

REGULATION OF CARDIAC METABOLISM BY AUTOPHAGY

by

Zhonggang Li

A dissertation submitted to the faculty of
The University of Utah
in partial fulfillment of the requirements for the degree of

Doctor of Philosophy

Department of Human Genetics

The University of Utah

December 2016

Copyright © Zhonggang Li 2016

All Rights Reserved

The University of Utah Graduate School

STATEMENT OF DISSERTATION APPROVAL

The dissertation of Zhonggang Li
has been approved by the following supervisory committee members:

<u>Dale Abel</u>	, Chair	<u>5/10/2016</u> Date
<u>Donald McClain</u>	, Member	<u>5/10/2016</u> Date
<u>Carl Thummel</u>	, Member	<u>5/10/2016</u> Date
<u>Charles Murtaugh</u>	, Member	<u>5/10/2016</u> Date
<u>Gabrielle Kardon</u>	, Member	<u>5/10/2016</u> Date

and by Lynn Jorde, Chair/Dean of
the Department/College/School of Human Genetics

and by David B. Kieda, Dean of The Graduate School.

ABSTRACT

Autophagy is a catabolic pathway that degrades damaged proteins and organelles in lysosome; however, the exact role of autophagy in cardiac function in physiological and pathological states is incompletely understood.

To investigate the role of autophagy in the heart, we generated a cardiac-specific autophagy-deficient mouse model with deletion of ATG3 gene (cATG3 KO) in cardiomyocytes. ATG3-deficient hearts exhibited reduced ATG3 protein and decreased autophagic flux. cATG3 KO mice developed cardiac contractile dysfunction at 4 weeks old in the absence of fibrosis. Mitochondrial function was impaired in cATG3 KO mouse hearts at 1 week old, which precedes cardiac contractile dysfunction. Interestingly, we found that NAD⁺ metabolic flux was altered in cATG3 KO mouse hearts, characterized by increased nicotinamide N-Methyltransferase (NNMT) expression and accelerated NAD⁺ degradation. NNMT overexpression was sufficient to cause mitochondrial dysfunction and NNMT inhibition prevented mitochondrial dysfunction in CQ-treated H9C2 cells. Moreover, nicotinamide mononucleotide (NMN), the precursor of NAD⁺, raised cardiac NAD⁺ content and rescued cardiac contractile dysfunction in cATG3 KO mice. These data suggest that autophagy plays an essential role in maintaining cardiac function by regulating NNMT expression and NAD⁺ homeostasis in the heart.

Exercise training has been shown to be beneficial for cardiac function, although the exact molecular mechanism is unclear. To investigate the role of autophagy in maintaining cardiac homeostasis under exercise conditions, mice with germline haplo-insufficiency of the autophagy regulator beclin 1 (Atg6) were subject to 6 weeks treadmill

training, and wild-type (WT) mice were used as control. Compared to WT mice, beclin 1 heterozygous mice exhibited impaired autophagy in response to exercise training. Interestingly, we found mitochondrial biogenesis and cardiac contractile function improvement was attenuated after exercise training in beclin 1 heterozygous mouse heart. These results indicate autophagy also plays an essential role for mediating the increase in cardiac function in response to exercise by promoting mitochondrial biogenesis.

TABLE OF CONTENTS

ABSTRACT	iii
LIST OF ABBREVIATIONS.....	vi
ACKNOWLEDGEMENTS	viii
INTRODUCTION	1
Autophagy Plays an Essential Role in Cellular Homeostasis.....	1
Autophagy and Heart Health	5
NAD ⁺ in Cellular Function.....	8
NAD ⁺ Is Emerging New Therapeutic Target for Heart Diseases	11
The Interaction Between Autophagy and NAD ⁺ Metabolism	12
Summary	13
References	14
CHAPTERS	
1 AUTOPHAGY MAINTAINS HEART FUNCTION BY MAINTAINING CARDIAC NAD ⁺ HOMEOSTASIS	25
Abstract.....	25
Introduction	25
Materials and Methods.....	27
Results.....	33
Discussion	41
References	47
2 AUTOPHAGY IS REQUIRED FOR IMPROVING CARDIAC PERFORMANCE FOLLOWING EXERCISE	68
Abstract.....	68
Introduction	69
Materials and Methods.....	70
Results.....	73
Discussion	76
References	81
CONCLUSION.....	92
References	96

LIST OF ABBREVIATIONS

3-MA: 3-Methyladenine

ADP: adenosine diphosphate

AMP: adenosine monophosphate

ATG: autophagy-related genes

ATP: Adenosine triphosphate

AMPK: 5' AMP-activated protein kinase

Co-IP: Co-Immunoprecipitation

Col: colchicine

CQ: chloroquine

DHE: dihydroethidium

GAPDH: glyceraldehyde-3-phosphate dehydrogenase

Het: heterozygous

HFD: high fat diet

I/R: ischemia and reperfusion

KO: knockout

MeNAM: N1-methyl-nicotinamide

NAD: nicotinamide adenine dinucleotide

NAM: nicotinamide

NMN: nicotinamide mononucleotide

NNMT: nicotinamide N-methyltransferase

OCR: oxygen consumption rate

PGC1: peroxisome proliferator-activated receptor-gamma coactivator 1

ROS: reactive oxidative species

SAM: S-adenosyl-1-methionine

shRNA: short hairpin RNA

siRNA: short interfering RNA

SIRT: sirtuins

TAC: transverse aortic constriction

TAG: triglyceride

TCA: tricarboxylic acid

TFR: transferrin receptor

PE: phosphatidylethanolamine

WT: wild-type

ACKNOWLEDGEMENTS

I would like to take this moment to express my sincere gratitude to my advisor and mentor, Dr. Abel, for providing me this precious opportunity to work in his lab. His valuable guidance, great personality, and his critical thinking have been of great value to me. His understanding, encouragement, and constant support are the corner-stone of my dissertation work.

I am grateful to all my committee members for providing their valuable critique and constructive suggestions throughout my graduate work.

I would like to thank my parents and my wife who devoted their retiring life to help me in my life. They are really supportive of my decision to pursue a Ph.D. degree outside of the P.R. China.

INTRODUCTION

Autophagy Plays an Essential Role in Cellular Homeostasis

Basic autophagy process

Autophagy is an essential cellular process to break down cellular components in a lysosome-dependent pathway. There are three major types of autophagy — macroautophagy, microautophagy, and chaperone-mediated autophagy [1, 2]. The term “autophagy” indicates macroautophagy if not specified.

In macroautophagy, certain long-lived proteins, damaged organelles and malformed proteins are sequestered in vacuoles termed as autophagosomes, and subsequently delivered to lysosomes for degradation [3] [4] [5]. Currently, 32 different autophagy-related genes (ATG) have been identified in yeast and many of these genes are found to be conserved in mammals, emphasizing the importance of autophagy in various biological processes [6].

Autophagy is a multistep process. Basically, there are 5 main steps, including vesicle nucleation, vesicle elongation, autophagosome structure formation, autophagosome fusion with lysosomes, and eventually, vesicle breakdown and degradation inside the lysosome (Figure 1.1) [5]. In the first step of autophagosome formation, cytoplasmic components, including damaged organelles, are sequestered by a unique double membrane called the phagophore. Complete sequestration by the elongating phagophore results in formation of the double-membraned autophagosome. LC3, a mammalian homolog of ATG8, targets autophagosome inner membrane and plays an important role in complete autophagosome formation [7].

In the course of autophagy, a cytosolic form of LC3 (LC3 I) is conjugated to phosphatidylethanolamine to form LC3-phosphatidylethanolamine conjugate (LC3 II), which is recruited to autophagosome membranes [1]. Thus, LC3 II/I ratio or LC3 II levels are commonly used as the marker of autophagosome formation and autophagy induction. After autophagosomes are formed, p62/SQSTM1 binds to LC3 II and is selectively degraded in lysosomes [8] [9]. Since p62/SQSTM1 has an ubiquitin-binding domain, ubiquitinated proteins can be recruited to the autophagosome membrane through their interaction with p62/SQSTM1 [9]. Therefore, p62/SQSTM1 can be regarded as an autophagic adapter for selective degradation of ubiquitinated proteins. Besides LC II level, cytosolic p62/SQSTM1 (p62) level is another marker of autophagic flux (Figure 1.2).

Autophagy regulatory machinery

Several autophagy-related proteins (ATG) are involved in the regulation of autophagy vesicle initiation and autophagosome membrane elongation. The most well studied ATG in autophagy is beclin 1, the mammalian orthologue of yeast ATG6. Beclin 1 plays an essential role in the initiation of autophagy. Under starvation or other stress conditions, beclin 1 is highly induced and dissociates from Bcl-2. The formed beclin 1-Vps34-Vps15 core complex is essential for the initiation of autophagy [10] [11]. With the heterozygous deletion of bclin 1, autophagy was partially inhibited in multiple tissues, and beclin 1 heterozygous mice are widely used as a universal model to study autophagy in multiple tissues, including in liver, heart and lung [11].

In autophagosome elongation, it has been well demonstrated that autophagy mainly depends on the function of ATG5, ATG7 and ATG3. ATG7 provides E1 conjugating enzyme activity to form an ATG12-ATG5-ATG16 conjugating tricomplex. ATG3 provides E2 conjugating enzyme activity to cleave LC3 I to LC3 II, and conjugates

LC3 II to phosphatidylethanolamine (PE) for selective targeting to the autophagosomal membrane. The conjugated LC3 II-PE promotes autophagosome membrane elongation and autophagosome maturation (Figure 1.3) [12-14].

In a recent study a small amount of autophagosome formation was found in ATG7 and ATG5 knockout (KO) MEFs when subjected to certain stressors, suggesting the existence of an ATG7/ATG5 independent autophagy pathway. This alternative pathway of autophagy was independent of LC3 processing, but still involved autophagosome formation from late endosomes [15]. But compared to the conventional LC3-dependent autophagy pathway, LC3-independent pathway contributes to a relatively minor component of autophagic flux in mammalian cells, and may be negligible in most cases.

Autophagy maintains cellular homeostasis

Autophagy is a constitutive process that maintains cellular homeostasis and serves an essential cellular quality control function. Under basal conditions, certain misfolded proteins and damaged organelles can be degraded and recycled by autophagy [2, 16]. Neuron-specific ATG7 knockout mice exhibited more ubiquitinated protein aggregates in the brain [17], ATG7-deficient hepatocytes showed accumulated peroxisomes [18], and ATG7 null β cells had abnormally Golgi structure [19]. ATG5 or ATG7-deficient skeletal muscle accumulated abnormal mitochondria and ubiquitin-positive proteins [20] [21]. These studies suggest that autophagy plays a crucial role by promoting ubiquitinated protein turnover, degrading aggregated proteins, as well as recycling damaged organelles.

Besides, activation of autophagy also serves as a means of providing nutrients and energy to sustain vital cellular functions during a variety of stress conditions, including nutrient starvation, growth factor withdrawal, oxidative stress, infection, and

hypoxia. In stress conditions, autophagy provides certain substrates for *de novo* protein synthesis and oxidative phosphorylation to maintain cellular biosynthesis and ATP production [22]. It has been found that ATG5 or ATG7 deficient mice exhibited reduced plasma and tissue amino acid levels, displayed signs of energy depletion and died within 1 day after birth probably due to nutrient depletion [23] [18]. Cells with ATG7 knockdown or treated with the autophagy inhibitors chloroquine (CQ) showed more cell death under growth factor deprivation conditions. And supplying autophagy-deficient cells with the TCA cycle substrate methylpyruvate enhanced ATP production and rescued cell viability under growth factor deprivation conditions [24]. Thus under multiple stress conditions, autophagy functions as a cellular survival mechanism by modulating protein synthesis and cellular energy homeostasis [25].

Autophagy is involved in various human diseases

Impaired autophagy was found to be associated with various human diseases such as neurodegeneration, myopathy, liver disease and type 2 diabetes [22]. In neurons, autophagy is believed to play a cytoprotective role by preventing protein aggregate formation. When ATG5 or ATG7 is deleted in neurons, these ATG7 or ATG5 KO mice show increased ubiquitinated aggregates and develop progressive neurodegeneration [26] [17]. In skeletal muscle, autophagy plays an essential role in maintaining muscle function, and muscle-specific ATG5 and ATG7 knockout mice showed muscle fiber dysfunction and develop severe muscle atrophy [20]. Besides neuron and skeletal muscle, the liver is another organ that is highly dependent on basal autophagy. ATG7 liver-specific KO mice showed increased triglyceride (TAG) levels, elevated total cholesterol levels and finally developed hepatomegaly, suggesting an essential role of autophagy in liver lipid metabolism regulation [27]. Autophagy has also been found to be associated with type 2 diabetes. β cell-specific ATG7 knockout mice

developed progressive β cell degeneration, hyperglycemia, loss of insulin production, and cellular hypertrophy when fed a high fat diet (HFD), suggesting an essential role of autophagy in maintaining β cell function [28]. Moreover, in diabetic patients and *db/db* mice, autophagic flux are both repressed, indicating decreased autophagy may contribute to diabetes development [29] [30].

Autophagy and Heart Health

Autophagy in the heart under basal conditions

Autophagy was also involved in multiple cardiovascular diseases. In one clinical study, mutations in genes encoding lysosome-associated membrane protein-2 (LAMP2), commonly known as Danon disease, were found to be strongly associated with profound myocardial hypertrophy and electrophysiologic defects, suggesting a causal relationship between autophagy defects and heart failure [31]. LAMP2 deficient mice were subsequently generated to study the role of LAMP2 in cardiac function. These LAMP2 deficient mice exhibited dramatically higher autophagic vacuole accumulation and decreased degradation of long-lived proteins in their cardiomyocytes. LAMP2 deficient mice developed severe cardiomyopathy and showed elevated mortality, indicating the critical role of LAMP2 in maintaining cardiac function [32].

In another mouse model, cardiac-specific deletion of ATG5 blocked autophagy in cardiomyocytes and caused cardiac contractile dysfunction [33]. Ultrastructural analyses of ATG5-deficient hearts demonstrated disorganized sarcomere structure and mitochondria misalignment [33]. These results indicate that constitutive autophagy is required for protein quality control and normal cardiomyocyte function. Isolated cardiomyocytes from ATG5-deficient hearts were more susceptible than cardiomyocytes isolated from control hearts to isoproterenol [33]. These results indicate ATG5 is required to maintain normal heart function, but the role of autophagy in the heart is still

unclear due to the diverse biological role of ATG5 beyond autophagy. For instance, ATG5 has pro-apoptotic effects through its interaction with Bcl family. Truncated ATG5 translocates from the cytosol to the mitochondria and associates with the antiapoptotic molecule Bcl-xL, which provokes apoptotic cell death. Thus the detrimental consequence of ATG5-deficiency in the heart could be the effect of activating apoptosis but not a secondary effect from autophagy inhibition [34].

Autophagy in the heart under pathological conditions

In human failing hearts from subjects with dilated cardiomyopathy, large amounts of autophagic cells have been observed [35], suggesting that cardiac autophagy may play a role in heart failure progression. In a mouse model with pressure overload induced by transaortic constriction (TAC), mice developed heart failure and showed greatly increased cardiac autophagy for at least 3 weeks [36]. And another study showed autophagy was upregulated between 1 and 12 hours after TAC but was downregulated below physiological levels 5 days after TAC [37].

Then more studies were conducted to investigate whether TAC-induced autophagy functions as a repair mechanism or contributes to cardiomyocyte cell death. In one study, using a whole body autophagy inhibition mouse model, heterozygous disruption of the beclin 1 gene, a protein required for early autophagosome initiation, decreased autophagy in cardiomyocytes and diminished pathological remodeling induced by pressure stress, suggesting cardiac autophagy may be a maladaptive response to hemodynamic stress. On the contrary, cardiac-specific ATG5 deficient mice developed severe cardiac dysfunction and left ventricular dilatation 1 week after TAC surgery [33], suggesting the protective role of autophagy in hemodynamic stress heart. The obvious inconsistency between these two models might be due to the fact that beclin 1 heterozygous mice exhibited disruption of autophagy but were not

completely abrogated; whereas ATG5-deficient mice showed complete autophagy deficiency in cardiomyocytes.

As a response to various stress conditions, autophagy has been found to be enhanced during ischemia and reperfusion (I/R) in the heart [38]. Forty minutes of ischemia caused more autophagosome formation, and reperfusion further increased autophagosome number, suggesting that I/R can induce autophagy in the heart [39]. Moreover, 30 minutes of ischemia and 2 hours of reperfusion induced LC3 II and beclin 1 in Langendorff hearts, indicating autophagy may be evoked in response to I/R [40]. Autophagy could play a detrimental role during I/R, since blocking autophagy with 3-methyladenine (3-MA) or LY294002 reduced cell death during glucose deprivation in cultured H9C2 cells [41], suggesting that autophagy contributes to cell death. Furthermore, inhibiting autophagy by beclin 1 knockdown or 3-Methyladenine (3-MA) treatment was sufficient to reduce cell death in cardiac myocytes after I/R stimulation [42]. Thus autophagy may play an adverse role during I/R in the heart.

Autophagy may also modulate cardiac aging. It has been known that autophagic flux dramatically declines in old mouse and rat hearts [43, 44]. In the previously described ATG5 KO mouse model, ATG5 KO mice developed age-related cardiac dysfunction at 8 months old [45], suggesting a beneficial role of autophagy in preventing age-related cardiomyopathy. Moreover, overexpression of Parkin, a protein essential for mitophagy (mitochondrial autophagy), ameliorated the age-related decline of cardiac function [46], providing more evidence that autophagy plays a protective role in the aging heart.

Exercise training, with multiple beneficial effects for cardiovascular health, is another well-known stress that robustly induces autophagic flux in the heart [47, 48]. Treadmill training increases autophagosome number in cardiac myocytes in LC3-GFP transgenic mice [49]. In recent studies, autophagic signaling, including LC3 and p62

levels, were significantly upregulated in rat cardiac muscle after chronic exercise treadmill training, supporting the idea that autophagy is induced in the heart during exercise training [50]. However, the exact role of exercise-induced autophagy in cardiac remodeling remains incompletely understood.

NAD⁺ in Cellular Function

NAD⁺ modulates cellular function

Nicotinamide adenine dinucleotide (NAD) is a central metabolic cofactor in cells either in its oxidized form (NAD⁺) or in its reduced form (NADH) [51]. NAD⁺ functions as a redox cofactor whose redox capacity is essential in cellular respiration. By using NAD⁺ and the electron transport chain, the cell can produce ATP in a more efficient way through oxidation of organic molecules in mitochondria [52]. NAD⁺ is also functional as a critical “coenzyme” in a wide range of enzymatic reactions. In the cytosolic compartment, NAD⁺ regulates glycolytic flux by modulating enzymatic activity of glycolytic enzymes, such as Glyceraldehyde 3-phosphate dehydrogenase (GAPDH) [53]. GAPDH modulates glycolysis rate, and its activity is largely affected by its co-substrate NAD⁺ concentration. Depletion of NAD⁺ by triggering Poly (ADP-ribose) polymerase 1 (PARP1) inhibits GAPDH activity and blocks glucose utilization in neuron cells [54]. Importantly, the reduction of glycolysis could be reversed by supplying 5 mM NAD⁺, suggestive of the importance of NAD⁺ content in regulating GAPDH activity and cellular glycolytic rates [55].

NAD⁺ can also regulate various biological reactions by modulation of sirtuin enzymatic activity. Seven sirtuins exist in mammalian cells (SIRT1-7), and all contain a conserved NAD-binding and catalytic domain [56]. The enzymatic activity of these sirtuins is highly dependent on NAD⁺, and connects cellular energy status with various biological functions, such as cell survival, inflammation, energy metabolism, and aging

[57]. For instance, NAD⁺ dependent enzyme SIRT1 regulates various biological functions depending on its tissue localization and plays a role in many pathophysiological processes, including obesity-associated metabolic diseases, cancer, adipose tissue differentiation, aging, cellular senescence, cardiac oxidative stress, neurodegeneration, inflammatory signaling and placental cell survival (Figure 1.4). Since its diverse role in regulating metabolic process and its activity is highly dependent on cellular NAD⁺ bioavailability, SIRT1 is regarded as a vital and sensitive energy sensor in adjusting biological systems.

NAD⁺ biosynthetic and breakdown machinery

Given its vital role in biological reactions, cellular NAD⁺ content is tightly controlled by multiple pathways. Basically, NAD⁺ metabolism is a balance between its biosynthesis and breakdown pathways (Figure 1.5).

There are two biosynthetic pathways that generate NAD⁺. One is called *de novo* biosynthesis and the other is salvage pathway. In the NAD⁺ *de novo* biosynthesis pathway, tryptophan is converted to NAD⁺ through niacin and then to NAD⁺; however, this *de novo* pathway is a relatively minor contributor to the total NAD pool in most organs [58]. Perhaps the more important NAD⁺ biosynthesis pathway is the salvage pathway, which can start either from nicotinic acid (NA), nicotinamide (NAM) or nicotinamide riboside (NR), all of which are present in the regular diet [59]. For example, NR is present in milk and can be used to synthesize NAD in eukaryotes [60]. More importantly, NR supplementation can also increase NAD⁺ levels and trigger NAD-related downstream signaling both in cultured mammalian cells and in mice [61], rendering NR an important dietary NAD⁺ precursor. Nicotinamide mononucleotide (NMN) is another key NAD⁺ intermediate that can be converted to NAD⁺ by one step reaction and becoming a prospective NAD⁺ precursor.

There are various enzymes that consume NAD^+ , such as previously described SIRT family proteins and GAPDH [57] [62]. These NAD^+ consumers utilize NAD as their co-substrate for enzymatic reaction, and degrade NAD to NAM. It should be noted that NAM can be recycled and synthesized to NAD^+ in salvage pathway.

For breakdown and clearance, NAM must be methylated to 1-methylnicotinamide (MeNAM) by nicotinamide N-methyltransferase (NNMT) [63], and then further oxidized to 1-methyl-2-pyridone-5-carboxamide (Me-2PY) and 1-methyl-4-pyridone-3-carboxamide (Me-4PY), which are excreted from tissue in urine [64]. Thus NNMT functions as the key enzyme in the NAD^+ breakdown and degradation pathway, although its role in metabolism remains to be fully elucidated.

NNMT in NAD^+ metabolism

NNMT is the enzyme that catalyzes the transfer of methyl groups from S-adenosyl-1-methionine (SAM) to NAM, generating S-adenosylhomocysteine (SAH) and MeNAM for NAD^+ breakdown. NNMT may be involved in multiple human diseases models. For example, NNMT was initially identified as a biomarker in a variety of human cancers, including in lung cancer, bladder cancer and colon cancer [65]. More studies show that NNMT is sufficient to promote the migration, invasion, proliferation and survival of cancer cells. NNMT also impairs the methylation potential of cancer cells by altering the cellular SAM/SAH ratio [66]. NNMT expression has also been shown to be tightly associated with Parkinson's disease, as evidenced by increased NNMT expression in the brains from patients with Parkinson's disease [67].

Recently, NNMT has recently been implicated in multiple metabolic diseases. MeNAM concentrations are increased in the urine from multiple type 2 diabetes models, including db/db mice, obese Zucker rats and type 2 diabetes patients, suggesting that NNMT activity might be increased in these diabetes models [68]. In a recent study,

NNMT mRNA and protein levels were found to be significantly induced in white adipose tissue (WAT) from adipose-specific GLUT4 knockout mice, an animal model with systemic insulin resistance. Interestingly, NNMT knockdown in WAT and liver was sufficient to protect against diet-induced obesity by increasing NAD⁺ levels and by increasing cellular energy expenditure [69]. This study highlights the important role of NNMT in maintenance of NAD⁺ homeostasis and therefore NNMT is emerging as a novel target for metabolic disease therapy.

NAD⁺ Is Emerging New Therapeutic Target for Heart Diseases

Altered NAD⁺ metabolism has been described in various forms of heart disease. In pathological cardiac hypertrophy, NAD⁺ levels are reduced in mouse hearts after transverse aortic constriction (TAC) [70]. Moreover, intracellular levels of NAD⁺ are also decreased in agonist-induced pathological cardiac hypertrophy models, but not in exercise-induced physiological hypertrophy [71]. These results suggest there is an association between NAD⁺ content and pathological cardiac hypertrophy. Interestingly, supplying mice with NAD⁺ prevented the development of cardiac hypertrophy and blunted fibrosis as a response to angiotensin II [71]. In a recent study, overexpression of nicotinamide phosphoribosyltransferase (NAMPT), the enzyme for NAD⁺ biosynthesis, in cardiomyocytes, preserved myocardial NAD⁺ levels [72]. These results illustrate the essential role of NAD⁺ in maintaining cardiac function under pressure overload conditions.

NAD⁺ also plays an important role in ischemia/reperfusion (I/R) in the heart. Following ischemia, NAD⁺ content is significantly reduced and this decline persists in 24 hours following reperfusion [73]. The depleted NAD⁺ during I/R is thought to contribute to myocyte damage. In an earlier study, nicotinamide-rich diets protected the heart against I/R in mice [74]. Moreover, restoring cardiac NAD⁺ levels by Nicotinic acid (NA)

or NMN administration was sufficient to reduce the infarct area after I/R [73, 75]. Cardiac-specific overexpression of NAMPT increased NAD⁺ content in the heart, and reduced apoptosis and myocardial infarction size following ischemia/reperfusion [76]. Therefore, NAD⁺ homeostasis plays a critical role in cardiac function under basal and stress conditions, but the molecular mechanisms that regulate NAD⁺ content in the heart remain incompletely understood.

The Interaction Between Autophagy and NAD⁺ Metabolism

Many studies support an association between autophagy and NAD⁺ homeostasis. In xeroderma pigmentosum (XP) disease, a neuron degenerative disorder, decreased autophagy was observed in the neurons from XP patients, which was accompanied by reduced NAD⁺ content and impaired SIRT1 signaling. Moreover, nicotinamide riboside (NR), the precursor of NAD⁺, is sufficient to rescue the autophagy deficiency and mitochondrial dysfunction phenotype, suggesting an interaction between NAD⁺ depletion and autophagy deficiency in neuron cells [77].

Dysfunctional autophagy has been widely observed in aging organisms and age-related diseases [78], and reduced NAD⁺ content is another feature of these aged organisms [79]. In a recent study, decreased autophagic flux and reduced NAD⁺ levels were found in oxidative stress-induced senescent fibroblasts, suggesting autophagy deficiency and NAD⁺ depletion are jointly involved in aging related cell death [80]. However, the mechanism linking autophagic flux and NAD⁺ homeostasis is unknown.

An association of autophagy deficiency and NAD⁺ depletion is also present in the failing heart. Transferrin receptor (TFR) knockout mice developed lethal cardiomyopathy due to iron deficiency in the heart. Interestingly, there was ineffective autophagy and altered NAD⁺ related gene expression in TFR deficient cardiomyocytes, suggestive of the association of autophagy and NAD⁺ metabolism in failing heart. Moreover,

administration of nicotinamide riboside (NR) raised cardiac NAD⁺ content, rescued the autophagy defect and ameliorated cardiomyopathy in TFR KO mice [81]. These results suggest a potential interaction between autophagy and NAD⁺ homeostasis in the heart.

Summary

Autophagy, as a cellular process to maintain cellular homeostasis, is altered in various heart diseases models. However, gaps remain in our knowledge regarding the relationship between autophagy and cardiac structure, function and metabolism. NAD⁺ is an important redox cofactor and plays a vital role in maintaining normal cardiac function. Based on previous studies, autophagy deficiency and NAD⁺ depletion coexist in the aging heart and in multiple heart failure models, indicating there might be an interaction between autophagy and NAD⁺ homeostasis in the heart. In the following study, we investigated the role of autophagy in the heart under basal and exercise-training conditions. And we sought to understand the interaction between autophagy and NAD⁺ metabolism in the heart.

References

1. Mizushima, N., Autophagy: process and function. *Genes Dev*, 2007. 21(22): p. 2861-73.
2. Parzych, K.R. and D.J. Klionsky, An overview of autophagy: morphology, mechanism, and regulation. *Antioxid Redox Signal*, 2014. 20(3): p. 460-73.
3. Nakatogawa, H., et al., Dynamics and diversity in autophagy mechanisms: lessons from yeast. *Nat Rev Mol Cell Biol*, 2009. 10(7): p. 458-67.
4. Mizushima, N., et al., Autophagy fights disease through cellular self-digestion. *Nature*, 2008. 451(7182): p. 1069-75.
5. Melendez, A. and B. Levine, Autophagy in *C. elegans*. *WormBook*, 2009: p. 1-26.
6. Glick, D., S. Barth, and K.F. Macleod, Autophagy: cellular and molecular mechanisms. *J Pathol*, 2010. 221(1): p. 3-12.
7. Kirisako, T., et al., The reversible modification regulates the membrane-binding state of Apg8/Aut7 essential for autophagy and the cytoplasm to vacuole targeting pathway. *J Cell Biol*, 2000. 151(2): p. 263-76.
8. Bjorkoy, G., et al., p62/SQSTM1 forms protein aggregates degraded by autophagy and has a protective effect on huntingtin-induced cell death. *J Cell Biol*, 2005. 171(4): p. 603-14.
9. Pankiv, S., et al., p62/SQSTM1 binds directly to Atg8/LC3 to facilitate degradation of ubiquitinated protein aggregates by autophagy. *J Biol Chem*, 2007. 282(33): p. 24131-45.
10. Liang, X.H., et al., Protection against fatal Sindbis virus encephalitis by beclin, a novel Bcl-2-interacting protein. *J Virol*, 1998. 72(11): p. 8586-96.
11. Kang, R., et al., The beclin 1 network regulates autophagy and apoptosis. *Cell Death Differ*, 2011. 18(4): p. 571-80.
12. Jia, W., et al., Autophagy, a novel pathway to regulate calcium mobilization in T lymphocytes. *Front Immunol*, 2013. 4: p. 179.
13. Levine, B., N. Mizushima, and H.W. Virgin, Autophagy in immunity and inflammation. *Nature*, 2011. 469(7330): p. 323-35.
14. Yamada, Y., et al., The crystal structure of Atg3, an autophagy-related ubiquitin carrier protein (E2) enzyme that mediates Atg8 lipidation. *J Biol Chem*, 2007. 282(11): p. 8036-43.
15. Nishida, Y., et al., Discovery of Atg5/Atg7-independent alternative macroautophagy. *Nature*, 2009. 461(7264): p. 654-8.
16. Yi, C., et al., Function and molecular mechanism of acetylation in autophagy regulation. *Science*, 2012. 336(6080): p. 474-7.

17. Komatsu, M., et al., Loss of autophagy in the central nervous system causes neurodegeneration in mice. *Nature*, 2006. 441(7095): p. 880-4.
18. Komatsu, M., et al., Impairment of starvation-induced and constitutive autophagy in Atg7-deficient mice. *J Cell Biol*, 2005. 169(3): p. 425-34.
19. Jung, H.S., et al., Loss of autophagy diminishes pancreatic beta cell mass and function with resultant hyperglycemia. *Cell Metab*, 2008. 8(4): p. 318-24.
20. Masiero, E., et al., Autophagy is required to maintain muscle mass. *Cell Metab*, 2009. 10(6): p. 507-15.
21. Thapaliya, S., et al., Alcohol-induced autophagy contributes to loss in skeletal muscle mass. *Autophagy*, 2014. 10(4): p. 677-90.
22. Murrow, L. and J. Debnath, Autophagy as a stress-response and quality-control mechanism: implications for cell injury and human disease. *Annu Rev Pathol*, 2013. 8: p. 105-37.
23. Kuma, A., et al., The role of autophagy during the early neonatal starvation period. *Nature*, 2004. 432(7020): p. 1032-6.
24. Lum, J.J., et al., Growth factor regulation of autophagy and cell survival in the absence of apoptosis. *Cell*, 2005. 120(2): p. 237-48.
25. Das, G., B.V. Shrivastava, and E.H. Baehrecke, Regulation and function of autophagy during cell survival and cell death. *Cold Spring Harb Perspect Biol*, 2012. 4(6).
26. Hara, T., et al., Suppression of basal autophagy in neural cells causes neurodegenerative disease in mice. *Nature*, 2006. 441(7095): p. 885-9.
27. Singh, R., et al., Autophagy regulates lipid metabolism. *Nature*, 2009. 458(7242): p. 1131-5.
28. Ebato, C., et al., Autophagy is important in islet homeostasis and compensatory increase of beta cell mass in response to high-fat diet. *Cell Metab*, 2008. 8(4): p. 325-32.
29. Masini, M., et al., Autophagy in human type 2 diabetes pancreatic beta cells. *Diabetologia*, 2009. 52(6): p. 1083-6.
30. Li, X., et al., Islet microvasculature in islet hyperplasia and failure in a model of type 2 diabetes. *Diabetes*, 2006. 55(11): p. 2965-73.
31. Arad, M., J.G. Seidman, and C.E. Seidman, Phenotypic diversity in hypertrophic cardiomyopathy. *Hum Mol Genet*, 2002. 11(20): p. 2499-506.
32. Stypmann, J., et al., LAMP-2 deficient mice show depressed cardiac contractile function without significant changes in calcium handling. *Basic Res Cardiol*, 2006. 101(4): p. 281-91.

33. Nakai, A., et al., The role of autophagy in cardiomyocytes in the basal state and in response to hemodynamic stress. *Nat Med*, 2007. 13(5): p. 619-24.
34. Yousefi, S., et al., Calpain-mediated cleavage of Atg5 switches autophagy to apoptosis. *Nat Cell Biol*, 2006. 8(10): p. 1124-32.
35. Kostin, S., et al., Myocytes die by multiple mechanisms in failing human hearts. *Circ Res*, 2003. 92(7): p. 715-24.
36. Zhu, H., et al., Cardiac autophagy is a maladaptive response to hemodynamic stress. *J Clin Invest*, 2007. 117(7): p. 1782-93.
37. Shirakabe, A., et al., Drp1-dependent mitochondrial autophagy plays a protective role against pressure overload-induced mitochondrial dysfunction and heart failure. *Circulation*, 2016. 133(13): p. 1249-63.
38. Hamacher-Brady, A., N.R. Brady, and R.A. Gottlieb, Enhancing macroautophagy protects against ischemia/reperfusion injury in cardiac myocytes. *J Biol Chem*, 2006. 281(40): p. 29776-87.
39. Hamacher-Brady, A., et al., Response to myocardial ischemia/reperfusion injury involves Bnip3 and autophagy. *Cell Death Differ*, 2007. 14(1): p. 146-57.
40. Gurusamy, N., et al., Cardioprotection by adaptation to ischaemia augments autophagy in association with BAG-1 protein. *J Cell Mol Med*, 2009. 13(2): p. 373-87.
41. Aki, T., et al., Phosphoinositide 3-kinase accelerates autophagic cell death during glucose deprivation in the rat cardiomyocyte-derived cell line H9c2. *Oncogene*, 2003. 22(52): p. 8529-35.
42. Valentim, L., et al., Urocortin inhibits beclin1-mediated autophagic cell death in cardiac myocytes exposed to ischaemia/reperfusion injury. *J Mol Cell Cardiol*, 2006. 40(6): p. 846-52.
43. De Meyer, G.R., G.W. De Keulenaer, and W. Martinet, Role of autophagy in heart failure associated with aging. *Heart Fail Rev*, 2010. 15(5): p. 423-30.
44. Wohlgemuth, S.E., et al., Autophagy in the heart and liver during normal aging and calorie restriction. *Rejuvenation Res*, 2007. 10(3): p. 281-92.
45. Taneike, M., et al., Inhibition of autophagy in the heart induces age-related cardiomyopathy. *Autophagy*, 2010. 6(5): p. 600-6.
46. Hoshino, A., et al., Cytosolic p53 inhibits Parkin-mediated mitophagy and promotes mitochondrial dysfunction in the mouse heart. *Nat Commun*, 2013. 4: p. 2308.
47. Gielen, S., G. Schuler, and V. Adams, Cardiovascular effects of exercise training: molecular mechanisms. *Circulation*, 2010. 122(12): p. 1221-38.

48. Driscoll, S.D., et al., Effects of exercise training and metformin on body composition and cardiovascular indices in HIV-infected patients. *AIDS*, 2004. 18(3): p. 465-73.
49. He, C., et al., Exercise-induced BCL2-regulated autophagy is required for muscle glucose homeostasis. *Nature*, 2012. 481(7382): p. 511-5.
50. McMillan, E.M., et al., Autophagic signaling and proteolytic enzyme activity in cardiac and skeletal muscle of spontaneously hypertensive rats following chronic aerobic exercise. *PLoS One*, 2015. 10(3): p. e0119382.
51. Berger, F., M.H. Ramirez-Hernandez, and M. Ziegler, The new life of a centenarian: signalling functions of NAD(P). *Trends Biochem Sci*, 2004. 29(3): p. 111-8.
52. Timashev, S.F., [Role of intermembrane electrical fields in electron and proton transport along the respiratory chain of mitochondria]. *Biofizika*, 1981. 26(6): p. 1027-32.
53. Schmalhausen, E.V., A.P. Pleten, and V.I. Muronetz, Ascorbate-induced oxidation of glyceraldehyde-3-phosphate dehydrogenase. *Biochem Biophys Res Commun*, 2003. 308(3): p. 492-6.
54. Ying, W., et al., Tricarboxylic acid cycle substrates prevent PARP-mediated death of neurons and astrocytes. *J Cereb Blood Flow Metab*, 2002. 22(7): p. 774-9.
55. Alano, C.C., et al., NAD⁺ depletion is necessary and sufficient for poly(ADP-ribose) polymerase-1-mediated neuronal death. *J Neurosci*, 2010. 30(8): p. 2967-78.
56. Frye, R.A., Phylogenetic classification of prokaryotic and eukaryotic Sir2-like proteins. *Biochem Biophys Res Commun*, 2000. 273(2): p. 793-8.
57. Nakagawa, T. and L. Guarente, SnapShot: sirtuins, NAD, and aging. *Cell Metab*, 2014. 20(1): p. 192-192 e1.
58. Houtkooper, R.H., et al., The secret life of NAD⁺: an old metabolite controlling new metabolic signaling pathways. *Endocr Rev*, 2010. 31(2): p. 194-223.
59. Magni, G., et al., Enzymology of NAD⁺ homeostasis in man. *Cell Mol Life Sci*, 2004. 61(1): p. 19-34.
60. Bieganowski, P. and C. Brenner, Discoveries of nicotinamide riboside as a nutrient and conserved NRK genes establish a Preiss-Handler independent route to NAD⁺ in fungi and humans. *Cell*, 2004. 117(4): p. 495-502.
61. Canto, C., et al., The NAD(+) precursor nicotinamide riboside enhances oxidative metabolism and protects against high-fat diet-induced obesity. *Cell Metab*, 2012. 15(6): p. 838-47.

62. Mouchiroud, L., R.H. Houtkooper, and J. Auwerx, NAD(+) metabolism: a therapeutic target for age-related metabolic disease. *Crit Rev Biochem Mol Biol*, 2013. 48(4): p. 397-408.
63. Scheller, T., et al., Mouse liver nicotinamide N-methyltransferase pharmacogenetics: biochemical properties and variation in activity among inbred strains. *Pharmacogenetics*, 1996. 6(1): p. 43-53.
64. Felsted, R.L. and S. Chaykin, N1-methylnicotinamide oxidation in a number of mammals. *J Biol Chem*, 1967. 242(6): p. 1274-9.
65. Roessler, M., et al., Identification of nicotinamide N-methyltransferase as a novel serum tumor marker for colorectal cancer. *Clin Cancer Res*, 2005. 11(18): p. 6550-7.
66. Ulanovskaya, O.A., A.M. Zuhl, and B.F. Cravatt, NNMT promotes epigenetic remodeling in cancer by creating a metabolic methylation sink. *Nat Chem Biol*, 2013. 9(5): p. 300-6.
67. Parsons, R.B., et al., High expression of nicotinamide N-methyltransferase in patients with idiopathic Parkinson's disease. *Neurosci Lett*, 2003. 342(1-2): p. 13-6.
68. Salek, R.M., et al., A metabolomic comparison of urinary changes in type 2 diabetes in mouse, rat, and human. *Physiol Genomics*, 2007. 29(2): p. 99-108.
69. Kraus, D., et al., Nicotinamide N-methyltransferase knockdown protects against diet-induced obesity. *Nature*, 2014. 508(7495): p. 258-62.
70. Pillai, J.B., et al., Poly(ADP-ribose) polymerase-1-dependent cardiac myocyte cell death during heart failure is mediated by NAD⁺ depletion and reduced Sir2alpha deacetylase activity. *J Biol Chem*, 2005. 280(52): p. 43121-30.
71. Pillai, V.B., et al., Exogenous NAD blocks cardiac hypertrophic response via activation of the SIRT3-LKB1-AMP-activated kinase pathway. *J Biol Chem*, 2010. 285(5): p. 3133-44.
72. Yano, M., et al., Monocyte-derived extracellular Nampt-dependent biosynthesis of NAD(+) protects the heart against pressure overload. *Sci Rep*, 2015. 5: p. 15857.
73. Yamamoto, T., et al., Nicotinamide mononucleotide, an intermediate of NAD⁺ synthesis, protects the heart from ischemia and reperfusion. *PLoS One*, 2014. 9(6): p. e98972.
74. Sukhodub, A., et al., Nicotinamide-rich diet protects the heart against ischaemia-reperfusion in mice: a crucial role for cardiac SUR2A. *Pharmacol Res*, 2010. 61(6): p. 564-70.
75. Trueblood, N.A., et al., Niacin protects the isolated heart from ischemia-reperfusion injury. *Am J Physiol Heart Circ Physiol*, 2000. 279(2): p. H764-71.

76. Hsu, C.P., et al., Nicotinamide phosphoribosyltransferase regulates cell survival through autophagy in cardiomyocytes. *Autophagy*, 2009. 5(8): p. 1229-31.
77. Fang, E.F., et al., Defective mitophagy in XPA via PARP-1 hyperactivation and NAD(+)/SIRT1 reduction. *Cell*, 2014. 157(4): p. 882-96.
78. Levine, B. and G. Kroemer, Autophagy in the pathogenesis of disease. *Cell*, 2008. 132(1): p. 27-42.
79. Yoshino, J., et al., Nicotinamide mononucleotide, a key NAD(+) intermediate, treats the pathophysiology of diet- and age-induced diabetes in mice. *Cell Metab*, 2011. 14(4): p. 528-36.
80. Han, X., et al., AMPK activation protects cells from oxidative stress-induced senescence via autophagic flux restoration and intracellular NAD elevation. *Aging Cell*, 2016.
81. Xu, W., et al., Lethal cardiomyopathy in mice lacking transferrin receptor in the heart. *Cell Rep*, 2015. 13(3): p. 533-45.

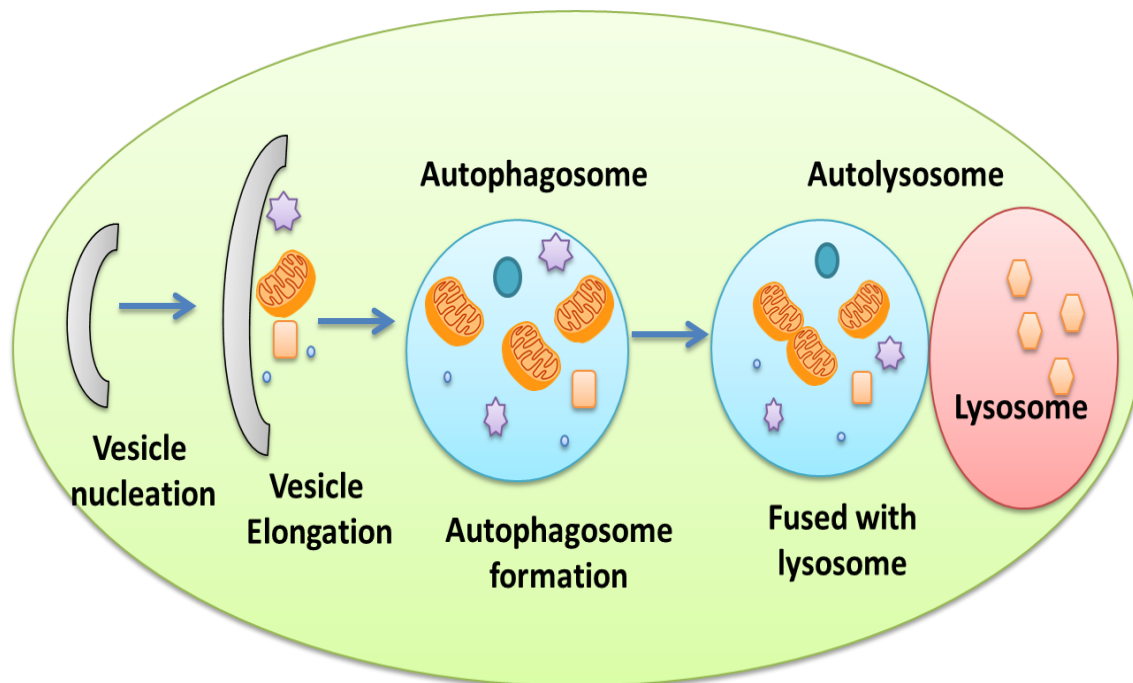


Figure 1.1 Autophagy is a multistep process, including vesicle nucleation, vesicle elongation, autophagosome formation, autophagosome fusion with the lysosome, vesicle breakdown and lysosomal degradation.

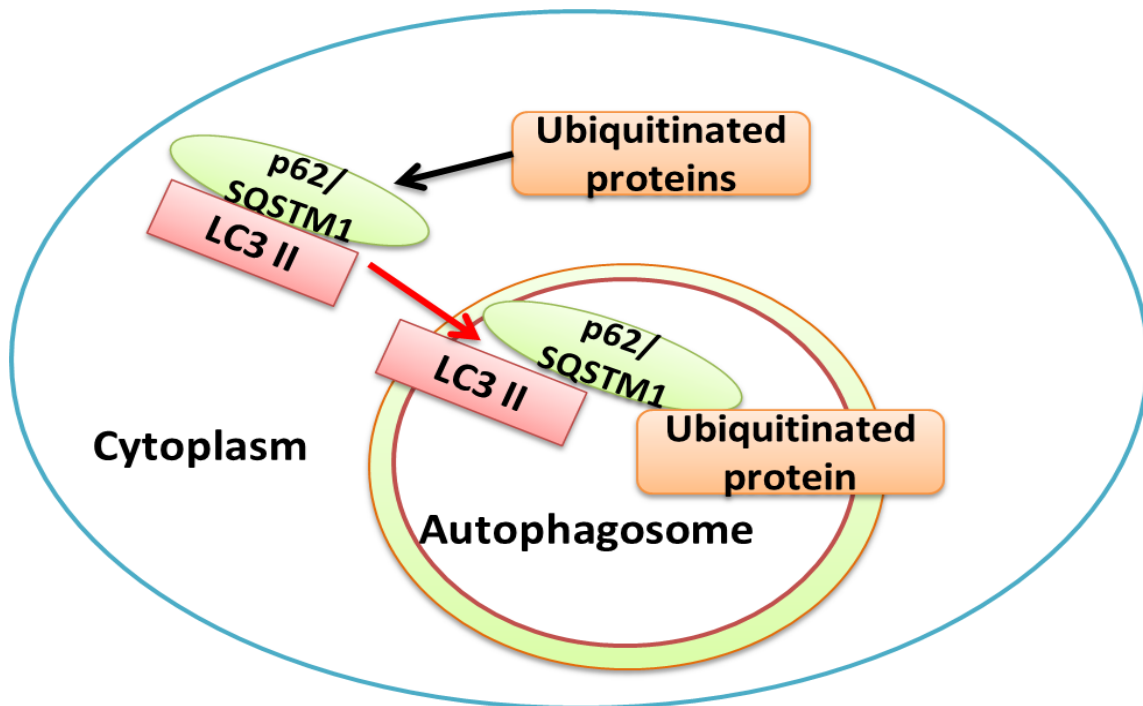


Figure 1.2 p62/SQSTM1 functions as an adaptor for protein selective degradation. p62/SQSTM1 can bind with ubiquitinated proteins and then bind to LC3 II for selective delivery of ubiquitinated proteins to autophagosome.

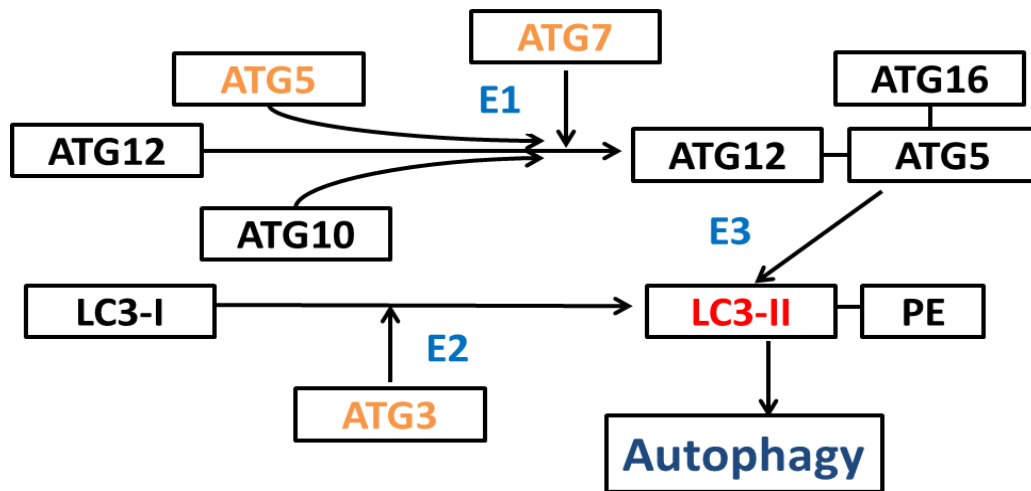


Figure 1.3 Autophagy-related (ATG) proteins and their interactions in the autophagy machinery. ATG7 functions as an E1 enzyme to form an ATG12–ATG5-ATG16 complex, providing E3 enzyme activity. ATG3 provides E2 enzyme activity, together with E3 enzyme, to conjugate LC3 II to the target lipid PE to form the autophagosome membrane.

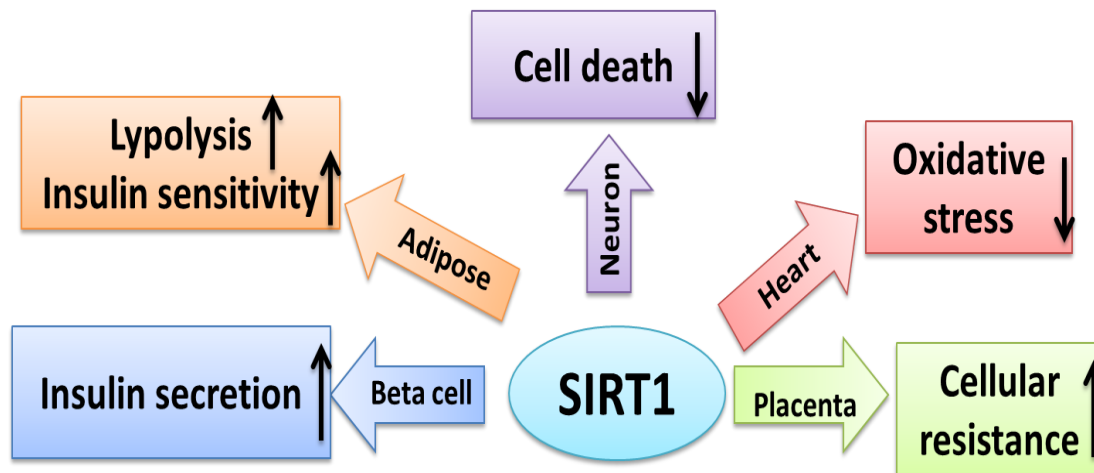


Figure 1.4 NAD⁺ dependent deacetylase SIRT1 plays a diverse role in mammalian cells in different tissues, including in neurons, adipocytes, beta cells, cardiomyocytes as well as placental cells.

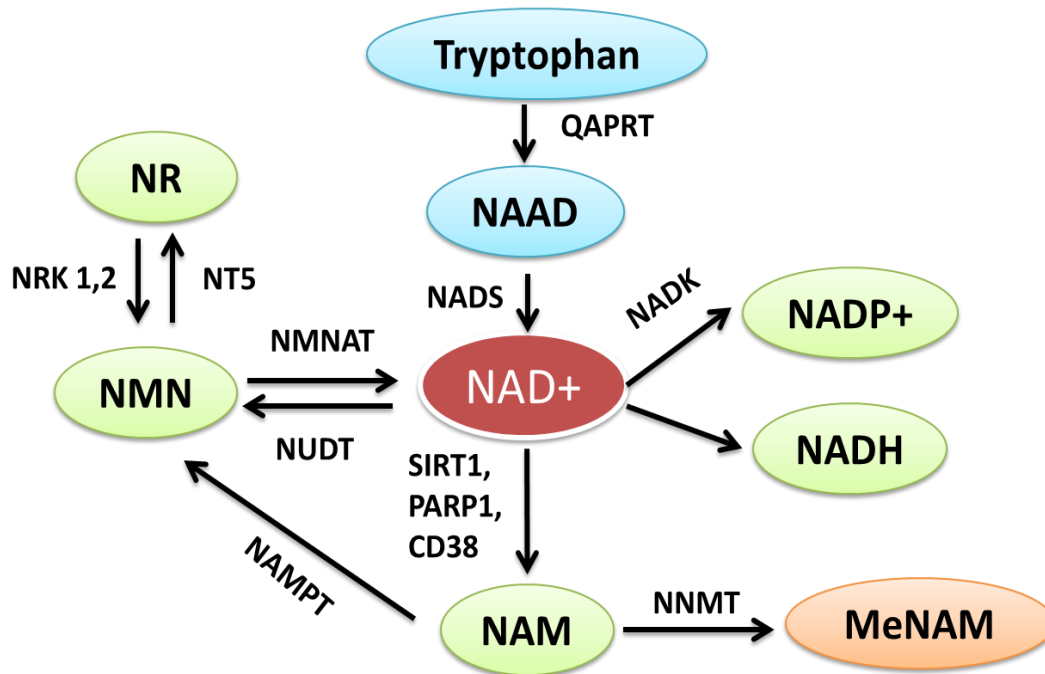


Figure 1.5 NAD⁺ can be converted from tryptophan through a de novo biosynthetic pathway, or recycled from nicotinamide riboside (NR) and nicotinamide mononucleotide (NMN) through the salvage pathway. For degradation and clearance, NAD⁺ can be degraded to nicotinamide (NAM) and cleared in the form of methylated-nicotinamide (MeNAM).

CHAPTER 1

AUTOPHAGY MAINTAINS HEART FUNCTION BY MAINTAINING CARDIAC NAD⁺ HOMEOSTASIS

Abstract

Autophagy is a catabolic pathway that degrades damaged proteins and organelles in lysosomes. Altered autophagy has been implicated in various cardiovascular diseases; however, a full understanding of the role of autophagy in cardiovascular homeostasis in physiological and pathophysiological states is still evolving. In this study, we generated a cardiac-specific autophagy-deficient mouse model with deletion of the ATG3 gene in cardiomyocytes. Compared to WT mice, cardiac-ATG3 knockout (cATG3 KO) mice exhibited cardiac contractile dysfunction and decreased mitochondrial respiration. Interestingly, NAD⁺ metabolism was altered in ATG3-deficient hearts, characterized by increased nicotinamide N-methyltransferase (NNMT) expression. NNMT overexpression repressed mitochondrial respiration, while NNMT inhibition prevented mitochondrial dysfunction in autophagy deficient cells. Replenishing cardiac NAD⁺ content by nicotinamide mononucleotide (NMN) restored cardiac contractile function in cATG3 KO mice. These data suggest autophagy plays an essential role in cardiac physiology by maintaining NAD⁺ homeostasis.

Introduction

Autophagy is an evolutionarily conserved catabolic process by which cells break down long-lived proteins and organelles to maintain cellular homeostasis [1]. Recent

evidence has indicated that autophagy plays a central role in regulating cardiac structure and function under physiological and pathophysiological conditions [2]. For example, the increase in autophagy during early phases of pressure overload may function as an adaptive response to prevent cardiomyocyte apoptosis [3]. However, repression of autophagy may promote the transition from compensated cardiac hypertrophy to heart failure [3]. Cardiac ATG5 knockout (cATG5 KO) mice developed age-related cardiomyopathy, suggesting that autophagy may also function as an anti-aging mechanism in the heart [4]. However many questions remain as to the exact role of autophagy in heart and these mechanisms need to be elucidated.

Nicotinamide adenine dinucleotide (NAD⁺) is an important coenzyme involved in numerous metabolic enzymatic reactions including glycolysis, fatty acid β -oxidation, and the tricarboxylic acid (TCA) cycle [5]. Reduced NAD⁺ levels correlate with reduced number and density of mitochondria in aging organs [6]. NAD⁺ can also serve as a substrate for poly (ADP-ribose) polymerases (PARPs) and class III NAD-dependent deacetylases (Sirtuins 1-7) [7, 8], which regulate diverse biological processes including those involved in the pathophysiology of cancer and metabolic diseases [9-12].

NAD⁺ plays a critical role in maintaining normal cardiac function. Impaired myocardial NAD⁺ homeostasis has been described in various cardiovascular diseases, including ischemia/reperfusion, myocardial infarction and dilated cardiomyopathy [13-16]. Moreover, boosting NAD⁺ by pharmacological approaches improved cardiac function in various heart failure animal models [16]. These results suggest NAD⁺ homeostasis as an emerging therapeutic target for heart failure.

ATG3 is a specific E2-like enzyme for the autophagosome conjugation system. It mediates the conversion of LC3 I to its active form LC3 II by conjugating phosphatidylethanolamine, which promotes autophagosome membrane elongation [17]. In previous studies, mice deficient in ATG3 gene were generated, and these ATG3-

deficient mice died 1 day after birth [18, 19]. In the present study, we sought to elucidate the role of autophagy in the heart by generating cardiac-specific ATG3 knockout (cATG3 KO) mice. Our results showed that cATG3 KO mice exhibited impaired autophagic flux in the heart and developed heart failure. Interestingly, we found that NAD⁺ metabolism was significantly changed in cATG3 KO mouse heart. Moreover, boosting cardiac NAD⁺ levels by nicotinamide mononucleotide (NMN) was sufficient to rescue cardiac contractile dysfunction in cATG3 KO mice. These results provide novel insights into the cross-talk between autophagy and NAD⁺ metabolism that impact cardiac function.

Materials and Methods

Animal experiments

This study protocol was approved by the Institutional Animal Care and Use Committees of the University of Utah, and the Carver College of Medicine of the University of Iowa.

Tissue harvest

Random fed or fasted mice were anesthetized by chloral hydrate, and hearts were immediately removed and rinsed in cold phosphate-buffered saline (PBS) before being snap frozen in liquid nitrogen. For metabolomics analyses, hearts were immediately removed, freeze-clamped and rapidly submerged in liquid nitrogen.

Cell culture and treatments

All reagents were purchased from Sigma (St. Louis, MO) unless stated otherwise. H9C2 (rat embryonic cardiomyoblasts, ATCC, Manassas, VA) and Ad-293 (ATCC, Manassas, VA) cells were maintained in DMEM (Invitrogen, Carlsbad, CA) with 25 mM glucose and 10% FBS (Thermo Scientific, Logan, UT).

SiRNA knockdown and virus transfection

For siRNA knockdown studies, H9C2 cells were transfected with 80 nM scramble or targeted siRNAs for 72 h using lipofectamine 2000 (Life Technologies, Eugene, OR). NNMT and GFP adenovirus were gifted from Dr. Pavlos Pissios from Beth Israel Deaconess Medical Center [20]. Cultured H9C2 cells were infected with adenovirus in DMEM medium with 25 mM glucose at a multiplicity of infection (MOI) of 10. Then the viral infected H9C2 cells were cultured for an additional 48 h.

Immunoprecipitation and immunoblotting

Total proteins were extracted from hearts or cultured H9C2 cells in lysis buffer, containing 50 mM HEPES (pH 7.5), 150 mM NaCl, 10% Glycerol, 1% Triton X-100, 1.5 mM MgCl₂, 1 mM EGTA, 10 mM Na₄P₂O₇, 100 mM NaF, and 1X Halt protease and phosphatase inhibitor cocktail (Thermo Scientific, Rockford, IL) [21]. The protein concentration was determined using a micro BCA Protein Assay kit (Thermo Scientific, Rockford, IL). Immunoprecipitation was performed with Millipore (Billerica, MA) provided protocols: 0.5 mg protein lysates in 1 ml lysis buffer containing both protease and phosphatase inhibitors were incubated with 10 µg PGC1α antibody (Santa Cruz Biotechnology, Santa Cruz, CA) at 4°C on a rocker for 3 h, and the antibody-protein complexes were later captured by protein A agarose beads (Millipore, Billerica, MA) by 1-h incubation on a rocker at 4°C. The immunocomplexes were then dissociated from the beads by boiling with 2× Tris-glycine SDS sample buffer (Invitrogen, Carlsbad, CA) containing 5% β-mercaptoethanol at 95°C for 10 min. The supernatant was used for Western blot analysis. For immunoblotting, previous extracted proteins were resolved on SDS-PAGE and analyzed by western blotting using the LI-COR Odyssey Imager (LI-COR Lincoln, NE), an infrared fluorescence based detection system. The following primary antibodies were used for immunoblotting: LC3 (L8918), ATG3 (A3231),

p62/SQSTM1 (P0067), and alpha-Tubulin (T8203) (Sigma-Aldrich, St. Louis, MO). Acetylated-Lysine (6952), Acetyl- α -Tubulin (Lys40), FOXO1 (2880), GAPDH (2118) and Parkin (4211) (Cell Signaling, Boston, MA). Ac-FKHR (D-19), NNMT (H-68), PGC1 α (H-300) and SIRT1 (B-10) antibodies (Santa Cruz Biotechnology, Santa Cruz, CA). NDUFA9 (complex I subunit), SDHA (complex II subunit), CytoC-regulatory core protein (complex III subunit), MTCO3 (complex IV subunit) and ATP5a (complex V subunit) antibodies (Abcam, Cambridge, MA).

Carnitine palmitoyltransferase (CPT) activity measurement

Mitochondria were isolated from fresh heart tissue as previously described [22]. Mitochondria were assayed in 1 ml of reaction buffer containing 20 mM HEPES, 1 mM EGTA, 220 mM sucrose, 40 mM KCl, 0.1 mM 5,5'-dithio-bis(2-nitrobenzoic acid) (DTNB), 1.3 mg/ml BSA, and 40 μ M palmitoyl-CoA. The reaction was started by the addition of 1 mM carnitine and was monitored at 412 nm for an additional 4 min with an ultraspectral 3000 spectrophotometer. The measured CPT activity was normalized to mitochondrial protein.

Citrate synthesis (CS) activity measurement

Heart tissue was homogenized on ice in homogenization buffer containing 20 mM HEPES and 10 mM EDTA at pH 7.4. Homogenates were subjected to two freeze and thaw cycles to liberate CS from the mitochondrial matrix and then diluted 1:10 to an approximate final protein concentration of 1 μ g/ μ l. The reaction was performed in 1 ml of reaction buffer containing 20 mM HEPES, 1 mM EDTA, 220 mM sucrose, 40 mM KCl, 0.1 mM DTNB, and 0.1 mM acetyl-CoA (pH 7.4 at 25°C). The reaction was started by the addition of 0.05 mM oxaloacetate and monitored for 3 min with an ultraspectral 3000 spectrophotometer. The result was normalized to protein content [22].

Electron microscopy

Cardiac tissue samples were removed and fixed in electron microscopy (EM) fixation buffer containing 2.5% glutaraldehyde and 1% paraformaldehyde. They were processed and overserved as previously described at the University of Utah Microscopy Core [23].

Echocardiography

Mice were anesthetized with 2% isoflurane gas with an inflow rate of 1 ml/min and placed on a heated stage (37°C). Chest hair was then removed with a topical depilatory agent before the echocardiogram. Fractional shortening (in %) was calculated as $100 \times [(LVDd - LVDs)/LVDd]$, where LVDd is the LV dimension at diastole and LVDs is the LV dimension at systole [22].

Glyceraldehyde 3 Phosphate Dehydrogenase (GAPDH)

activity measurement

Heart tissue was homogenized and GAPDH activity was measured as described according to manufacturer's manual (Abcam, Cambridge, MA). NAD⁺ was added to the reaction buffer for a final concentration of 10 mM.

Histology

Myocardial fragments were stained with H&E (Thermo Scientific, Rockford, IL), Masson's trichrome (Sigma-Aldrich, St. Louis, MO) or wheat germ agglutinin (Abcam, Cambridge, MA). Stained slides were analyzed as previously described [24].

Measurement of apoptosis

Apoptosis was assessed in heart tissue using In Situ Cell Death Detection Kits (Roche, Madison, WI) following the supplier's protocol.

Mitochondrial function in saponin-permeabilized cardiac fibers

LV subendocardial muscle fibers were used to measure mitochondrial respiration rates and ATP synthesis as previously described [25]. Respiration rates were determined in the presence of substrate palmitoyl-carnitine (VO), after stimulation with 1 mM ADP (VADP), and after addition of 1 µg/ml of the ATP synthase inhibitor oligomycin (VOligo). ATP synthesis rate was measured in fibers after stimulation with 1mM ADP.

Mitochondrial oxygen consumption and glycolysis analysis

The oxygen consumption and glycolytic rate were measured in cultured H9C2 cells as described before [26]. H9C2 cells are seeded in Seahorse (Seahorse XF Analyzers, Seahorse Bioscience, North Billerica, MA) cell culture plates. The basal oxygen consumption (OCR) and extracellular acidification (ECAR) rates were measured to establish baseline rates. The cells are then metabolically perturbed by following compounds in succession: 1 µg/ml oligomycin (Sigma-Aldrich, St. Louis, MO), 0.5 µg/ml FCCP (Sigma-Aldrich, St. Louis, MO), 1 µg/ml rotenone (Sigma-Aldrich, St. Louis, MO).

NAD⁺ metabolic tracer assay

WT mice or cATG3 KO mice were intraperitoneally injected with heavy-isotope labeled nicotinamide riboside (¹³C, D double labeled NR). At 0, 30 and 60 min after heavy-isotope labeled NR i.p. administration, mice were sacrificed and hearts were harvested. NAD⁺ and its metabolites were measured using LC-MS as shown in previous studies [27].

NAD⁺ metabolite measurement

Hearts and livers from WT and cATG3 KO mice were freeze-clamped and prepared for metabolomics analysis using LC-MS as shown in our previous studies [27].

NMN administration

β -Nicotinamide mononucleotide (NMN, N3501, Sigma-Aldrich, St. Louis, MO) was prepared in PBS and injected daily and continued for 7 days. NMN solution was administered intraperitoneally to 3-week-old mice at a dosage of 500 mg/kg body weight once a day for for 7 days. PBS (pH 7.4, Thermo Scientific, Rockford, IL) was injected in controls.

Electron microscopy

Cardiac tissue samples were removed and fixed in electron microscopy (EM) fixation buffer containing 2.5% glutaraldehyde and 1% paraformaldehyde. All samples were processed and analyzed as previously described, at the University of Utah Microscopy Core [23].

Echocardiography

Mice were anesthetized with 2% isoflurane gas with an inflow rate of 1 ml/min and placed on a heated stage (37°C). Chest hair was then removed with a topical depilatory agent before the echocardiogram. Fractional shortening (in %) was calculated as $100 \times [(LVd_d - LVd_s)/LVd_d]$, where LVd_d is the LV dimension at diastole and LVd_s is the LV dimension at systole [22].

Quantitative PCR

Total RNA was extracted from H9C2 cardiomyocytes using TRIzol reagent (Invitrogen), purified with the RNeasy kit (Qiagen, Valencia, CA) and reverse transcribed. Quantitative real-time PCR was performed using SYBR Green I with ROX as an internal reference dye. The expression level was normalized to the levels of RPL13A transcript. The primer sequences used for quantitative real-time PCR are listed in Table 2.1.

Statistical analysis

Statistical analyses were performed using GraphPad Prism 6. All data are presented as mean \pm SEM. Statistical significance ($p < 0.05$) was determined by one-way ANOVA then followed by unpaired Student's t-test.

Results

cATG3 KO mice exhibited blocked autophagic flux in heart

under fed and starvation conditions

We crossed mice bearing floxed ATG3 alleles with transgenic mice expressing Cre recombinase under the control of α -myosin heavy chain promoter (α -MyHC). ATG3 flox/flox, α -MyHC-Cre- littermates were used as wild-type (WT) controls (Figure 2.1A). Compared to WT mice, cardiac-specific ATG3 KO (cATG3 KO) mice exhibited significantly reduced ATG3 protein expression in the heart (Figure 2.1B). The LC3 II/I ratio was significantly decreased in cATG3 KO mouse heart but unchanged in their liver, skeletal muscle or adipose tissue (Figure 2.1C, 2.1D). SQSTM1/p62 was highly accumulated in cATG3 KO mouse heart (Figure 2.1C), indicating inhibition of autophagic flux. After 48 h of nutrient deprivation, autophagy was dramatically increased in WT mice hearts; however, this autophagy induction following starvation was totally blunted in ATG3-deficient hearts (Figure 2.1D).

cATG3 KO mice developed cardiac contractile dysfunction

and heart failure

Echocardiogram data showed that at 4 months of age, cATG3 KO mice exhibited decreased fractional shortening compared with their WT littermates in both males and females (30.94 ± 0.90 % vs. 41.45 ± 1.44 %, $p < 0.001$; 33.21 ± 3.35 % vs. 44.90 ± 1.00 %, $p < 0.001$), suggestive of impaired cardiac contractile function (Figure 2.2A). Moreover, cATG3 KO mice exhibited reduced fractional shortening under both

fed and starvation conditions (Figure 2.2B).

We also found a 17% increase in ratio of heart weight (HW) to tibia length (BW) (7.04 ± 0.23 vs. 6.07 ± 0.16 mg/mm, $p < 0.001$) (Table 2.2). Moreover, the expression levels of atrial natriuretic peptide (ANP) and brain natriuretic peptide (BNP) were significantly increased in ATG3-deficient hearts, indicating the existence of cardiac remodeling and pathological cardiac hypertrophy (Figure 2.2C). However, histological changes, such as inflammation, fibrosis, cardiomyocytes size, or apoptosis, were absent in cATG3 KO mice heart at 4 months of age (Figure 2.2D,E).

Impaired fatty acid oxidation and increased lipid accumulation in cATG3 KO mouse hearts

As adult heart's main source of fuel, fatty acids are transported to the mitochondria to undergo β -oxidation and generate ATP. Fatty acids not used for energy production can be esterified to tri-acyl glycerol (triglyceride, TAG) to provide an intracellular pool for fatty acids storage [28]. We observed that the expression levels of fatty acid oxidation (FAO) genes were decreased by up to 40% in cATG3 KO mice heart (Figure 2.S1A), accompanied by decreased carnitine palmitoyltransferase (CPT) activity (Figure 2.S1B) and increased TAG accumulation (Figure 2.S1C). The myocardial lipid accumulation in cATG3 KO mice hearts was confirmed using oil red O staining of sections (Figure 2.S1D), suggestive of impaired fatty acid oxidation and lipid accumulation in ATG3-deficient hearts.

Mitochondrial respiration was impaired and mitochondrial content was lost in cATG3 KO mouse hearts

Since mitochondria play a critical role in maintaining cardiac function, and mitochondrial dysfunction appears to be a critical factor in causing various heart diseases, we assessed mitochondrial function using saponin-permeabilized cardiac

fibers. Fibers obtained from cATG3 KO mouse heart revealed impaired palmitoyl-carnitine supported ADP-stimulated mitochondrial oxygen consumption (VADP) and ATP production rate at 4 months old (Figure 2.3A,B). However, ATP/O ratios were not changed in cATG3 KO mice heart, suggestive of preserved mitochondrial coupling (data not shown). Citrate synthase activity, which reflects mitochondrial oxidation capacity [29], was also significantly reduced in cATG3 KO mouse heart (Figure 2.3C).

Moreover, protein expression levels of mitochondrial complexes were decreased in cATG3 KO mouse hearts (Figure 2.3D), accompanied by a trend towards reduced mitochondrial DNA copy number (data not shown). We used transmission electron microscopy (TEM) to observe the morphology and structure of mitochondria in fixed heart sections. We found more abnormal morphology or disarrayed alignment in cATG3 KO mice hearts (Figure 2.3E). Together, these data showed that mitochondrial content was reduced and function was impaired in cATG3 KO mouse heart.

We then investigated the potential mechanism by which mitochondrial content was reduced in cATG3 KO mouse heart. Since mitochondrial content is a balance between producing new mitochondria through biogenesis and clearing damaged ones through autophagy, we suspected mitochondrial biogenesis was impaired in ATG3-deficient hearts. Indeed, the expression PGC1 α , the master regulator of mitochondrial biogenesis, was downregulated in cATG3 KO mouse heart (Figure 2.3F). We also found the mRNA expression of other mitochondrial biogenesis markers, including NRF1, NRF2 and TFAM, was all decreased in ATG3-deficient heart (data not shown). Thus impaired mitochondrial biogenesis may account for mitochondrial content loss in cATG3 KO mouse heart.

Mitochondrial dysfunction precedes age-dependent cardiac

contractile dysfunction in cATG3 KO mice

We monitored cardiac function in a cohort of cATG3 KO mice and their WT littermates after birth. Cardiac dysfunction occurred in cATG3 KO mice at as early as 4 weeks old, while at 1 week and 2 weeks after birth, cardiac function in cATG3 KO mice was preserved (Figure 2.S2A). We then harvested heart tissues from 1-week-old and 4-week-old cATG3 KO mice and their WT littermates. We found reduced citrate synthesis activity and decreased mitochondrial complexes at 1-week-old cATG3 KO mice, when cardiac function is normal (Figure 2.S2B,C), suggesting mitochondrial dysfunction precedes heart failure in cATG3 KO mice.

Moreover, we conducted metabolomics analysis for metabolic intermediates in 1-week-old and 4-week-old mouse heart samples. Most of the tricarboxylic acid (TCA) cycle intermediates, including succinic acid and malic acid, were significantly reduced in cATG3 KO mice heart at 1 week old (Figure 2.S2D). These results indicate metabolic flux to TCA was partially blocked in 1-week-old ATG3-deficient heart, suggestive of inhibited mitochondrial function.

Blocked glycolytic flux and decreased GAPDH activity

in ATG3-deficient hearts

We further investigated the mechanism by which autophagy modulates mitochondrial function guided by the data generated from metabolomics. We first measured amino acid concentrations in cardiac extracts in 1-week-old and 4-week-old mice. Contrary to the previously reported findings in livers, we did not observe any change in amino acid levels from cATG3 KO mouse heart at 1 week and 4 weeks of age (Table 2.3). Surprisingly, we found the glucose metabolism was dramatically altered in cATG3 KO mouse heart at 1 week and 4 weeks old. For example, when

compared to age-matched WT control mouse heart, there was a two-fold increase in glucose-6-phosphate in 1-week-old and five-fold increase in 4-week-old ATG3-deficient heart. The accumulation of glycolytic intermediates suggests the existence of a switch in substrate utilization for energy production in ATG3-deficient hearts, with a preference for glucose rather than fatty acid [30]. More interestingly, we noticed that the accumulated glycolytic intermediates were over-represented by those in the early stages of glycolysis, whereas downstream intermediates were unchanged or even reduced (Figure 2.S3).

To further investigate the mechanism by which glycolytic pathway was blocked in ATG3-deficient heart, we found the glycolysis was blocked in the step catalyzed by Glyceraldehyde 3-phosphate dehydrogenase (GAPDH). GAPDH is an NAD-dependent enzyme that catalyzes the sixth step of glycolysis [31], and inhibited GAPDH activity could reduce glycolytic flux and lead to accumulation of early stage intermediates. Indeed, we found that GAPDH activity in cATG3 KO mice hearts were significantly decreased (Figure 2.S4A) without any changes in expression level (Figure 2.S4B). Supplying exogenous NAD⁺ (10mM) was sufficient to normalize GAPDH activity in ATG3-deficient hearts (Figure 2.S4A), suggesting that NAD⁺ depletion might account for the inhibited GAPDH activity and impaired glycolytic flux in cATG3 KO mice hearts. Moreover, we also demonstrated that total protein acetylation in cATG3 KO mice heart was increased (Figure 2.S4C). This difference was unlikely due to the increased acetyl-CoA levels, since there was a trend towards decreased acetyl-CoA in cATG3 KO mice hearts (Figure 2.S4D). Sirtuins (SIRT) are a class of proteins that possess deacetylase activity that regulate various metabolic processes in a NAD⁺-dependent manner [32]. Two of the known downstream acetylated target proteins of SIRT1, FOXO1 and PGC1 α [33], were hyperacetylated in cATG3 KO mice hearts compared to WT controls (Figure 2.S4E,F), suggestive of decreased SIRT1 activity in

ATG3-deficient hearts.

Altered NAD⁺ metabolic flux in cATG3 KO mouse hearts

Based on the observation of decreased GAPDH activity and increased protein acetylation in cATG3 KO mouse hearts, we hypothesized that NAD⁺ metabolism may be altered in cATG3 KO mouse hearts. We therefore measured NAD⁺ and its metabolites under basal conditions or after 7 days of nicotinamide riboside (NR) treatment. Although cATG3 KO mice exhibited unchanged NAD⁺ content in the heart under basal conditions, they showed significantly lower cardiac NAD⁺ levels following NR supplementation, suggestive of altered NAD⁺ metabolic rate (Figure 2.4A).

Besides NAD⁺, cATG3 KO mice also exhibited reduced NAD⁺ related metabolites, including nicotinamide acid mononucleotide (NAMN), nicotinic acid riboside (NAR), nicotinamide adenine dinucleotide (NAAD), nicotinamide mononucleotide (NMN) and nicotinamide (NAM) after NR administration (Table 2.4). On the contrary, NAD⁺ degradation products, including methylated-nicotinamide (MeNAM), Me-4PY and Me-2PY (Figure 2.4B), showed a trend towards increase in cATG3 KO mouse hearts after NR administration.

To further investigate NAD⁺ metabolism in cATG3 KO mouse hearts, we used isotope-labeled NR to determine NAD⁺ metabolic flux (Figure 2.4C). Consistent with our earlier findings in NR administration, ATG3-deficient hearts exhibited significantly lower NAD⁺ and NAM enrichment, but higher MeNAM enrichment (Figure 2.4D,E). These findings are consistent with the hypothesis that NAD degradation was accelerated in cATG3 KO mouse heart. We also measured the mRNA expression of NAD⁺ related enzymes, and found that NRK1, NAMPT, NMNAT3 and NNMT were significantly induced in cATG3 KO mouse hearts (Figure 2.4F), indicating increased NAD⁺ synthesis and degradation in ATG3-deficient heart.

Induced NNMT when autophagy inhibited in cardiomyocytes

Nicotinamide N-Methyltransferase (NNMT) is the enzyme for converting NAM to MeNAM in NAD⁺ metabolism [34]. Since we observed increased MeNAM production following NR administration and more labeled MeNAM enrichment in cATG3 KO mouse heart (Figure 2.S5B,E), we hypothesized NNMT might be induced in ATG3-deficient heart, which may contribute to altered NAD⁺ metabolism and affects cardiac function.

Indeed, we found that NNMT protein levels were increased in cATG3 KO mouse hearts relative to WT mouse hearts (Figure 2.S5A). In addition to mice with constitutive cATG3 KO, we also generated inducible cardiac-specific ATG3 KO mice using a tamoxifen-inducible Mer-Cre-Mer cardiomyocyte-restricted transgene [35]. In cardiac inducible ATG3 knockout (CIATG3 KO) mice, we found decreased ATG3 expression and autophagy inhibition 1 week after tamoxifen injection (Figure 2.S5B). Interestingly, although cardiac function was preserved at this time point (data not shown), CIATG3 KO mice exhibited significantly increased NNMT expression in their hearts (Figure 2.S5B), suggesting that NNMT accumulation may be an early event before heart failure in autophagy-deficient hearts.

To further study whether NNMT induction is directly mediated by an ATG3 dependent pathway or is secondary to the change in autophagy, we applied pharmacological approaches to inhibit autophagic flux in the heart using colchicine (Col) and chloroquine (CQ) respectively [36] [37]. Blocked autophagic flux with Col or CQ in WT mice led to NNMT accumulation in the hearts relative to PBS treated controls (Figure 2.S5C,D). With ATG3 gene knockdown, autophagy was inhibited and NNMT protein expression was induced (Figure 2.S5E). Similarly, blocking autophagy by ATG5 knockdown also increased NNMT expression in H9C2 cells (Figure 2.S5F).

NNMT overexpression caused NAD⁺ depletion and repressed mitochondrial respiration in cardiomyocytes

Our data indicated that autophagy inhibition may precipitate NNMT accumulation in cardiomyocytes. To further elucidate the role of NNMT in cardiomyocytes, we overexpressed NNMT in H9C2 cells using an adenovirus vector harboring NNMT cDNA and used ad-GFP as control. Compared to ad-GFP controls, following NNMT overexpression in H9C2 cells (Figure 2.5A), cellular NAD⁺ and nicotinamide (NAM) levels were both significantly reduced, and the NAD⁺ metabolite MeNAM was highly accumulated (Figure 2.5B).

Since NNMT is specifically localized in the mitochondrial fraction of hearts and H9C2 cells (Figure 2.5C), we hypothesized that NNMT induction exerts some effects on mitochondrial function. Indeed, NNMT overexpression impaired mitochondrial respiration under both basal and FCCP-stimulated conditions (Figure 2.5D).

NNMT inhibition normalized mitochondrial dysfunction in the autophagy deficient cardiomyocytes

ATG3 silencing inhibited autophagy and reduced mitochondrial respiration in cultured H9C2 cells (Figure 2.S5E, Figure 2.6A). Interestingly, we observed that NNMT silencing was sufficient to rescue mitochondrial dysfunction in ATG3 knockdown cells (Figure 2.6B,C), suggesting that the adverse effect of ATG3 deletion in mitochondrial function may be NNMT dependent.

Similarly, CQ, the autophagy inhibitor, reduced autophagic flux and increased NNMT protein expression in cultured H9C2 cells (Figure 2.6D). Consistent with the NNMT accumulation, CQ treatment led to NAM depletion and MeNAM accumulation in H9C2 cells, suggestive of increased NNMT activity in CQ-treated cells (Figure 2.6E). Allosteric inhibition of NNMT activity by its end product MeNAM rescued CQ-induced

mitochondrial dysfunction in H9C2 cells (Figure 2.6F). These data revealed that mitochondrial dysfunction in autophagy deficient cells might be through NNMT dependent manner.

NMN increased cardiac NAD⁺ content and restored cardiac contractile function in cATG3 KO mice

Nicotinamide mononucleotide (NMN) is an intermediate of the NAD⁺ biosynthesis pathway and is found to be protective in hearts by increasing cardiac NAD⁺ content [13, 16]. After 7 days of NMN i.p. injection, the autophagy defect in cATG3 KO mouse hearts was unchanged (Figure 2.7A). However, NAD⁺ and its metabolites, including NADH, NADP⁺ and NADPH, were also significantly increased in WT and cATG3 KO mouse hearts (Figure 2.7B). Consistent with increased NAD⁺ content following NMN administration, NMN normalized protein hyperacetylation of FOXO1 in cATG3 KO mice hearts (Figure 2.7C). Citrate synthesis activity was also restored in cATG3 KO mouse hearts, suggestive of improved mitochondrial function (Figure 2.7D). Importantly, cardiac dysfunction in cATG3 KO mice was completely rescued after NMN supplementation (Figure 2.7E).

The mitochondrial biogenesis defect was not rescued by NMN treatment in cATG3 KO mice heart. Instead, NMN reduced mitochondrial biogenesis in both WT and cATG3 KO mice hearts, as evidenced by reduced mtDNA copy number, suggesting NMN may have adverse effect on mitochondrial biogenesis in the heart (Figure 2.7F,G).

Discussion

The present study revealed an essential role of autophagy in maintaining cardiac function by generating cardiac-specific ATG3 deficient mice. We compared bioenergetics of hearts in cATG3 KO mice and WT mice. We found that cATG3-deficient hearts showed decreased mitochondrial oxygen consumption and energy

production. Moreover, we demonstrated that mitochondrial dysfunction precipitated by ATG3 deletion precedes cardiac contractile dysfunction, suggesting a critical role for mitochondrial dysfunction in heart failure development in this model. We also found that when ATG3 was deleted *in vitro*, mitochondria in cardiomyocytes became dysfunctional, characterized by decreased oxygen consumption rate, suggesting that autophagy may modulate mitochondrial function in a cell-autonomous manner. This is consistent with earlier findings in ATG7 KO MEFs, which exhibited reduced oxygen consumption rate relative to WT MEFs [38]. Our *in vivo* and *in vitro* data further confirm that autophagy deficiency impairs mitochondrial function in cardiomyocytes.

It is widely accepted that autophagy might play a role in mitochondrial function maintenance [19], but the exact mechanism is still unclear. One proposed mechanism is that autophagy may function to clear dysfunctional mitochondria to maintain its quality. In the previously generated ATG5 KO mice, ATG5-deficient hearts showed disorganized sarcomeric structure and mitochondrial alignment both in adult and developing hearts [3] [4]. We indeed found that ATG3-deficient hearts showed abnormal mitochondrial morphology and reduced mitochondrial content, which may contribute to the decreased mitochondrial function.

There is a change in the cardiac metabolic substrate preference from carbohydrates to fatty acids during the perinatal period, but the mechanism of this transition are incompletely understood. Interestingly, our studies revealed that cATG3-deficient hearts exhibited impaired mitochondrial biogenesis and altered substrate preference since the age of 1 week. Autophagy is thought to be involved in mitochondrial quality control by clearing damaged mitochondria through lysosomal pathways, but its role in regulating mitochondrial biogenesis is incompletely understood. Here, for the first time we demonstrate that intact autophagy could be a prerequisite for mitochondrial biogenesis in neonatal and adult hearts.

There is a burst of mitochondrial biogenesis gene induction, such as PGC1 α , NRF1 and NRF2, in the heart after birth, which may mediate the metabolic switch from glucose to fatty acids as the predominant energy substrate in the maturing heart [39]. We also observed impaired mitochondrial substrate metabolism and accumulation of glucose metabolites in heart tissue, suggesting that ATG3-deficient hearts could be more reliant on glucose as its main substrate, potentially as a consequence of impaired mitochondrial biogenesis. Consistent with our study, a recent study found mitophagy defective hearts showed a similar inhibition in metabolic transition in perinatal hearts, characterized by reduced mitochondrial biogenesis and impaired fatty acid metabolism [40]. Thus autophagy may play an essential in promoting mitochondrial biogenesis and regulating metabolic switch process in perinatal hearts.

Importantly, our results revealed that autophagy is involved in the regulation of NAD⁺ metabolism in cardiomyocytes. NAD⁺ functions as the most important electron carrier used in oxidative phosphorylation for cardiac fuel supply [41], and impaired myocardial NAD⁺ metabolism has been implicated in cardiomyopathy [42] [13]. Our findings revealed that, although the NAD⁺ level was not depleted, NAD⁺ metabolic flux was increased in ATG3-deficient heart, which is also accompanied by increased protein acetylation. In failing cardiac tissue from heart failure patients, there were increased levels of acetylated mitochondrial proteins. Moreover, elevated levels of mitochondrial protein acetylation were detected at the earliest stages of heart failure in animal models [43]. Therefore, it is important to illustrate how protein hyperacetylation contributes to heart failure in our model in future studies.

Sirtuin (SIRT) family may connect NAD⁺ homeostasis to protein acetylation and mitochondrial function in the heart. Among seven sirtuins family proteins, SIRT1 is a NAD-dependent deacetylase that removes acetyl groups from various proteins, and promotes mitochondrial biogenesis by deacetylation of PGC1 α in various tissues [44].

Thus we hypothesized that ATG3-deficient hearts may exhibit impaired mitochondrial biogenesis in a NAD⁺-SIRT1 dependent manner. For this reason, we supplemented cATG3 KO mice with NMN, a precursor of NAD⁺ in the heart [13]. Although NAD⁺ content was increased and Foxo1 hyperacetylation normalized in ATG3-deficient hearts, which could be expected to be associated with improved SIRT1 activity, we did not observe a rescue of the mitochondrial biogenesis defect in ATG3-deficient hearts. Indeed, we found that NMN decreased mitochondrial biogenesis and reduced mitochondrial content in WT mice hearts. These results are consistent with a recent finding that SIRT1 overexpression in rat triceps muscle resulted in impaired mitochondrial biogenesis and decreased expression of mitochondrial proteins, rather than their expected improvement of mitochondrial biogenesis [45]. The detailed mechanism is still unclear so far, but these results, at least, might lead to a re-examination of the role of NAD⁺ and SIRT1 in mitochondrial biogenesis in the heart.

Nicotinamide N-methyltransferase (NNMT) is the enzyme that converts nicotinamide (NAM) to 1-methyl-nicotinamide (MeNAM), which is further degraded and cleared from tissues [46] [47]. NNMT expression levels are altered in various disease conditions, for example, NNMT is increased in lung cells with non-small lung cancer [48], in neurons in Parkinson's diseases [49], as well as in adipocytes in subjects with obesity and type 2 diabetes s [50], [51]. We observed NNMT mRNA and protein expression levels were induced in ATG3-deficient hearts as well as in the hearts of mice in which autophagy was inhibited. We also independently observed this in other autophagy deficient animal models, such as cardiac-specific inducible ATG3 KO mice and following colchicine and chloroquine treatment [52]. These results indicate that NNMT induction might be a common response to autophagy inhibition in cardiomyocytes. But the molecular mechanism by which NNMT induction in autophagy deficient cells is still unclear. Interestingly, mRNA expression level of NNMT was also

significantly increased in ATG3 SiRNA treated or CQ-treated H9C2 cells (data not shown), indicating NNMT induction by autophagy inhibition may be in transcriptional level. These results were consistent with the previous finding in type 2 diabetic animal models, where NNMT mRNA was upregulated in liver and adipose tissue. In future studies, NNMT promoter reporter construct may facilitate the screen of potential transcriptional factors which connects NNMT transcription and autophagy.

We then investigated the role of NNMT in the regulation of cardiomyocyte metabolism. Earlier studies observed that NNMT knockdown increased NAD^+ content and oxygen consumption in rat adipocytes [53], but its role in cardiomyocytes was not previously studied. When NNMT was overexpressed in cultured cardiomyocytes, we found that NNMT overexpression caused cellular NAD^+ pool depletion and increased cellular nicotinamide methylation and clearance. Importantly, we identified NNMT as a mitochondria-localized protein. NNMT overexpression impaired mitochondrial respiration and led to a switch from mitochondrial respiration to glycolysis in cultured cardiomyocytes. This metabolic switch is consistent with our *in vivo* observations in cATG3 KO mouse hearts. It raised the possibility that NNMT induction in autophagy-deficient cardiomyocytes may contribute to impaired mitochondrial respiration leading to a metabolic switch towards glycolysis as the predominant fuel supply in these cardiomyocytes.

The detailed mechanism by which NNMT modulates mitochondrial function is incompletely understood. In a recent study, supplementation of high-fat diet with NNMT inhibitor MeNAM decreased serum and liver cholesterol and liver triglyceride levels in mice [20], suggesting the involvement of NNMT in metabolic diseases, but the role of NNMT in mitochondria was never investigated before. With NNMT knockdown or using the NNMT inhibitor MeNAM, we were able to blunt the adverse effect on mitochondrial function caused by ATG3 knockdown or CQ treatment in cultured cardiomyocytes.

These results suggest that NNMT induction may contribute importantly to mitochondrial dysfunction when autophagy is inhibited.

Here we describe a novel NAD⁺ regulation pathway by autophagy. Under nutrient starvation, autophagy is induced as a well-known stress response to degrade proteins and organelles to provide energy. In addition to this well-established role, increased autophagy also enhanced cellular NAD⁺ content by downregulating NNMT expression and preventing NAD⁺ degradation. This altered NAD⁺ metabolism may trigger certain biological signaling and function as a cellular survival mechanism when nutrient is deprived.

Finally, we replenished cardiac NAD⁺ levels using its precursor NMN, and we found that mitochondrial dysfunction and cardiac contractile dysfunction were completely rescued in cATG3 KO mice hearts, suggesting that altered NAD⁺ metabolism could be an important cause of heart failure in ATG3-deficient hearts. Although mitochondrial function was improved after NMN treatment, the defect in mitochondrial biogenesis in cATG3 KO mice hearts was not prevented. It is likely that a mechanism other than NAD⁺ might be responsible for the link between autophagy and mitochondrial biogenesis in the heart. In summary, our results showed that ATG3 deletion in the heart impaired cardiac autophagy, which induced NNMT and increased NAD⁺ catabolism. As a consequence, cardiac mitochondria became dysfunctional and cardiac contractile function was impaired. These results render NNMT and NAD⁺ flux a potential targets for modulating cardiac dysfunction that is mediated by impaired autophagy.

References

1. Mizushima, N. and B. Levine, Autophagy in mammalian development and differentiation. *Nat Cell Biol*, 2010. 12(9): p. 823-30.
2. Cao, D.J., T.G. Gillette, and J.A. Hill, Cardiomyocyte autophagy: remodeling, repairing, and reconstructing the heart. *Curr Hypertens Rep*, 2009. 11(6): p. 406-11.
3. Nakai, A., et al., The role of autophagy in cardiomyocytes in the basal state and in response to hemodynamic stress. *Nat Med*, 2007. 13(5): p. 619-24.
4. Taneike, M., et al., Inhibition of autophagy in the heart induces age-related cardiomyopathy. *Autophagy*, 2010. 6(5): p. 600-6.
5. Chiarugi, A., et al., The NAD metabolome--a key determinant of cancer cell biology. *Nat Rev Cancer*, 2012. 12(11): p. 741-52.
6. Pittelli, M., et al., Pharmacological effects of exogenous NAD on mitochondrial bioenergetics, DNA repair, and apoptosis. *Mol Pharmacol*, 2011. 80(6): p. 1136-46.
7. Koch-Nolte, F., et al., Emerging roles of NAD⁺ and its metabolites in cell signaling. *Sci Signal*, 2009. 2(57): p. mr1.
8. Ziegler, M., New functions of a long-known molecule. Emerging roles of NAD in cellular signaling. *Eur J Biochem*, 2000. 267(6): p. 1550-64.
9. Mouchiroud, L., et al., The NAD(+)/Sirtuin pathway modulates longevity through activation of mitochondrial UPR and FOXO signaling. *Cell*, 2013. 154(2): p. 430-41.
10. Mouchiroud, L., R.H. Houtkooper, and J. Auwerx, NAD(+) metabolism: a therapeutic target for age-related metabolic disease. *Crit Rev Biochem Mol Biol*, 2013. 48(4): p. 397-408.
11. Yoshino, J., et al., Nicotinamide mononucleotide, a key NAD(+) intermediate, treats the pathophysiology of diet- and age-induced diabetes in mice. *Cell Metab*, 2011. 14(4): p. 528-36.
12. Burgos, E.S., NAMPT in regulated NAD biosynthesis and its pivotal role in human metabolism. *Curr Med Chem*, 2011. 18(13): p. 1947-61.
13. Yamamoto, T., et al., Nicotinamide mononucleotide, an intermediate of NAD⁺ synthesis, protects the heart from ischemia and reperfusion. *PLoS One*, 2014. 9(6): p. e98972.
14. Wang, P., et al., NAMPT and NAMPT-controlled NAD metabolism in vascular repair. *J Cardiovasc Pharmacol*, 2015.
15. Wang, X., et al., Discovery of novel inhibitors and fluorescent probe targeting NAMPT. *Sci Rep*, 2015. 5: p. 12657.

16. Karamanlidis, G., et al., Mitochondrial complex I deficiency increases protein acetylation and accelerates heart failure. *Cell Metab*, 2013. 18(2): p. 239-50.
17. Sou, Y.S., et al., The Atg8 conjugation system is indispensable for proper development of autophagic isolation membranes in mice. *Mol Biol Cell*, 2008. 19(11): p. 4762-75.
18. Radoshevich, L. and J. Debnath, ATG12-ATG3 and mitochondria. *Autophagy*, 2011. 7(1): p. 109-11.
19. Lee, J., S. Giordano, and J. Zhang, Autophagy, mitochondria and oxidative stress: cross-talk and redox signalling. *Biochem J*, 2012. 441(2): p. 523-40.
20. Hong, S., et al., Nicotinamide N-methyltransferase regulates hepatic nutrient metabolism through Sirt1 protein stabilization. *Nat Med*, 2015. 21(8): p. 887-94.
21. Zhu, Y., et al., Mechanistic target of rapamycin (Mtor) is essential for murine embryonic heart development and growth. *PLoS One*, 2013. 8(1): p. e54221.
22. Riehle, C., et al., PGC-1beta deficiency accelerates the transition to heart failure in pressure overload hypertrophy. *Circ Res*, 2011. 109(7): p. 783-93.
23. Boudina, S., et al., Mitochondrial energetics in the heart in obesity-related diabetes: direct evidence for increased uncoupled respiration and activation of uncoupling proteins. *Diabetes*, 2007. 56(10): p. 2457-66.
24. Mandarim-de-Lacerda, C.A., Stereological tools in biomedical research. *An Acad Bras Cienc*, 2003. 75(4): p. 469-86.
25. Boudina, S., et al., Reduced mitochondrial oxidative capacity and increased mitochondrial uncoupling impair myocardial energetics in obesity. *Circulation*, 2005. 112(17): p. 2686-95.
26. Dott, W., et al., Modulation of mitochondrial bioenergetics in a skeletal muscle cell line model of mitochondrial toxicity. *Redox Biol*, 2014. 2: p. 224-33.
27. Trammell, S.A. and C. Brenner, Targeted, LCMS-based metabolomics for quantitative measurement of NAD⁺ metabolites. *Comput Struct Biotechnol J*, 2013. 4: p. e201301012.
28. Ruberg, F.L., Myocardial lipid accumulation in the diabetic heart. *Circulation*, 2007. 116(10): p. 1110-2.
29. Larsen, S., et al., Biomarkers of mitochondrial content in skeletal muscle of healthy young human subjects. *J Physiol*, 2012. 590(Pt 14): p. 3349-60.
30. Zhou, L., et al., Regulation of myocardial substrate metabolism during increased energy expenditure: insights from computational studies. *Am J Physiol Heart Circ Physiol*, 2006. 291(3): p. H1036-46.
31. Knight, R.J., et al., Inhibition of glyceraldehyde-3-phosphate dehydrogenase in post-ischaemic myocardium. *Cardiovasc Res*, 1996. 32(6): p. 1016-23.

32. Hall, J.A., et al., The sirtuin family's role in aging and age-associated pathologies. *J Clin Invest*, 2013. 123(3): p. 973-9.
33. Canto, C. and J. Auwerx, Targeting sirtuin 1 to improve metabolism: all you need is NAD(+)? *Pharmacol Rev*, 2012. 64(1): p. 166-87.
34. Brenner, C., Metabolism: Targeting a fat-accumulation gene. *Nature*, 2014. 508(7495): p. 194-5.
35. Sohal, D.S., et al., Temporally regulated and tissue-specific gene manipulations in the adult and embryonic heart using a tamoxifen-inducible Cre protein. *Circ Res*, 2001. 89(1): p. 20-5.
36. Xiao, Y., et al., Suppressed autophagy flux in skeletal muscle of an amyotrophic lateral sclerosis mouse model during disease progression. *Physiol Rep*, 2015. 3(1).
37. Perry, C.N., et al., Novel methods for measuring cardiac autophagy in vivo. *Methods Enzymol*, 2009. 453: p. 325-42.
38. Wu, J.J., et al., Mitochondrial dysfunction and oxidative stress mediate the physiological impairment induced by the disruption of autophagy. *Aging (Albany NY)*, 2009. 1(4): p. 425-37.
39. Wang, P., et al., Peroxisome proliferator-activated receptor δ is an essential transcriptional regulator for mitochondrial protection and biogenesis in adult heart. *Circ Res*, 2010. 106(5): p. 911-9.
40. Gong, G., et al., Parkin-mediated mitophagy directs perinatal cardiac metabolic maturation in mice. *Science*, 2015. 350(6265): p. aad2459.
41. Ferro, A.M. and E. Kun, Macromolecular derivatives of NAD⁺ in heart nuclei: poly adenosine diphosphoribose and adenosine diphosphoribose proteins. *Biochem Biophys Res Commun*, 1976. 71(1): p. 150-4.
42. Yano, M., et al., Monocyte-derived extracellular Nampt-dependent biosynthesis of NAD(+) protects the heart against pressure overload. *Sci Rep*, 2015. 5: p. 15857.
43. Horton, J.L., et al., Mitochondrial protein hyperacetylation in the failing heart. *JCI Insight*, 2016. 2(1).
44. Rahman, S. and R. Islam, Mammalian Sirt1: insights on its biological functions. *Cell Commun Signal*, 2011. 9: p. 11.
45. Higashida, K., et al., Effects of resveratrol and SIRT1 on PGC-1 α activity and mitochondrial biogenesis: a reevaluation. *PLoS Biol*, 2013. 11(7): p. e1001603.
46. Zhou, S.S., D. Li, and Y. Zhou, Management of nicotinamide N-methyltransferase overexpression: inhibit the enzyme or reduce nicotinamide intake? *Diabetologia*, 2015. 58(9): p. 2191-2.

47. Kannt, A., et al., Management of nicotinamide N-methyltransferase overexpression: inhibit the enzyme or reduce nicotinamide intake? Reply to Zhou S, Li D, Zhou Y [letter]. *Diabetologia*, 2015. 58(9): p. 2193-4.
48. Sartini, D., et al., Nicotinamide N-methyltransferase in non-small cell lung cancer: promising results for targeted anti-cancer therapy. *Cell Biochem Biophys*, 2013. 67(3): p. 865-73.
49. Williams, A.C., L.S. Cartwright, and D.B. Ramsden, Parkinson's disease: the first common neurological disease due to auto-intoxication? *QJM*, 2005. 98(3): p. 215-26.
50. Lee, Y.H., et al., Microarray profiling of isolated abdominal subcutaneous adipocytes from obese vs non-obese Pima Indians: increased expression of inflammation-related genes. *Diabetologia*, 2005. 48(9): p. 1776-83.
51. Salek, R.M., et al., A metabolomic comparison of urinary changes in type 2 diabetes in mouse, rat, and human. *Physiol Genomics*, 2007. 29(2): p. 99-108.
52. Ju, J.S., et al., Quantitation of "autophagic flux" in mature skeletal muscle. *Autophagy*, 2010. 6(7): p. 929-35.
53. Kraus, D., et al., Nicotinamide N-methyltransferase knockdown protects against diet-induced obesity. *Nature*, 2014. 508(7495): p. 258-62.

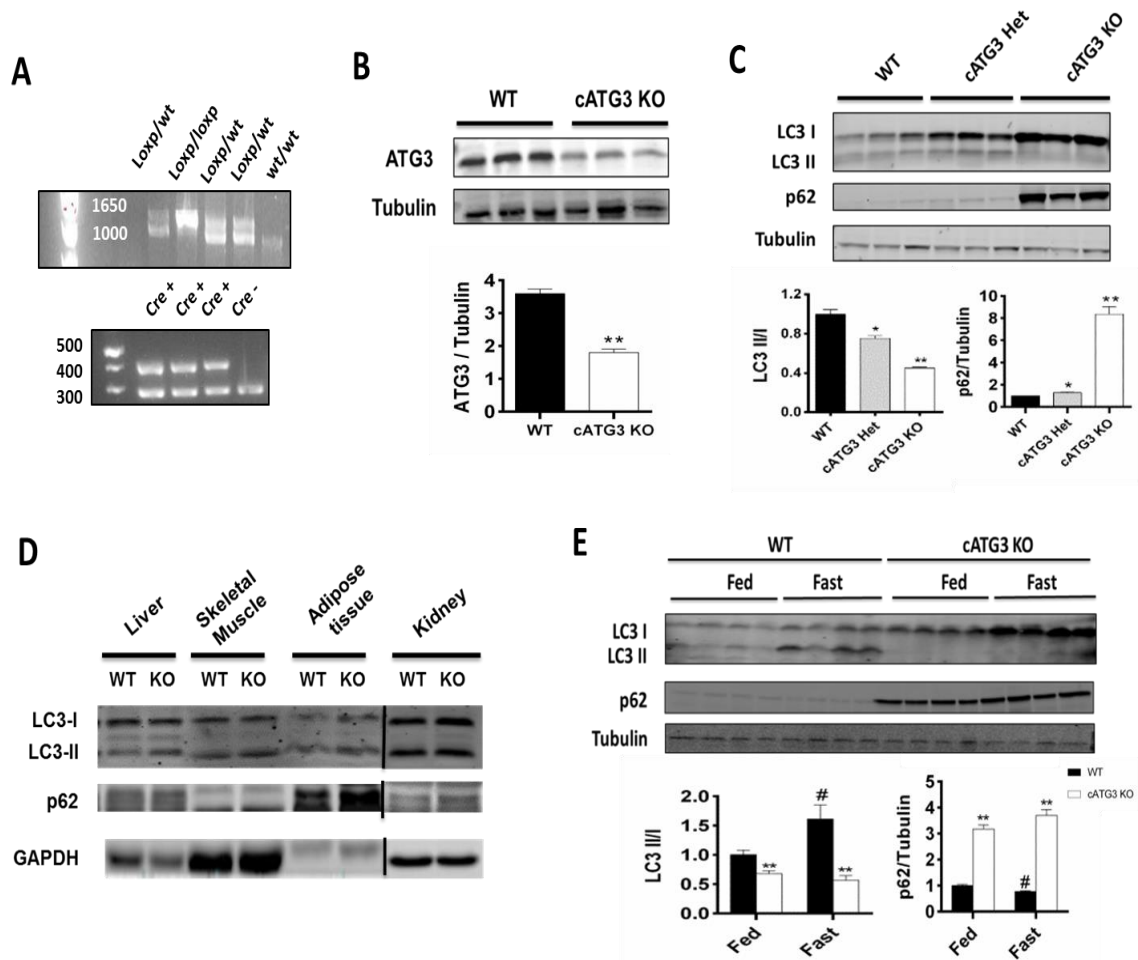


Figure 2.1 Cardiac specific ATG3 deletion blocks autophagic flux in 4-month-old mouse hearts. (A) Genotyping of ATG3 flox/flox and alpha-MHC CRE. (B) ATG3 protein content in whole heart lysates from WT and cATG3 KO mice, n=3. (C) LC3 and p62 protein content in WT, cATG3 heterozygous and cATG3 KO hearts, n=3. (D) LC3 and p62 protein content in liver, skeletal muscle, adipose tissue and kidney from WT and cATG3 KO mice, n=2. (E) LC3 and p62 levels were measured in WT and ATG3-deficient heart under random-fed conditions or after 48 h starvation, n=4. **p<0.01, *p<0.05 when compared to WT.

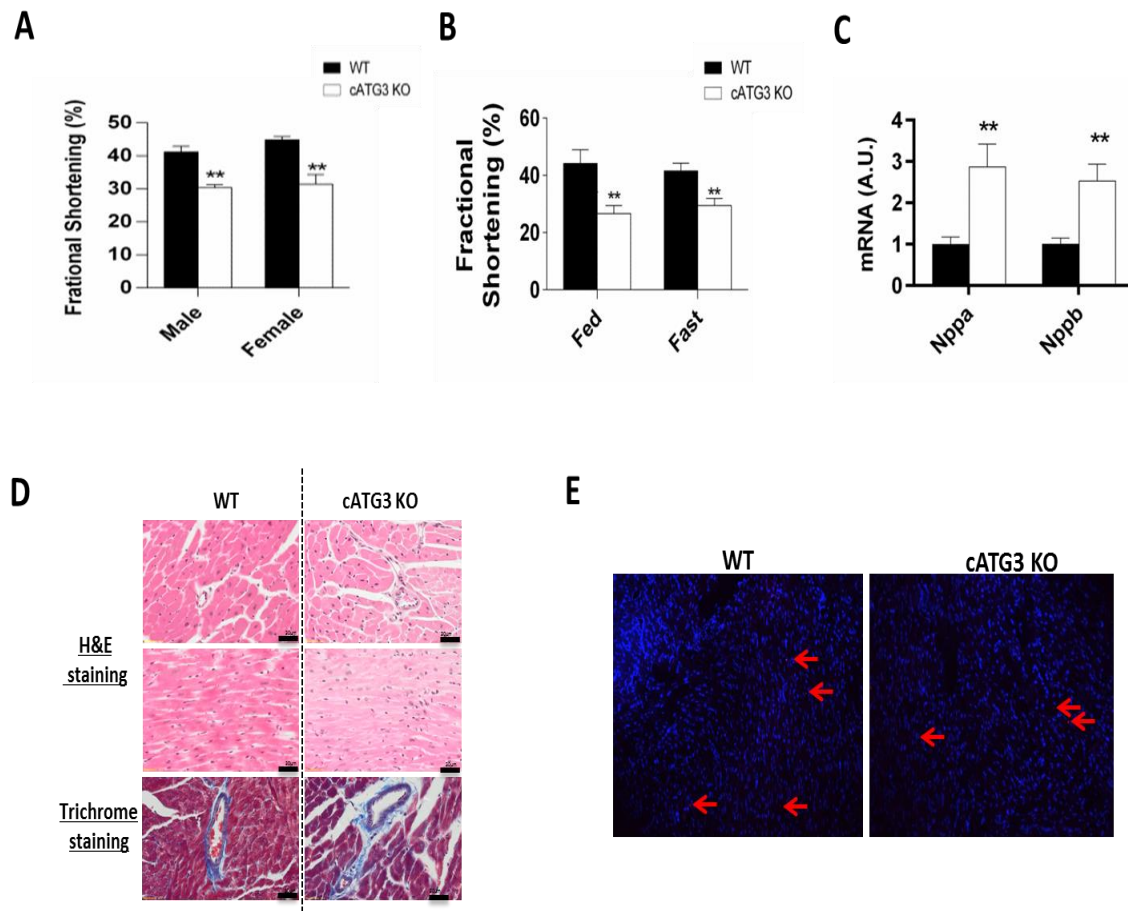


Figure 2.2 cATG3 KO developed cardiac contractile dysfunction in the absence of histological changes at 4 months old. (A) Fractional shortening in WT and cATG3 KO male and female mice measured by echocardiography under anesthesia with isoflurane, n=6-8. (B) Fractional shortening in WT and cATG3 KO mice under random-fed conditions or after 48 hours starvation, n=4. (C) ANP and BNP mRNA expression levels in WT and ATG3-deficient hearts, n=6. (D) Representative H&E staining and trichrome staining in WT mice and cATG3 KO mice hearts, n=3. (E) Representative TUNEL staining in WT and ATG3-deficient hearts, n=3. **p<0.01 when compared to WT.

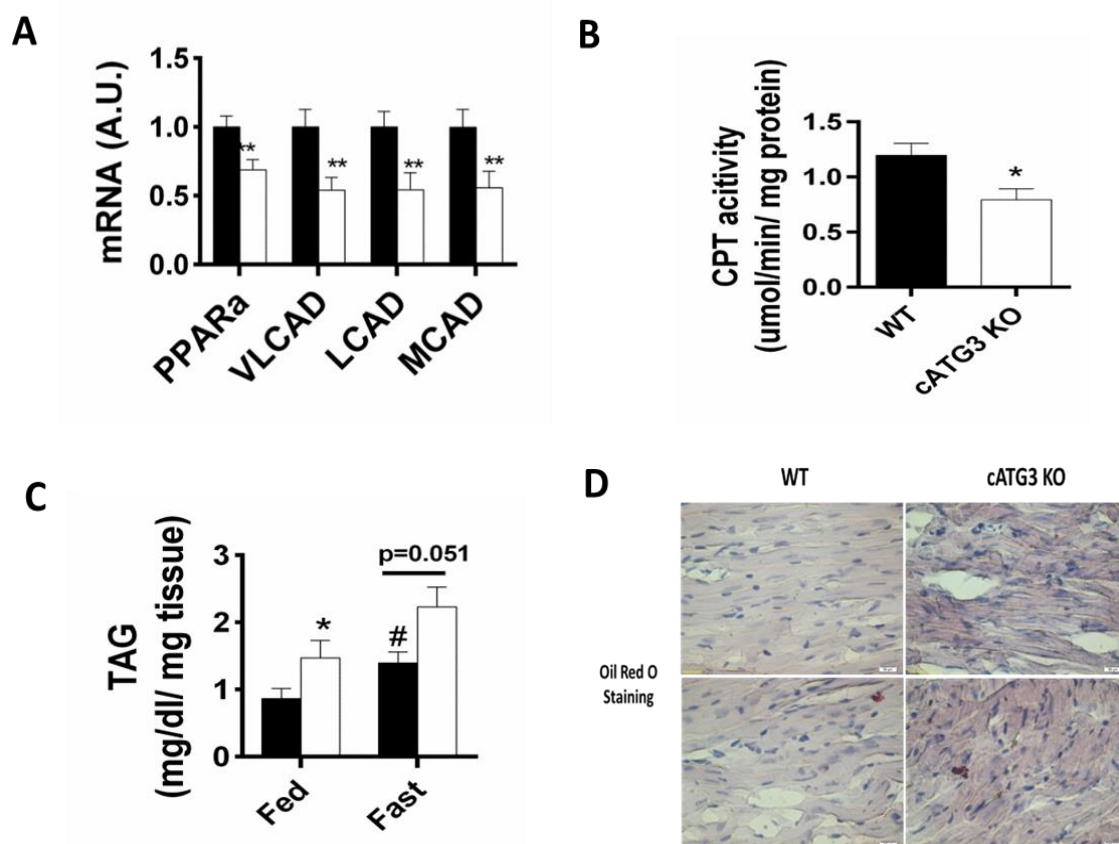


Figure 2.S1 Fatty acid oxidation was repressed in 4-month-old ATG3-deficient hearts. (A) mRNA levels of transcripts encoding fatty acid beta oxidation proteins in WT and ATG3-deficient hearts, n=6. (B) Carnitine palmitoyltransferase (CPT) activity was determined in isolated cardiac mitochondria from WT and cATG3 KO mice, n=6. (C) Triglyceride levels were measured in WT and ATG3-deficient hearts under random-fed conditions or after 48 hours of starvation, n=4. (D) Representative oil red O staining of frozen sections from WT and cATG3 KO mice hearts, n=3. **p<0.01, *p<0.05 versus WT. #p<0.05 versus random fed group.

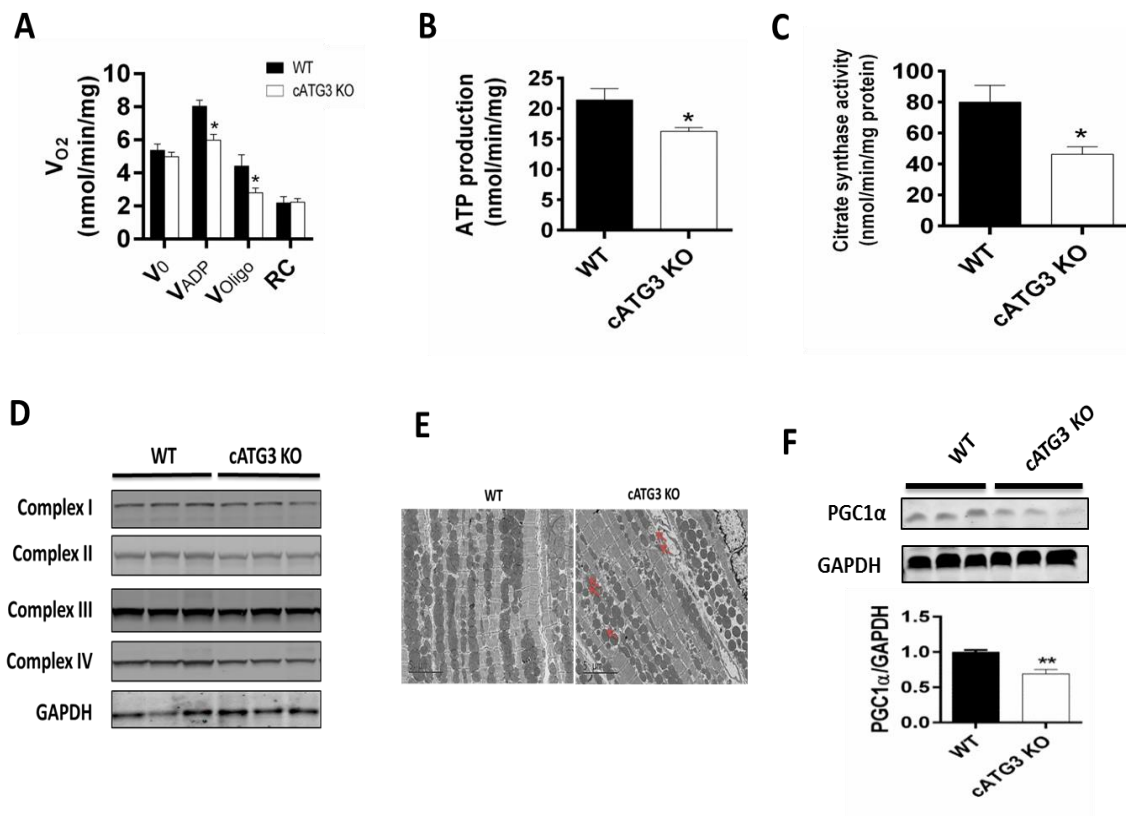


Figure 2.3 Mitochondrial function was decreased in 4-month-old ATG3-deficient hearts. (A) Oxygen consumption rate was measured in WT and cATG3 KO mouse hearts fibers, n=6. (B) ATP production rate was measured in cardiac fibers following stimulation with ADP, n=6. (C) Citrate synthase activity was measured in WT and cATG3 KO mice hearts, n=6. (D) Mitochondrial electron transport complex expression in WT and ATG3-deficient heart, n=3. (E) Mitochondrial morphology and structure in WT and ATG-deficient heart sections by transmission electron microscopy, n=5. (F) PGC-1 α protein levels in WT and cATG3 KO mice hearts, n=3. **p<0.01, *p<0.05 when compared to WT.

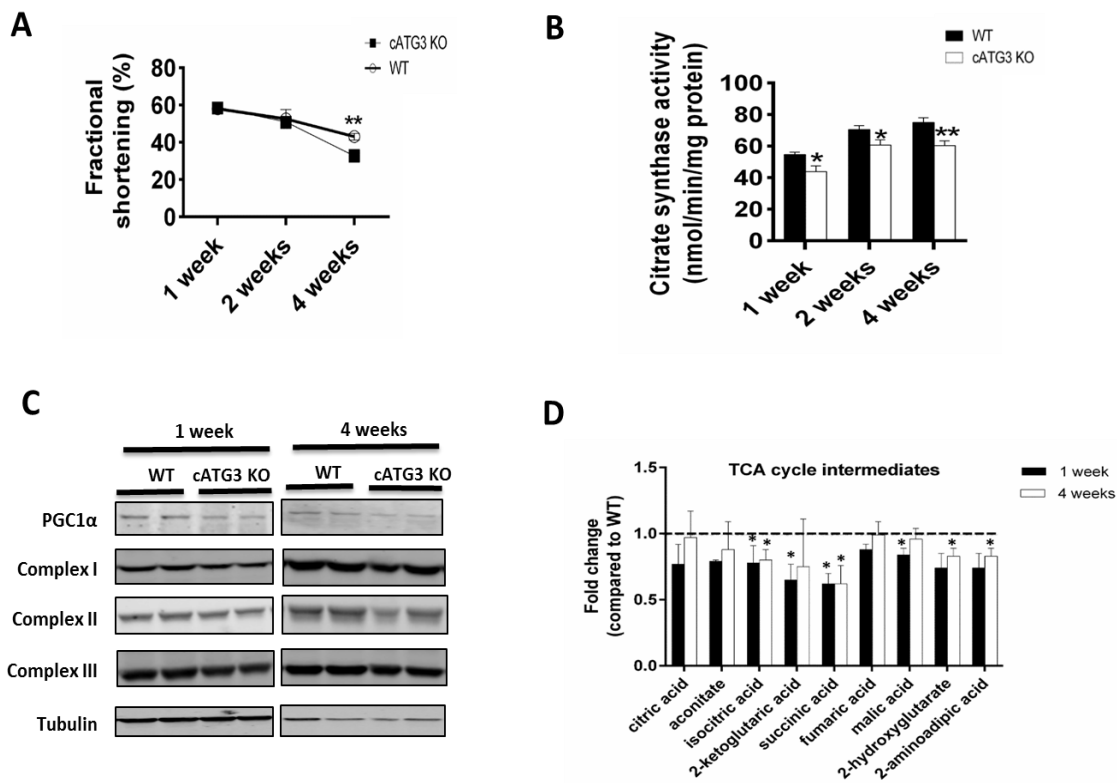


Figure 2.S2 Cardiac mitochondrial dysfunction precedes cardiac dysfunction in cATG3 KO mice. (A) Fractional shortening at 1 week, 2 weeks and 4 weeks of age in WT and cATG3 KO mice, $n=3-6$. (B) Citrate synthase activity in 1-week-old, 2-week-old and 4-week-old WT and cATG3 KO mouse hearts, $n=6$. (C) PGC-1 α and mitochondrial complex expression levels were measured in 1-week-old and 4-week-old WT and ATG3-deficient hearts, $n=2$. (D) Tricarboxylic acid cycle (TCA cycle) intermediates in 1-week-old and 4-week-old ATG3 KO mouse hearts, shown as fold change compared to age matched WT controls, $n=5-6$. ** $p<0.01$, * $p<0.05$ when compared to WT.

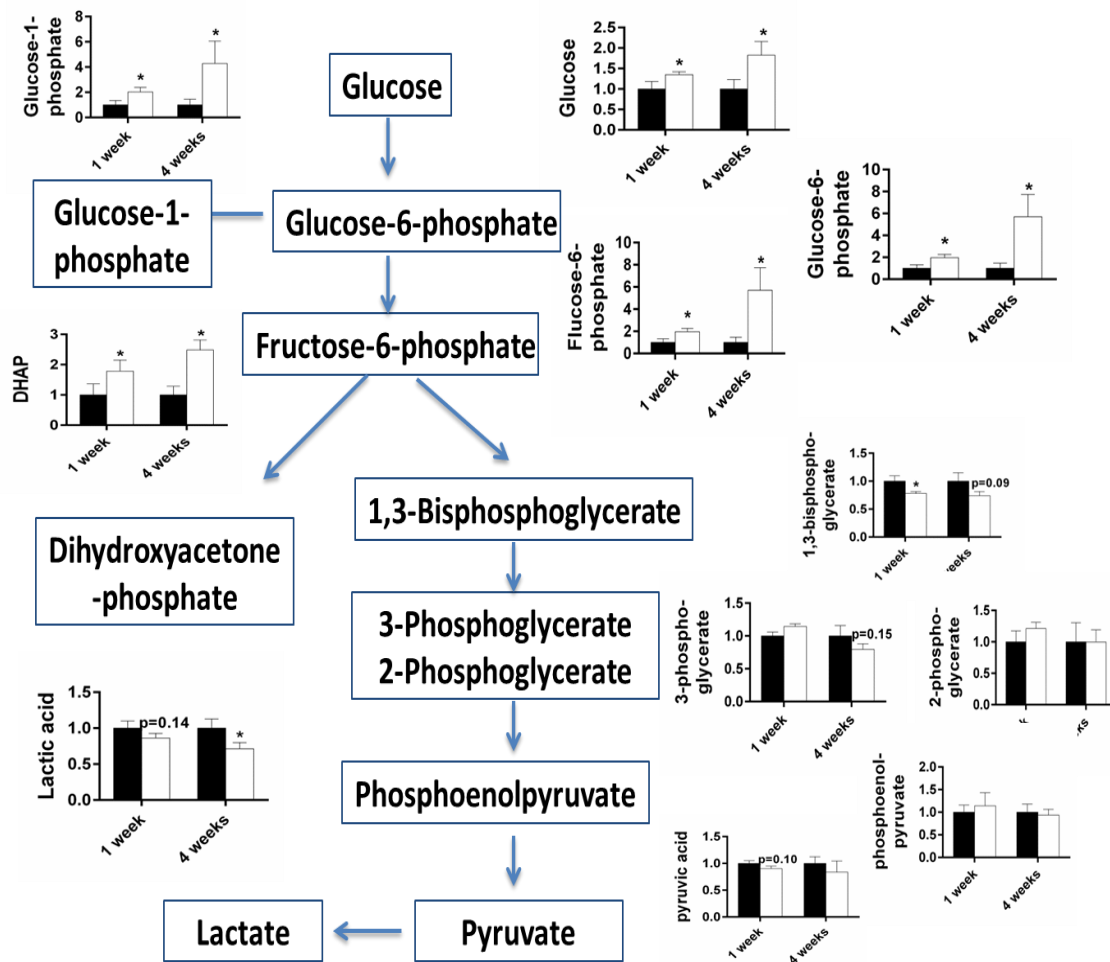


Figure 2.S3 Glycolytic intermediates in 1-week-old and 4-week-old WT and ATG3-deficient hearts. All metabolites were measured using GC-MS, n=5-6. **p<0.01, *p<0.05 when compared to WT.

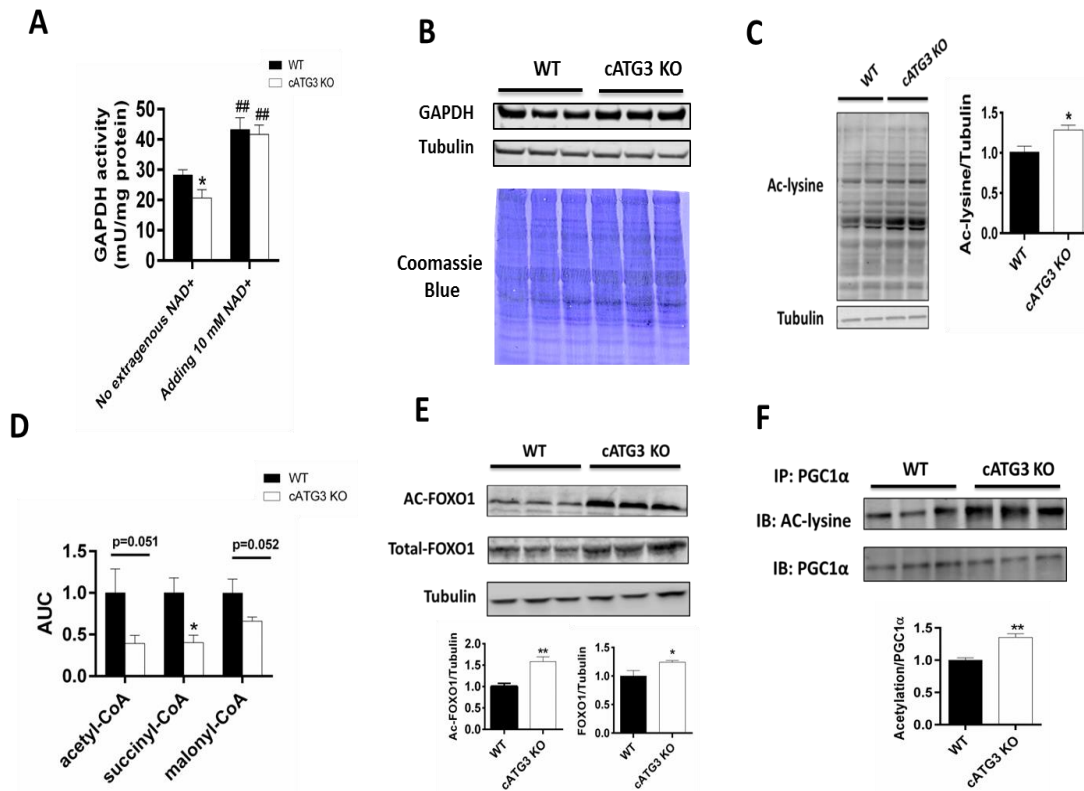


Figure 2.S4 cATG3 KO mice exhibited protein hyperacetylation in mouse heart at 4 weeks. (A) GADPH activity measurement in WT and ATG3-deficient hearts without or with exogenous NAD⁺ supplementation, n=6. (B) GADPH protein levels in WT and ATG3-deficient hearts, n=3. (C) Total protein acetylation in WT and ATG3-deficient hearts, n=3. (D) Acetyl-CoA, Succinyl-CoA and malonyl-CoA levels in WT and ATG3-deficient hearts, n=3-5. (E) Foxo1 and Ac-Foxo1 expression levels in WT and ATG3-deficient hearts, n=3. (F) PGC-1 α acetylation in WT and ATG-deficient hearts using Co-Immunoprecipitation, n=3. **p<0.01, *p<0.05 when compared to WT.

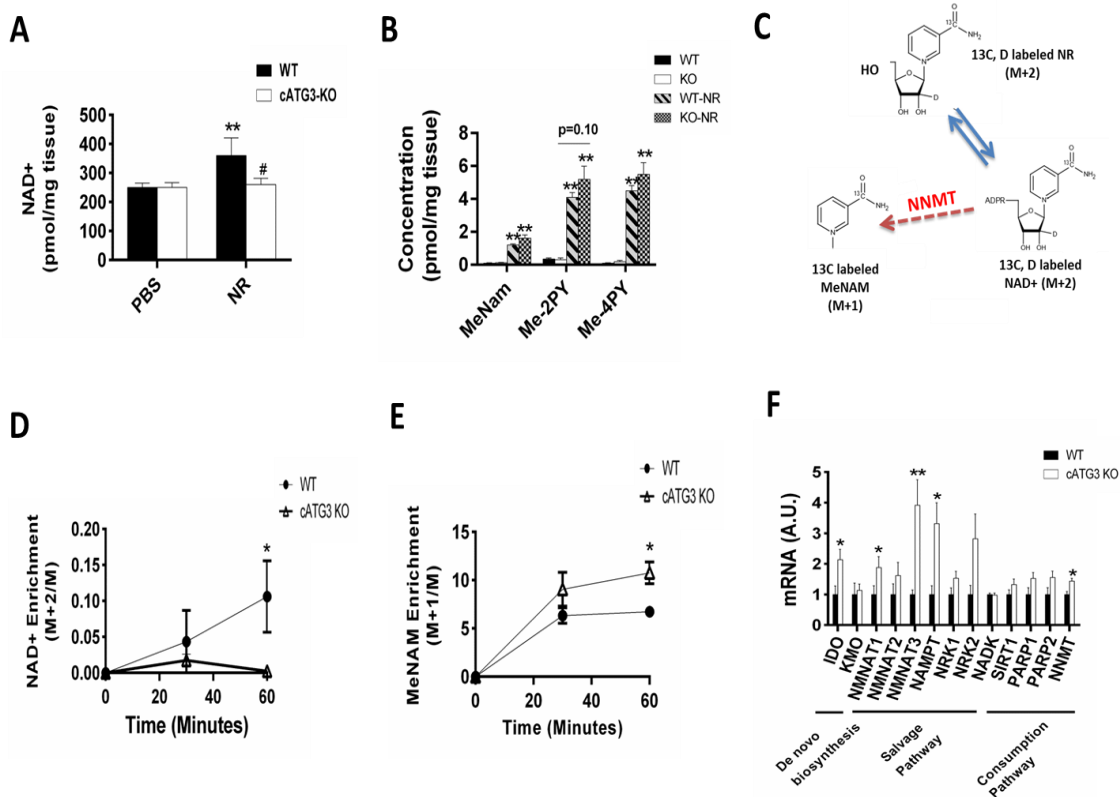


Figure 2.4 NAD⁺ metabolism was altered in cATG3 KO mouse heart at 6 weeks. (A) NAD⁺ content was measured in WT and ATG3-deficient hearts after PBS or Nicotinamide riboside (NR) administration, n=6. (B) Measurement of NAD⁺ breakdown products, including MeNAM, Me-2PY and Me-4PY in WT and ATG3-deficient hearts after PBS or NR administration, n=6. (C) Schematic depicting use of isotope-labeled NR to trace NAD⁺ metabolism in the heart. (D) NAD⁺ enrichment in WT and ATG3-deficient hearts at 0, 30 min and 60 min after isotope-labeled NR injection, n=4. (E) Me-NAM enrichment in WT and ATG3-deficient hearts at 0, 30 min and 60 min after isotope-labeled NR injection, n=4. (F) NAD⁺ related enzyme mRNA expression levels in WT and ATG3-deficient hearts, n=6. **p<0.01, *p<0.05 when compared to WT.

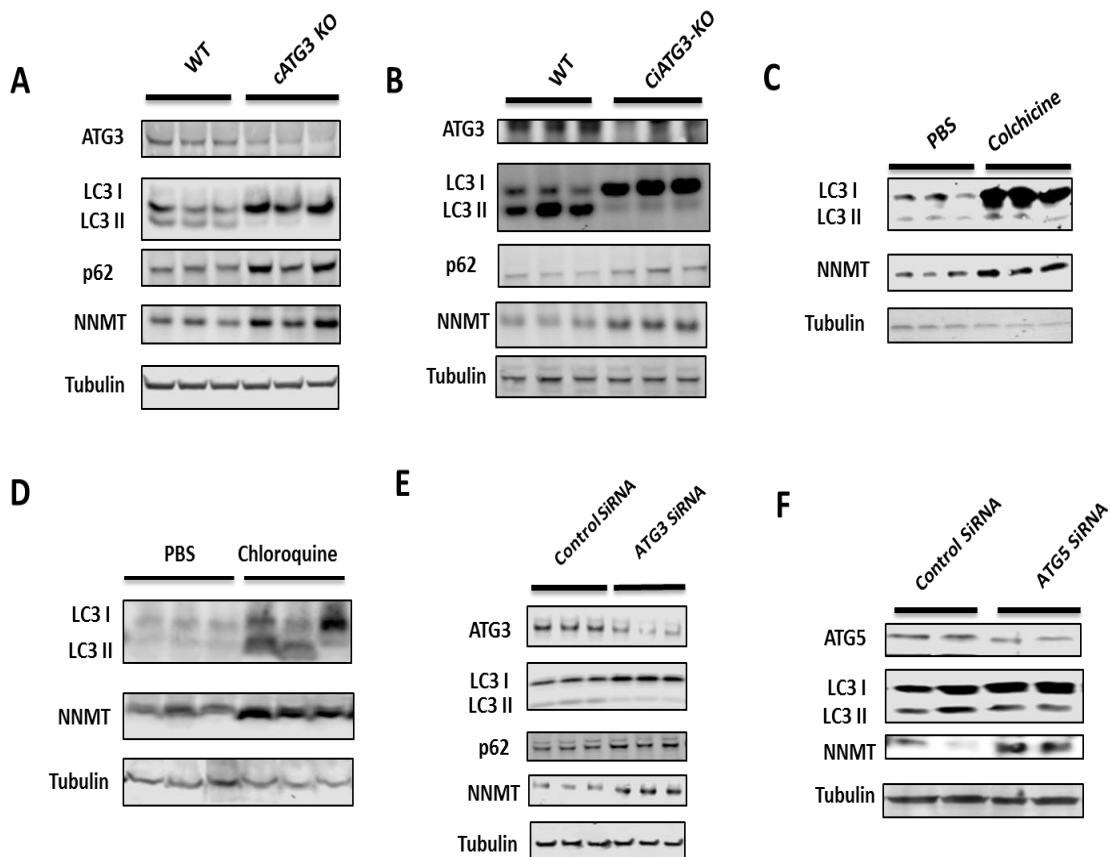


Figure 2.S5 Autophagy inhibition induces NNMT accumulation in cardiomyocytes *in vivo* and *in vitro*. (A) ATG3, LC3 and NNMT protein levels in WT and cATG3 KO mouse hearts, n=3. (B) ATG3, LC3 and NNMT protein levels in WT and inducible ATG3 KO mouse hearts 1 week after tamoxifen injection, n=3. (C) LC3 and NNMT expression protein in PBS or Colchicine (Col) treated hearts, n=3. (D) LC3 and NNMT protein levels in PBS or Chloroquine (CQ) treated hearts, n=3. (E) ATG3, LC3, p62 and NNMT expression in ATG3 SiRNA treated H9C2 cells, n=3. Scrambled SiRNA was used as control, n=3. (F) ATG5, LC3 and NNMT protein expression in ATG5 SiRNA treated H9C2 cells, n=2. Scrambled SiRNA was used as control.

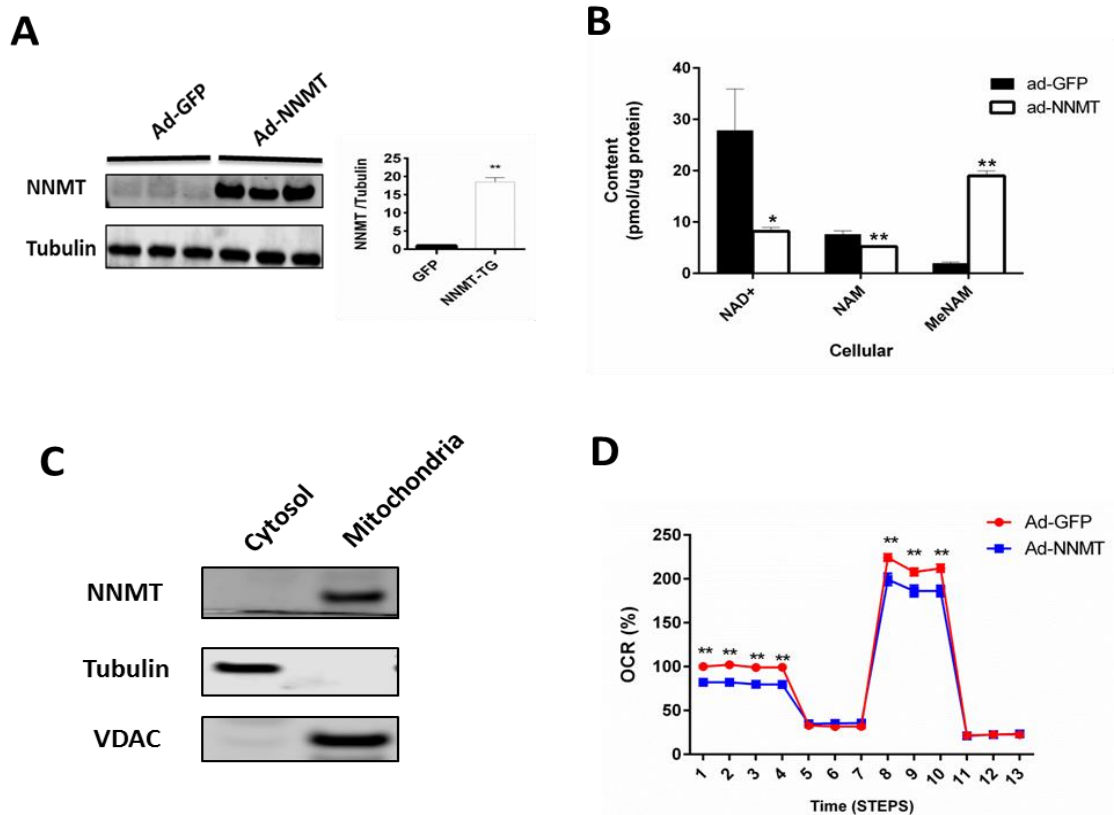


Figure 2.5 NNMT overexpression depletes NAM and represses mitochondrial respiration in cultured cardiomyocytes. (A) NNMT expression following adenoviral transfection of GFP or NNMT in cultured H9C2 cells, n=3. (B) Measurement of NAD⁺, nicotinamide (NAM) and MeNAM in ad-GFP or ad-NNMT transfected H9C2 cells, n=6. (C) Detection of NNMT expression in cytosolic or mitochondrial fraction from WT hearts. (D) Oxygen consumption rates in ad-GFP or ad-NNMT transfected H9C2 cells, n=6-8. **p<0.01, *p<0.05 when compared to ad-GFP group.

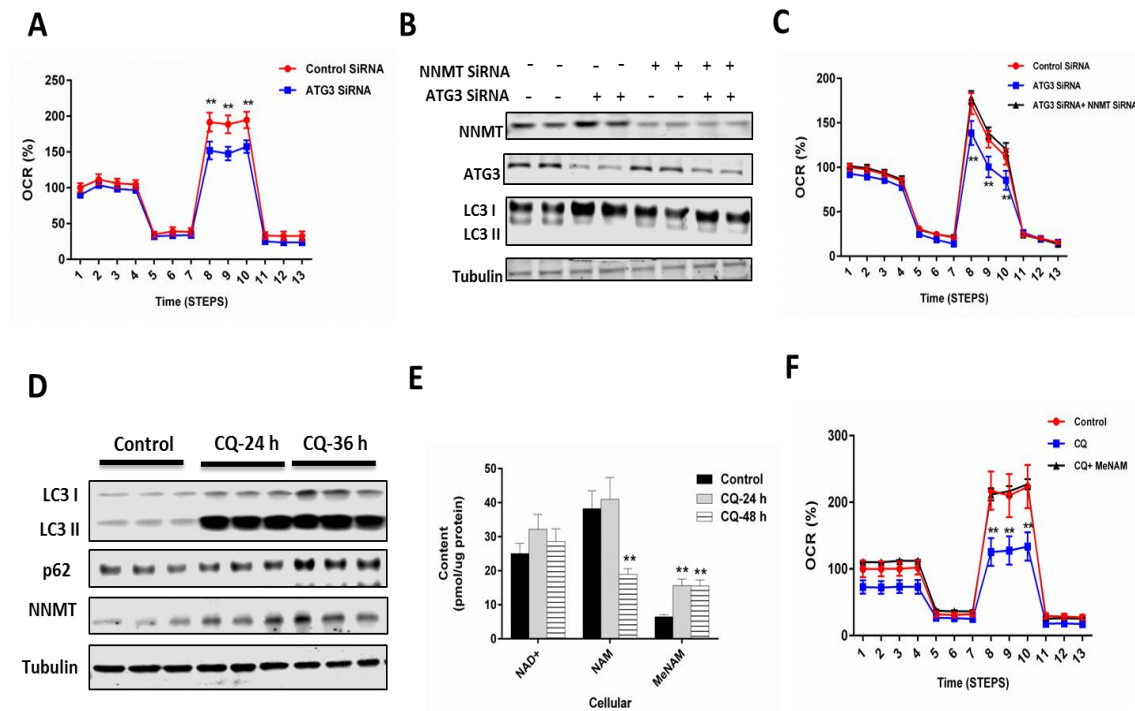


Figure 2.6 NNMT inhibition prevented mitochondrial dysfunction induced by autophagy inhibition in cultured cardiomyocytes. (A) Oxygen consumption rate measurement in ATG3 SiRNA treated H9C2 cells. Scrambled SiRNA was used as control, n=6-8. (B) NNMT, ATG3 and LC3 expression in ATG3, NNMT and double knockdown H9C2 cells. Scrambled SiRNA was used as control, n=2. (C) Oxygen consumption rate measurement in control, ATG3 knockdown and double knockdown H9C2 cells, n=5-6. (D) LC3 and NNMT expression in PBS or CQ treated H9C2 cells. H9C2 cells were treated with 80 μ M CQ for 24 or 48 hours, and subjected to 3 hours HBSS starvation before harvest, n=3. (E) NAD⁺, NAM and MeNAM measurement in CQ treated H9C2 cells. H9C2 cells were treated with 20 μ M CQ for 24 or 48 hours, and subject to 3 hours HBSS starvation before harvest. PBS treatment was used as control, n=3. (F) Oxygen consumption rate measurement in control, CQ or CQ with MeNAM treated H9C2 cells, n=6-8. **p<0.01, *p<0.05 when compared to PBS treated group.

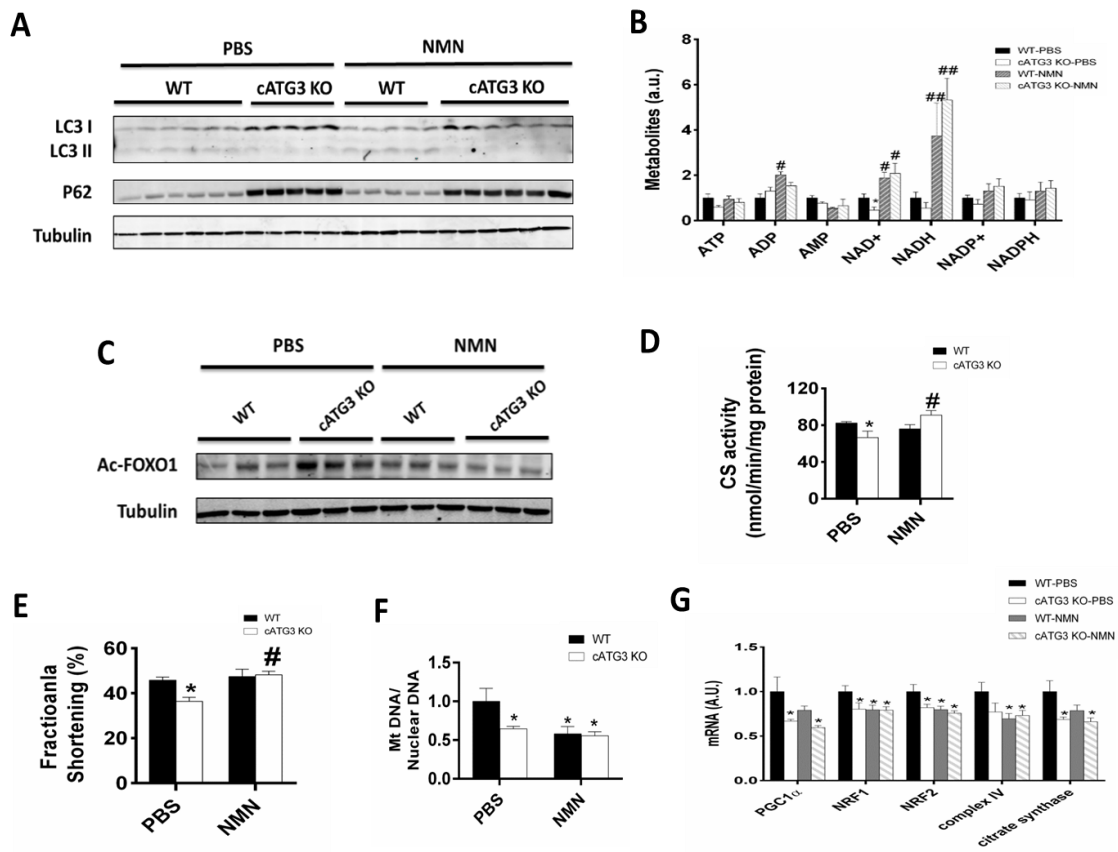


Figure 2.7 NMN increased cardiac NAD⁺ content and rescued cardiac contractile dysfunction in 4-week-old cATG3 KO mice. (A) LC3 and p62 expression levels in PBS or NMN-treated hearts from WT and cATG3 KO mouse hearts, n=5-6. (B) Bioenergetics metabolites measurement in PBS or NMN-treated WT and cATG3 KO mice, n=4-6. (B) Ac-Foxo1 expression levels in whole heart lysates, n=3. (D) Citrate synthase activity measurement in WT and cATG3 KO mouse hearts, n=6. (E) Fractional shortening in WT and ATG3-deficient hearts after PBS or NMN treatment, n=6. (F) mtDNA copy number in PBS or NMN-treated hearts from WT and cATG3 KO mice heart, n=6. (G) Mitochondrial-related nuclear mRNA expression in WT and cATG3 KO mice heart following PBS or NMN administration for 7 days, n=6. **p<0.01, *p<0.05 when compared WT mice, #p<0.05, ##p<0.01 when compared to PBS treated mice.

Table 2.1 Primer sequences for RT-qPCR.

Gene	Forward	Reverse
RPL13a	CTCTGGCCTTTTCCTTTTTG	CCGAAGAAGGGAGACAGTTC
NNMT	GATTGCACGCCTCAACTTCT	GAACCAGGAGCCTTTGACTG
NMRK1	CTTGAAGCTTGCTCTGCGAC	CTCCGTTTGTACACCACCA
NMRK2	AAGCCCCAGGACCAAATAGC	GCGTGCAAACCTTGTGTGGAT
PARP1	CACCTTCCAGAAGCAGGAGA	GCAGCGAGAGTATCCCAAG
SIRT1	GACACAGAGACGGCTGGAAC	CAGACCCTCAAGCCATGTTT
NMAPT	TCACGGCATTCAAAGTAGGA	GCAGAAGCCGAGTTCAACAT
NMNAT3	CAGAAGCACCACAGGGATTG	CCTGCAGCACGTTTACAGTC
NMNAT2	ATCCCGCCAATCACAATAAA	GCAGCTTCAATCCCATCACT
NMNAT1	TGAGTCCATGGGGAGAAGTT	AGGACTAGGGCCGTTTGG
SOD1	CGGCGGATGAAGAGAGGCA	TCACACGATCTTC AATGGACACA
Catalase	GCAGATACCTGTGAACTGTC	GTAGAATGTCCGCACCTGAG
ANP	ATGGGCTCCTTCTCCATCA	CCTGCTTCCTCAGTCTGCTC
BNP	GGATCTCCTGAAGGTGCTGT	TTCTTTTGTGAGGCCTTGGT
ATG3	ATCTGTTTCCAACAATCCAC	GAGTATTCGGATGAATTGGA
Cyto-C	ATCTCCACGGTCTGTTCCGGG	TCCCCAGGTGATGCCTTTGT
PGC-1	GTAAATCTGCGGGATGATGG	AGCAGGGTCAAATCGTCTG
SOD2	CAGACCTGCCTTACGACTATGG	CTCGGTGGCGTTGAGATTGTT
D-loop	GATTAGACCCG ATACCATCGAGAT	GGTTCTTACTTC AGGGCCATCA
Ndufv1	CCAAAACCCAGTGATCCAGC	CTTCCCCACTGGCCTCAAG

Table 2.2 Heart weight and heart weight/tibia length in 4-week-old and 4-month-old mice. **p<0.01, *p<0.05 when compared WT mice, n=12-16.

Age		WT	cATG3 KO
4 Weeks	Heart weight (mg)	88.36 ± 2.96	94.10 ± 3.46
	Heart weight/Tibia length (mg/mm)	4.88 ± 0.18	5.30 ± 0.10*
4 months	Heart weight (mg)	112.16 ± 2.73	126.15 ± 3.31**
	Heart weight/Tibia length (mg/mm)	6.07 ± 0.16	7.04 ± 0.23 **

Table 2.3 Amino acid levels in 1-week-old and 4-week-old cATG3 KO mouse hearts. The relative change of each amino acid in ATG3-deficient hearts is represented as the fold changed compared to their aged matched WT mice. **p<0.01, *p<0.05 when compared WT mice, n=6.

Amino acid	1 week		4 weeks	
	Mean	SE	Mean	SE
lysine	0.88	0.06	0.74	0.09
valine	1.08	0.04	1.03	0.05
leucine	1.04	0.03	0.86	0.02
isoleucine	1.06	0.05	1.05	0.05
threonine	0.99	0.04	1.08	0.05
homoserine	0.94	0.05	1.14	0.05
glycine	0.94	0.05	1.14	0.05
serine	0.79	0.10	1.76	0.41
alanine	0.87	0.04	0.87	0.06
glutamic acid	1.18	0.05	0.88	0.04
glutamine	0.98	0.06	0.92	0.07
proline	0.96	0.09	0.85	0.10
aspartic acid	1.04	0.08	0.87	0.09
asparagine	1.11	0.09	1.02	0.08
methionine	0.96	0.02	0.98	0.08
cysteine	1.06	0.24	1.79*	0.38
homocysteine	0.99	0.18	0.92	0.17
phenylalanine	0.97	0.03	0.92	0.04
tyrosine	0.98	0.09	1.04	0.05
tryptophan	1.02	0.02	0.90	0.08
histidine	0.78	0.04	0.66	0.07
N-methylalanine	1.04	0.03	1.43	0.20
sarcosine	0.96	0.08	0.80	0.15
4-hydroxyproline	1.02	0.19	0.83	0.14
ornithine	0.91	0.07	1.03	0.07
N-acetylaspartate	1.48*	0.16	1.19	0.30
β-alanine	1.33*	0.11	0.80	0.13

Table 2.4 NAD⁺ related metabolites in WT and cATG3 KO mouse hearts after PBS or NR administration. #p<0.05, ##p<0.01 when compared to PBS treated mice, n=6.

Metabolites (nmol/mg tissue)	WT-PBS		KO-PBS		WT-NR		KO-NR	
	Mean	SE	Mean	SE	Mean	SE	Mean	SE
NADP	21	1.2	20	1.4	22	4.2	20	1.4
NAAD	0.1	0.02	0.15	0.07	21##	4.3	13##	3.2
NMN	0.77	0.04	0.76	0.09	1.7##	0.23	1.1##	0.15
NAR	0.02	0.01	0.01	0.01	0.15##	0.01	0.08	0.01
ADPR	10	1.4	12	2.2	11	1.6	8.8	1.1
NAMN	NA	NA	NA	NA	0.78	0.06	0.51	0.08
Uridine	2.5	0.61	3.9	1.7	2.9	0.84	1.9	0.45
Cytidine	2.8	0.92	2.7	1.4	2.4	0.56	1.8	0.32
Inosine	1.8	0.68	11	4.9	3.8	2	1.2	0.21
Nam	48	4.9	47	4.3	340##	25	240##	54

Table 2.5 Sequence for SiRNA.

Gene	Sense	Anti-Sense
ATG7	GGAUACAAGCUUGGCUG CUACUUCU	AGAAGUAGCAGCCAAGC UUGUAUCC
ATG5	AUCUGAGCUAUCCAGACAA	UUGUCUGGAUAGCUCAGAU
Control	UAAGGCUAUGAAGAGAUAC	GUAUCUCUUCAUAGCCUUA
ATG3	GGUGUUCAUAUGUAUCUUUT	AAAGAUACAUAUGAACACCAA
NNMT	UGUUCGAGAUGCCGUGGAA	GAACCAAGGGACCGGAGAA

CHAPTER 2

AUTOPHAGY IS REQUIRED FOR IMPROVING CARDIAC PERFORMANCE FOLLOWING EXERCISE

Abstract

Autophagy is an evolutionarily conserved catabolic process that degrades proteins and organelles to maintain cellular homeostasis. Recent studies showed that exercise training induces autophagy in the heart; however, it is still unclear how exercise-induced autophagy regulates cardiovascular function. In this study, we investigated the role of autophagy in cardiac function using wild-type (WT) mice and beclin 1 heterozygous mice following 6 weeks of treadmill training. After exercise training, beclin 1 heterozygous mice showed impaired autophagy relative to WT mice. As a consequence, although exhibiting similar cardiac hypertrophic responses, cardiac function improvement and enhanced mitochondrial oxidative capacity were blunted in beclin 1 heterozygous mice after 6 weeks of chronic training. Exercise-induced mitochondrial biogenesis was prevented in beclin 1 heterozygous mice, which may be due to the impaired AMPK activation in autophagy deficient hearts. Moreover, beclin 1 heterozygous mice showed impaired anti-oxidant gene expression and increased ROS production in response to exercise training. Thus, autophagy may promote cardiac mitochondrial biogenesis, increase cardiac mitochondrial function, decrease ROS production and improve cardiac contractile function in response to chronic exercise training.

Introduction

Autophagy is an essential process by which cells break down their own components to maintain cellular homeostasis [1, 2]. In this process, certain long-lived proteins, damaged organelles and malformed proteins are degraded and recycled by the lysosomes. Autophagy has been implicated in various cardiovascular diseases, such as ischemia/reperfusion, pressure-overload induced cardiomyopathy as well as chronic heart failure [3] [1].

Exercise, particularly endurance exercise training, improves cardiac function in health and disease conditions [4]. For instance, in a large and prospective study, exercise training shows significant beneficial effect for old patients with coronary artery disease and heart failure [5]. Exercise mediates benefits not only by reducing cardiovascular risk factors, such as diabetes or hypertension, but also by directly improving cardiac function [6] [7, 8]. One beneficial effect of endurance exercise training in the heart is by increasing cardiac energy metabolism [9] [10], but detailed mechanism by which exercise increases cardiac bioenergetics and maintains cardiac function is incompletely understood.

Exercise was recently reported to induce autophagy in skeletal muscle and cardiac muscle [11], and this study revealed an essential role of autophagy in regulating skeletal muscle glucose homeostasis. However, the mechanisms by which exercise-induced autophagy improves cardiac performance or reduces cardiac injury were not pursued. In the present study, we observed that beclin 1 heterozygous mice did not induce autophagy in response to exercise, and exhibited blunted improvement in cardiac function and mitochondrial oxidative capacity after endurance exercise training, which may be due to in part to impaired AMPK activation and reduced mitochondrial biogenesis. Thus these results revealed an essential role of autophagy in exercise-induced cardiac function improvement.

Materials and Methods

Animal experiments

This study protocol was approved by the Institutional Animal Care and Use Committee of University of Utah, and the Carver College of Medicine of the University of Iowa.

Acute treadmill training

Twelve-week-old mice are acclimated to and trained on a 10-degree treadmill incline for 3 days. On day 1, mice were subjected to run for 5 min at 8 m/min. On day 2 mice they were subjected to run for 5 min at 8 m/min followed by another 5 min at 10 m/min. On day 3, mice were subjected to a speed of 17 m/min for 60 min. Mice were sacrificed at 60 min after last exercise training.

Chronic treadmill exercise training

Twelve-week-old mice were trained with 10-degree uphill incline for 60 min at an initial speed of 5 m/min for 5 min, followed by a speed of 10m/min for 5 min, and a final speed of 17 m/min for 50 min. Mice were sacrificed at 60 min after last exercise training.

Maximum running speed and exhaustion running

Twelve-week-old mice were subject to 10-degree uphill incline treadmill training at an initial speed of 5 m/min for 5 min, and were then followed by increasing speed of 2 m/min every min, until the mice stopped running.

Lactate measurement

Serum lactate levels were measured using a lactate assay kit (MAK064, Sigma) following manufacturer's protocol. Briefly, lactate concentration was determined by an enzymatic assay, which results in a colorimetric (570 nm)/ fluorescent ($\lambda_{ex} = 535$ nm/ $\lambda_{em} = 587$ nm) product that is proportionate to the lactate concentration.

Tissue harvest

Mice were anesthetized by chloral hydrate 0.5 h after acute or chronic exercise training. Hearts were then immediately removed and rinsed in cold PBS before being snap-frozen in liquid nitrogen.

Immunoblotting

Total proteins were extracted from hearts or cultured H9C2 cells in a lysis buffer containing 50 mM HEPES (pH 7.5), 150 mM NaCl, 10% Glycerol, 1% Triton X-100, 1.5 mM MgCl₂, 1 mM EGTA, 10 mM Na₄P₂O₇, 100 mM NaF, and 1X Halt protease and phosphatase inhibitor cocktail (Thermo Scientific, Rockford, IL). Protein concentration was determined by a Micro BCA Protein Assay kit (Pierce). For immunoblotting, previously extracted proteins were resolved on SDS-PAGE and analyzed by western blotting using the LI-COR Odyssey Imager (LI-COR), an infrared fluorescence based detection system. The following primary antibodies were used for immunoblotting. LC3 (L8918) and p62/SQSTM1 (P0067) antibodies were from purchased from Sigma (St. Louis, MO). GAPDH (2118) antibodies were purchased from Cell Signaling (Boston, MA). PGC1 α (H-300) and SIRT1 (B-10) antibodies were purchased from Santa Cruz (Santa Cruz,CA).

Citrate synthesis (CS) activity measurement

Heart tissue was homogenized on ice in homogenization buffer containing 20 mM HEPES and 10 mM EDTA at pH 7.4. Homogenates were subjected to two freeze and thaw cycles to liberate CS from the mitochondrial matrix and then diluted 1:10 to an approximate final protein concentration of 1 μ g/ μ l. The reaction was performed in 1 ml of reaction buffer containing 20 mM HEPES, 1 mM EDTA, 220 mM sucrose, 40 mM KCl, 0.1 mM DTNB, and 0.1 mM acetyl-CoA (pH 7.4 at 25°C). The reaction was started by the addition of 0.05 mM oxaloacetate and monitored for 3 min with an ultraspectral 3000

spectrophotometer. The result was normalized to protein content.

Mitochondrial respiration in cardiac fibers

LV subendocardial muscle fibers were used to measure mitochondrial respiration rates and ATP synthesis as previously described. Respiration rates were determined in the presence of substrate palmitoyl-carnitine (VO), after stimulation with 1 mM ADP (VADP), and after addition of 1 µg/ml of the ATP synthase inhibitor oligomycin (VOligo). ATP synthesis rate was measured in fibers after stimulation with 1mM ADP.

Electron microscopy

Cardiac tissue samples were removed and fixed in electron microscopy (EM) fixation buffer containing 2.5% glutaraldehyde and 1% paraformaldehyde. They were processed and at the University of Utah Microscopy Core.

Echocardiography

Mice were anesthetized with 2% isoflurane gas with an inflow rate of 1 ml/min and placed on a heated stage (37°C). Chest hair was then removed with a topical depilatory agent before the echocardiogram. Fractional shortening (in %) was calculated as $100 \times [(LVDD - LVDs)/LVDD]$, where LVDD is the LV dimension at diastole and LVDs is the LV dimension at systole.

Quantitative PCR

RNA extraction and quantitative real-time PCR were performed on total RNA that was extracted from heart tissue using TRIzol reagent (Invitrogen, Carlsbad, CA), purified with the RNeasy kit (Qiagen, Valencia, CA) and reverse transcribed. Quantitative real-time PCR was performed using SYBR Green I with ROX as an internal reference dye. The expression level was normalized to the levels of RPL13A transcript. The primer sequences used for quantitative real-time PCR are listed in Table 3.1.

Statistical analysis

Statistical analyses were performed using GraphPad Prism 6. All data are presented as mean \pm SEM. Statistical significance ($p < 0.05$) was determined by one-way ANOVA and followed by an unpaired Student's t-test.

Results

Exercise-induced autophagy was impaired in beclin 1

heterozygous mouse hearts

Since it has been reported that beclin 1 heterozygous mice exhibited exercise intolerance [11], it was important to optimize the chronic exercise training protocol. We initially failed to find any significant difference in the maximum running speed between WT mice and beclin 1 heterozygous mice (Figure 3.1A). Using our chosen running protocol (17 m/min for 1 hour), serum lactate levels in WT and beclin 1 heterozygous mice were significantly lower than when they were ran to exhaustion (Figure 3.1B). This indicates that WT and beclin 1 heterozygous mice were not exhausted under our chosen chronic running protocol.

After 1 hour acute exercise, beclin 1 protein expression was induced in WT mouse hearts, but not in beclin 1 heterozygous mouse hearts (Figure 3.1C). Moreover, we found that the LC3 II/I ratio, which is used as an index of autophagy induction, was increased in WT mice but blunted in beclin 1 heterozygous mice (Figure 3.1C), consistent with defective autophagy in beclin 1 heterozygous mouse hearts following exercise training.

Exercise-induced cardiac contractile function improvement

was blunted in beclin 1 heterozygous mice

After 6 weeks of exercise training, WT and beclin 1 heterozygous mice showed similar reductions in body weight. The heart weight increase was also comparable

between WT and beclin 1 heterozygous mice (Figure 3.2 A,B). When heart weight was normalized to tibia length, there was no significant difference between WT and beclin 1 heterozygous mice, indicating an equivalent exercise-induced cardiac hypertrophic response (Figure 3.2 C). However, after 6 weeks of exercise training, cardiac contractile function, measured by fractional shortening (FS), was significantly increased in WT mice. However, this increased FS was largely prevented in beclin 1 heterozygous mice after endurance exercise training (Figure 3.2D).

Exercise enhanced cardiac mitochondrial oxidative capacity

in WT mice but not in beclin 1 heterozygous mice

Mitochondria play an essential role in maintaining cardiac function [12]. We assessed mitochondrial function in saponin-permeabilized cardiac fibers from chronic exercise trained WT and beclin 1 heterozygous mice. Palmitoyl-carnitine supported ADP-stimulated mitochondrial oxygen consumption (VADP) and ATP production rates were induced in WT mouse heart fibers relative to sedentary WT hearts (Figure 3.3 A,B). This induction of oxygen consumption and ATP production were blunted in beclin 1 heterozygous mouse hearts after exercise training (Figure 3.3 A,B). ATP/O ratios were similar in all groups, indicating that there were no differences between the groups in mitochondrial coupling in response to exercise training (Figure 3.3 C).

Citrate synthase is a key enzyme in the TCA cycle and its activity is often used as a marker of mitochondrial function [13]. After 6 weeks of exercise training, citrate synthase activity was significantly induced in WT mouse hearts but not in beclin 1 heterozygous mouse hearts, indicating impaired mitochondrial function enhancement in beclin 1 heterozygous mice following endurance training (Figure 3.3 D).

Exercise-induced mitochondrial mass increase was blunted

in beclin 1 heterozygous mice

We used transmission electron microscopy (TEM) to evaluate the morphology and structure of mitochondria in fixed heart sections. Mitochondrial size was significantly increased in exercised WT and beclin 1 heterozygous mice heart relative to their sedentary controls (Figure 3.4 A,B). Interestingly, we observed that mitochondrial coverage area, or mitochondrial density, was significantly lower in beclin 1 heterozygous mice heart when compared to WT mice heart in exercise group (Figure 3.4 C,D). Given the equivalence in cardiac mitochondrial size, the reduced mitochondrial density indicates beclin 1 heterozygous mice may have reduced mitochondrial number.

Beclin 1 heterozygous mice showed impaired exercise-induced

cardiac mitochondrial biogenesis

After endurance exercise training, WT mice showed increased expression of nuclear-encoded genes that promote mitochondrial biogenesis, including PGC1 α , NRF1, NRF2 and TFAM. However, the induction of these mitochondrial biogenesis genes was blunted in beclin 1 heterozygous mice (Figure 3.5 A). Moreover, mtDNA copy number, another marker of mitochondrial number, was reduced in beclin 1 heterozygous mice heart relative to exercise WT control mice (Figure 3.5 B).

Beclin 1 heterozygous mice exhibited AMPK inactivation in

the heart after chronic exercise training

After endurance exercise training, AMPK is activated in the hearts of WT mice but not in beclin 1 heterozygous mouse hearts (Figure 3.6 A). Its downstream target, acetyl coA carboxylase (ACC), was also significantly higher in WT mouse hearts after exercise training, but this was totally blunted in beclin 1 heterozygous mouse hearts (Figure 3.6 A). ADP/ATP ratio, which is an important regulator of AMPK activation in the

heart, was equivalently increased in WT and beclin 1 heterozygous mouse hearts (Figure 3.6 B), suggesting that AMPK inactivation in beclin 1 heterozygous mouse heart after exercise might occur via a mechanism that is independent of the ADP/ATP ratio.

Beclin 1 heterozygous mice exhibited impaired anti-oxidant gene expression and increased ROS production

Following exercise training, many anti-oxidant genes, including SOD1, SOD2, catalase, and UCP2, were significantly induced. It is assumed that these changes would minimize oxidative stress –induced cardiac damage. Interestingly, expression levels of anti-oxidant genes were increased in WT hearts but depressed in beclin 1 heterozygous mouse hearts after chronic exercise training (Figure 3.7 A), suggesting that beclin 1 heterozygous mouse hearts may be more susceptible to oxidative stress-induced cardiac damage. We then measured reactive oxidative species (ROS) production in WT and beclin 1 heterozygous mice heart after 0, 40 min and 60 min acute treadmill exercise training. Relative to WT mice, beclin 1 heterozygous mice produced significantly more ROS in their hearts (Figure 3.7 B).

Discussion

The present study demonstrated that beclin 1 heterozygous knockout mice exhibited impaired exercise-induced autophagy in the heart, accompanied by blunted mitochondrial biogenesis and reduced anti-oxidant response, and did not increase cardiac function after chronic exercise training. These results suggest an essential role of autophagy in promoting mitochondrial biogenesis and modulating cardiac bioenergetics during exercise conditions.

We confirmed that beclin 1 heterozygous mice were a suitable animal model to study exercise-induced autophagy in the heart. Beclin 1, the mammalian orthologue of the yeast ATG6, plays a central role in autophagy initiation [14]. Beclin 1 KO mice were

embryonic lethal, and therefore cannot be used to model exercise training [15]. Beclin 1 heterozygous mice, on the contrary, were viable, developed normally, but exhibited reduced autophagy under stress conditions [16]. As such we reasoned that this could represent a good model for studying the role of autophagy in the cardiac adaptations to exercise training. Compared to WT mouse hearts, the LC3II/I ratio in beclin 1 heterozygous mice heart did not increase in response to exercise training, suggesting impaired exercise-induced autophagy in beclin 1 heterozygous mice.

Exercise training exerts its beneficial effects on cardiac function in various models, including in humans, rats and mice [17] [18] [19] [20]. Consistent with these studies, we also found that exercise training improved cardiac performance in WT mice, characterized by increased left ventricular function, measured by echocardiography. However this enhancement in contractile function was blunted in beclin1 heterozygous mice, suggesting that autophagy may be an important mediator of exercise-induced cardiac remodeling.

Cardiac hypertrophy is a general term that describes increased cardiac mass in response to exercise, which could be either physiological or pathological hypertrophy. In mild, early hypertrophy, cardiac myocyte contractile performance may be enhanced as a consequence [21]. We found that beclin 1 heterozygous mice, although showing impaired autophagy in the heart, exhibited a similar increase in heart weight as well as left ventricular posterior wall thickness after training in exercise-induced cardiac hypertrophy.

Mitochondria are the main organelles for energy fuel metabolism in the heart and they play an essential role in regulating cardiac bioenergetics [22] [23]. We observed that ADP-stimulated cardiac fiber respiration and ATP production rate were induced in WT mouse hearts after exercise training, but not in beclin 1 heterozygous mouse hearts. The exercise-induced increase in citrate synthase activity, which is the marker of

mitochondrial function improvement, was also prevented in beclin 1 heterozygous mice. These data revealed that autophagy might be required for promoting mitochondrial biogenesis and increasing mitochondrial oxidative capacity in the heart following exercise training. This difference was not necessarily reflected by changes in mitochondrial morphology, since WT and beclin 1 heterozygous mice heart exhibited similar increases in mitochondrial size after exercise training. However mitochondrial coverage area, or mitochondrial density, was significantly lower in trained beclin 1 heterozygous mice heart relative to their WT trained controls. Furthermore, we found mtDNA copy number was increased in WT mice heart in response to exercise training, but this increase was blunted in beclin 1 heterozygous mouse heart. Since the mitochondrial size was similar between WT and beclin 1 heterozygous mouse heart, the reduced density reflected decreased mitochondrial number in beclin 1 heterozygous mouse heart after exercise training.

Interestingly, we observed that exercise-induced induction of mitochondrial biogenesis genes, such as PGC1 α , NRF1, NRF2 and TFAM, were prevented in beclin 1 heterozygous mouse hearts. Exercise-induced mitochondrial biogenesis is characterized by mitochondrial proliferation with increased mitochondrial mass, which contributes to cardiac function improvement [9]. Mitochondrial biogenesis is an adaptive response to stress conditions, and plays an essential role in maintaining cardiac function. Interestingly, we found this process was blunted in beclin 1 heterozygous mouse hearts, which may contribute to the attenuated mitochondrial and cardiac function improvement after exercise. Because mitochondrial mass is a balance between mitochondrial biogenesis and autophagy [24], attenuated mitochondrial biogenesis might be a secondary effect of autophagy deficiency in beclin 1 heterozygous mouse hearts. Our results are consistent with a recent study in skeletal muscle, where autophagy was shown to be required for mitochondrial biogenesis during myoblast differentiation [25].

Consistently, in a very recent publication, autophagic flux inhibitor colchicine abolished mitochondrial biogenesis following swimming exercise training in skeletal muscle [26]. These results, together with our finding in the heart, indicate autophagy may be involved in mitochondrial biogenesis signaling following exercise training in skeletal muscle and in the heart.

To further investigate the molecular mechanism by which mitochondrial biogenesis was blunted in beclin 1 heterozygous mouse hearts, we measured AMP-activated protein kinase (AMPK) phosphorylation. AMPK is an enzyme that is activated in response to energy stress, including fasting or exercise training [27]. Its activation promotes increased expression of PGC-1 α to increase mitochondrial biogenesis signaling in response to energy deficiency [28]. Beclin 1 heterozygous mice heart exhibited a blunted AMPK activation as a response to exercise training, which may be the potential mechanism by which mitochondrial biogenesis was impaired in beclin 1 heterozygous heart following exercise-training. AMPK is activated in part by changes in the ADP/ATP ratio, NAD⁺-SIRT1 pathway, LKB1 phosphorylation, or by increased Ca²⁺ intracellular flux in the heart [29]. We found that ADP/ATP ratio was equally increased in WT and beclin 1 heterozygous mouse heart, indicating that AMPK inactivation in beclin 1 heterozygous mouse heart is through an ADP/ATP independent pathway. Besides ADP/ATP ratio, cellular NAD⁺ is another important factor to regulate AMPK activation. For instance, resveratrol, the well-known SIRT1 activator, activates AMPK in cultured HepG2 cells and mouse liver in SIRT1 dependent manner. And it is known that NAM, the SIRT1 inhibitor, downregulates SIRT1 and AMPK activity in cultured HepG2 cells [30]. In our previous studies in cardiac-specific ATG3 KO mice model, we found autophagy may regulate cardiac NAD⁺ homeostasis and SIRT1 activity in cardiomyocytes (data not shown). Therefore, future studies are required to understand whether NAD⁺ metabolism and SIRT1 activity are altered in beclin 1 heterozygous mice,

which may be a potential mechanism by which autophagy regulates AMPK activation and mitochondrial biogenesis induced by exercise.

Finally, we found that exercise-caused ROS production was increased in beclin 1 heterozygous mouse heart when compared to WT mice. And this is consistent with the reduced anti-oxidant gene expression levels in beclin 1 heterozygous mouse heart. The molecular mechanisms by which AMPK acts to modulate cellular reactive oxidative species (ROS) levels is through activating FoxO1 (forkhead box O1) by phosphorylation at Thr (649) and increasing FoxO1-dependent transcription of anti-oxidant genes expression, including SOD2 and catalase [31]. This new finding in liver cells was consistent with our finding in beclin 1 heterozygous mouse heart following exercise training, with impaired AMPK activation, blunted anti-oxidant response and more ROS production.

Since anti-oxidant defense plays an important role in preventing cardiac dysfunction under stress conditions [32], we may think this impaired anti-oxidant defense and increased ROS may further contribute to cardiac contractile dysfunction in beclin 1 heterozygous mice after exercise training. To further testify the importance of anti-oxidant response under exercise conditions, anti-oxidant reagent may be used to see whether cardiac function could be improved after exercise training when autophagy is inhibited in following studies.

In summary, exercise-induced autophagy was impaired in beclin 1 heterozygous mice, accompanied by blunted mitochondrial biogenesis, increased cardiac ROS production and attenuated cardiac contractile improvement. This study illustrates a novel connection between autophagy and mitochondrial function in the heart under exercise conditions, probably through activating AMPK and promoting mitochondrial biogenesis. Moreover, we also revealed the essential role of autophagy in the cardiac adaptation to exercise training.

References

1. Rothermel, B.A. and J.A. Hill, Autophagy in load-induced heart disease. *Circ Res*, 2008. 103(12): p. 1363-9.
2. Levine, B., N. Mizushima, and H.W. Virgin, Autophagy in immunity and inflammation. *Nature*, 2011. 469(7330): p. 323-35.
3. Nishida, K., et al., The role of autophagy in the heart. *Cell Death Differ*, 2009. 16(1): p. 31-8.
4. Mann, N. and A. Rosenzweig, Can exercise teach us how to treat heart disease? *Circulation*, 2012. 126(22): p. 2625-35.
5. Adams, V., et al., Exercise training in patients with chronic heart failure promotes restoration of high-density lipoprotein functional properties. *Circ Res*, 2013. 113(12): p. 1345-55.
6. Teichert, M., et al., How useful are prescribing indicators based on the DU90% method to distinguish the quality of prescribing between pharmacotherapy audit meetings with different levels of functioning? *Eur J Clin Pharmacol*, 2007. 63(12): p. 1171-7.
7. Flynn, K.E., et al., Effects of exercise training on health status in patients with chronic heart failure: HF-ACTION randomized controlled trial. *JAMA*, 2009. 301(14): p. 1451-9.
8. O'Connor, C.M., et al., Efficacy and safety of exercise training in patients with chronic heart failure: HF-ACTION randomized controlled trial. *JAMA*, 2009. 301(14): p. 1439-50.
9. Vettor, R., et al., Exercise training boosts eNOS-dependent mitochondrial biogenesis in mouse heart: role in adaptation of glucose metabolism. *Am J Physiol Endocrinol Metab*, 2014. 306(5): p. E519-28.
10. Wang, H., et al., Exercise prevents cardiac injury and improves mitochondrial biogenesis in advanced diabetic cardiomyopathy with PGC-1alpha and Akt activation. *Cell Physiol Biochem*, 2015. 35(6): p. 2159-68.
11. He, C., et al., Exercise-induced BCL2-regulated autophagy is required for muscle glucose homeostasis. *Nature*, 2012. 481(7382): p. 511-5.
12. Porter, G.A., Jr., et al., Bioenergetics, mitochondria, and cardiac myocyte differentiation. *Prog Pediatr Cardiol*, 2011. 31(2): p. 75-81.
13. Larsen, S., et al., Biomarkers of mitochondrial content in skeletal muscle of healthy young human subjects. *J Physiol*, 2012. 590(Pt 14): p. 3349-60.
14. Kang, R., et al., The Beclin 1 network regulates autophagy and apoptosis. *Cell Death Differ*, 2011. 18(4): p. 571-80.

15. Yue, Z., et al., Beclin 1, an autophagy gene essential for early embryonic development, is a haploinsufficient tumor suppressor. *Proc Natl Acad Sci U S A*, 2003. 100(25): p. 15077-82.
16. Qu, X., et al., Promotion of tumorigenesis by heterozygous disruption of the beclin 1 autophagy gene. *J Clin Invest*, 2003. 112(12): p. 1809-20.
17. Ehsani, A.A., et al., Improvement of left ventricular contractile function by exercise training in patients with coronary artery disease. *Circulation*, 1986. 74(2): p. 350-8.
18. Ypenburg, C., et al., Myocardial contractile reserve predicts improvement in left ventricular function after cardiac resynchronization therapy. *Am Heart J*, 2007. 154(6): p. 1160-5.
19. Cazorla, O., et al., Effects of high-altitude exercise training on contractile function of rat skinned cardiomyocyte. *Cardiovasc Res*, 2006. 71(4): p. 652-60.
20. Schober, T. and B.C. Knollmann, Exercise after myocardial infarction improves contractility and decreases myofilament Ca²⁺ sensitivity. *Circ Res*, 2007. 100(7): p. 937-9.
21. Hart, G., Exercise-induced cardiac hypertrophy: a substrate for sudden death in athletes? *Exp Physiol*, 2003. 88(5): p. 639-44.
22. Goldenthal, M.J., H.R. Weiss, and J. Marin-Garcia, Bioenergetic remodeling of heart mitochondria by thyroid hormone. *Mol Cell Biochem*, 2004. 265(1-2): p. 97-106.
23. Kiebish, M.A., et al., Dysfunctional cardiac mitochondrial bioenergetic, lipidomic, and signaling in a murine model of Barth syndrome. *J Lipid Res*, 2013. 54(5): p. 1312-25.
24. Cooper, M.P., Interplay of mitochondrial biogenesis and oxidative stress in heart failure. *Circulation*, 2013. 127(19): p. 1932-4.
25. Sin, J., et al., Mitophagy is required for mitochondrial biogenesis and myogenic differentiation of C2C12 myoblasts. *Autophagy*, 2015: p. 0.
26. Ju, J.S., et al., Autophagy plays a role in skeletal muscle mitochondrial biogenesis in an endurance exercise-trained condition. *J Physiol Sci*, 2016.
27. Bungard, D., et al., Signaling kinase AMPK activates stress-promoted transcription via histone H2B phosphorylation. *Science*, 2010. 329(5996): p. 1201-5.
28. Zong, H., et al., AMP kinase is required for mitochondrial biogenesis in skeletal muscle in response to chronic energy deprivation. *Proc Natl Acad Sci U S A*, 2002. 99(25): p. 15983-7.
29. Qi, D. and L.H. Young, AMPK: energy sensor and survival mechanism in the ischemic heart. *Trends Endocrinol Metab*, 2015. 26(8): p. 422-9.

30. Suchankova, G., et al., Concurrent regulation of AMP-activated protein kinase and SIRT1 in mammalian cells. *Biochem Biophys Res Commun*, 2009. 378(4): p. 836-41.
31. Yun, H., et al., AMP-activated protein kinase mediates the antioxidant effects of resveratrol through regulation of the transcription factor FoxO1. *FEBS J*, 2014. 281(19): p. 4421-38.
32. Niu, Y., et al., Antioxidant treatment improves neonatal survival and prevents impaired cardiac function at adulthood following neonatal glucocorticoid therapy. *J Physiol*, 2013. 591(Pt 20): p. 5083-93.

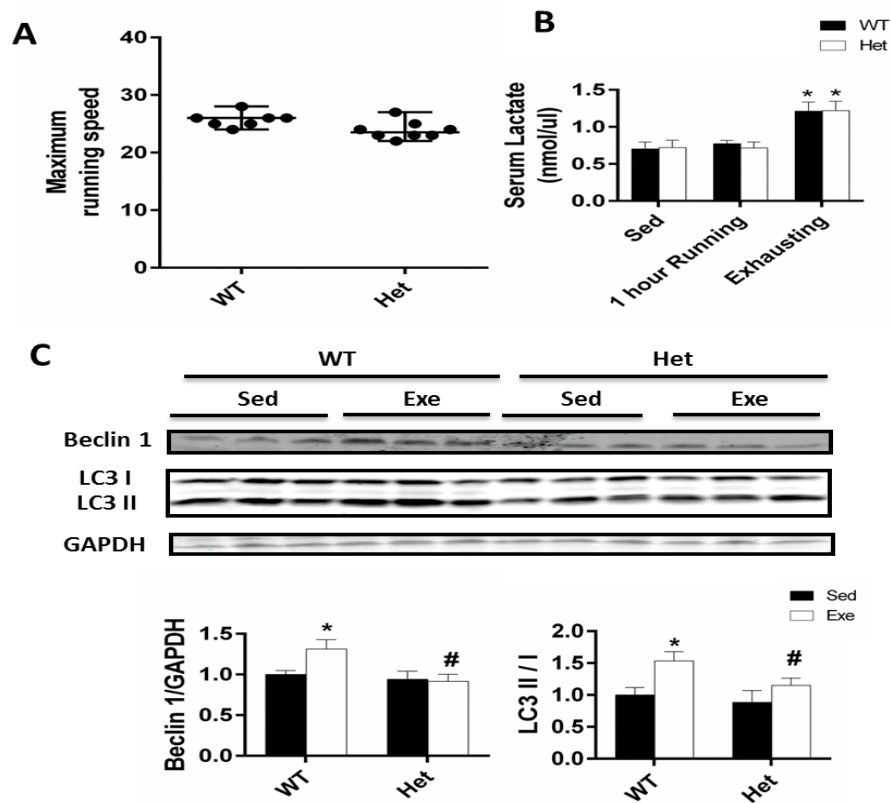


Figure 3.1 Exercise-induced autophagy is impaired in Beclin 1 Het mice. (A) The maximum running speed was determined with increased running speed until mice were exhausted, $n=7-8$. (B) Serum lactate levels from sedentary, after 1 hour running and in exhausted WT and beclin 1 heterozygous mice, $n=6$. (C) Protein levels of beclin 1 and LC3 in WT and beclin 1 heterozygous mouse hearts under sedentary conditions or following 60 min acute exercise training, $n=3$. * $p<0.05$ compared to sedentary mice, # $p<0.05$ compared to WT mice.

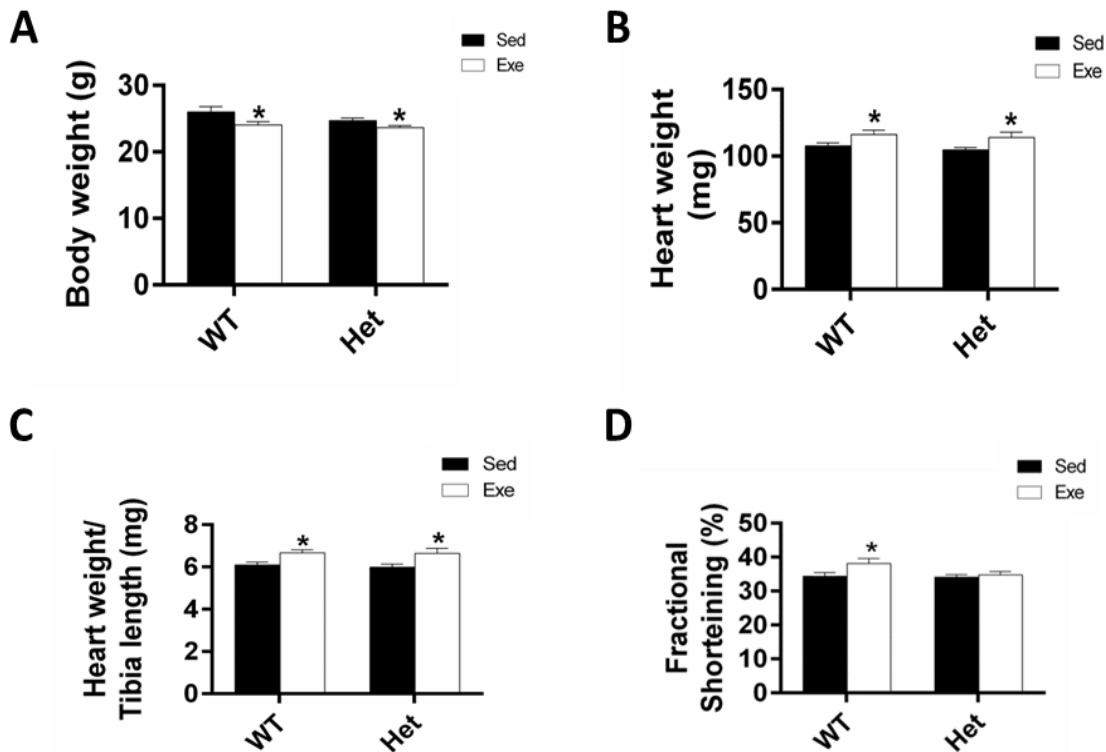


Figure 3.2 Beclin 1 heterozygous mice and WT mice exhibited equivalent cardiac hypertrophic response to training, but beclin 1 heterozygous mice failed to improve cardiac contractile function after exercise. (A) Body weight, Heart weight in chronic exercise trained or sedentary WT and beclin 1 heterozygous mice, n=6. (B, C) Heart weight, and heart weight/tibia length in chronic exercise trained or sedentary WT and beclin 1 heterozygous mice, n=6. (D) Fractional shortening measured in chronic exercise trained or sedentary mice, n=12. *p<0.05 compared to sedentary mice,

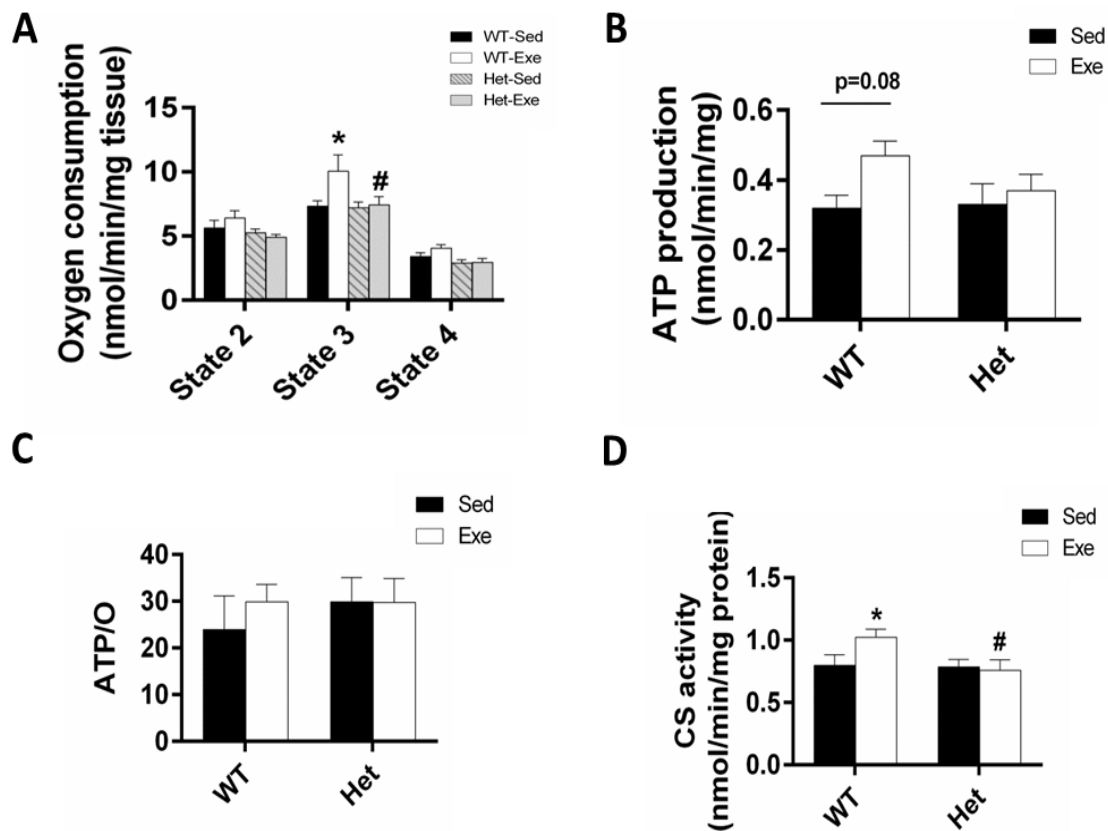


Figure 3.3 Exercise-induced augmentation of mitochondrial respiratory capacity is blunted in beclin 1 heterozygous mice. (A) Oxygen consumption rate was measured in WT and beclin 1 heterozygous mouse heart fibers under sedentary or after exercise training conditions, $n=6$. (B-C) ATP production rate, or ATP/O ratio was measured in cardiac fibers following stimulation with ADP, $n=6$. (D) Citrate synthase activity in WT and beclin 1 heterozygous mouse hearts under sedentary conditions or after exercise training, $n=6$. * $p<0.05$ compared to sedentary mice, # $p<0.05$ compared to WT mice.

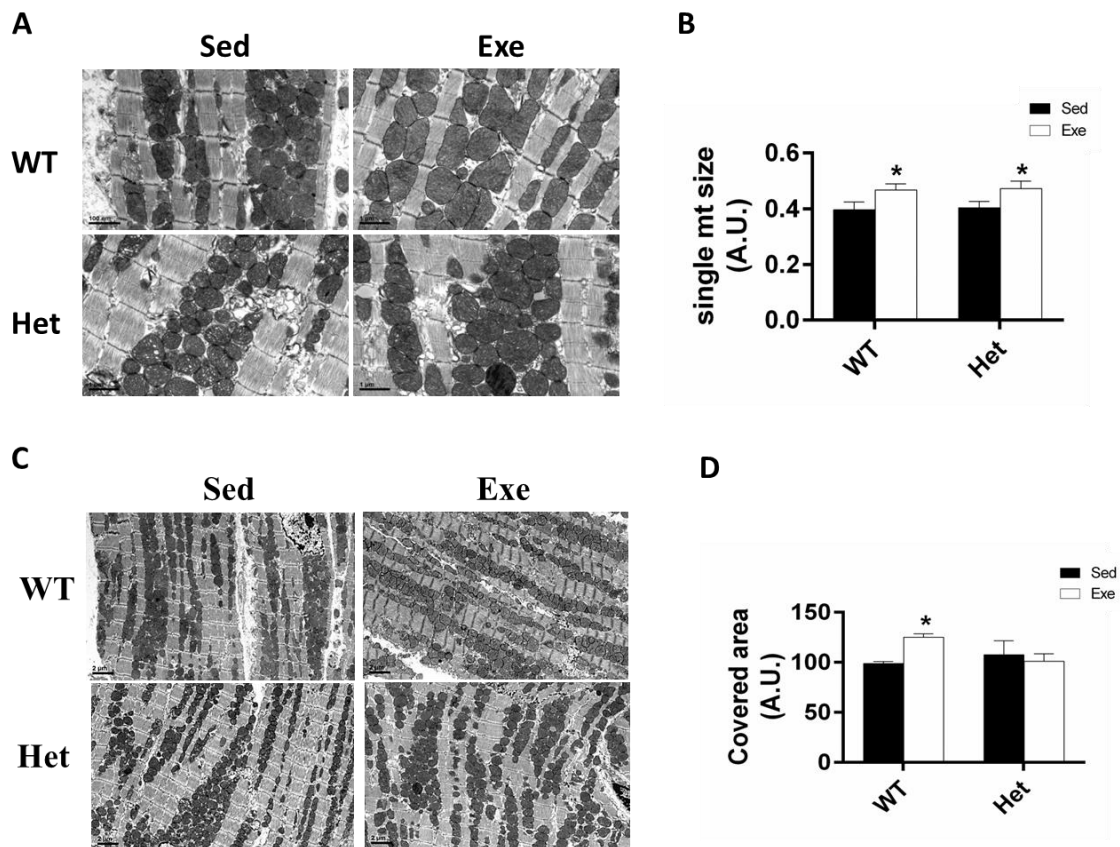


Figure 3.4 Beclin 1 heterozygous mice exhibited similar increase in mitochondrial size but reduced mitochondrial density after exercise. (A) Representative images of mitochondria from sedentary or chronic trained mouse hearts, $n=6$. (B) Normalized mitochondrial size from sedentary or chronic trained mouse hearts, $n=6$. (C) Representative images of mitochondria from sedentary or chronic trained mouse hearts, $n=6$. (D) Normalized mitochondrial density in sedentary or chronic trained mouse hearts, $n=6$. * $p<0.05$ compared to sedentary mice.

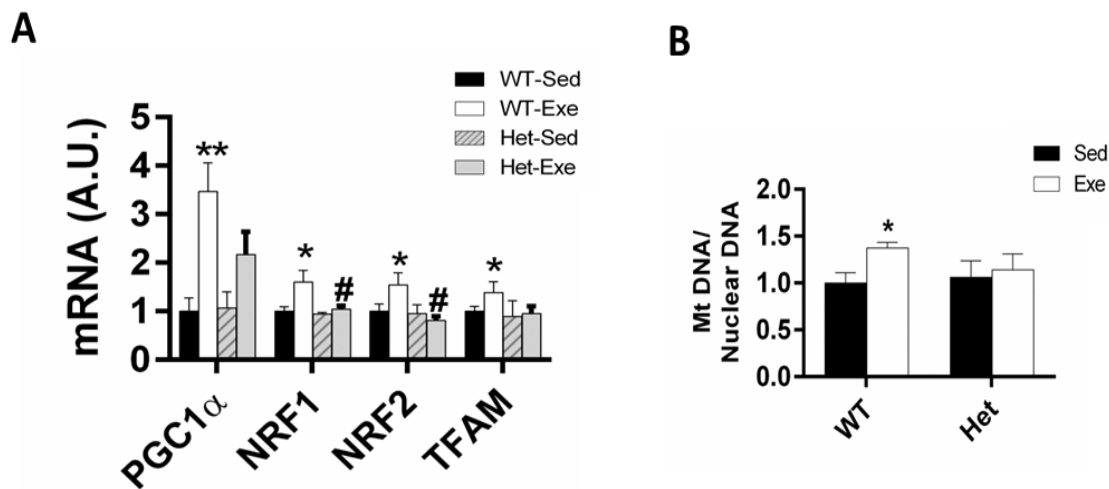


Figure 3.5 Exercise-induced mitochondrial biogenesis was impaired in beclin 1 heterozygous mouse hearts. (A) mRNA expression of nuclear –encoded genes that regulate mitochondrial biogenesis in sedentary or chronic trained mouse hearts, n=6. (B) mtDNA copy number measurement in sedentary or chronic trained mouse hearts, n=8. *p<0.05 compared to sedentary mice, #p<0.05 compared to WT mice.

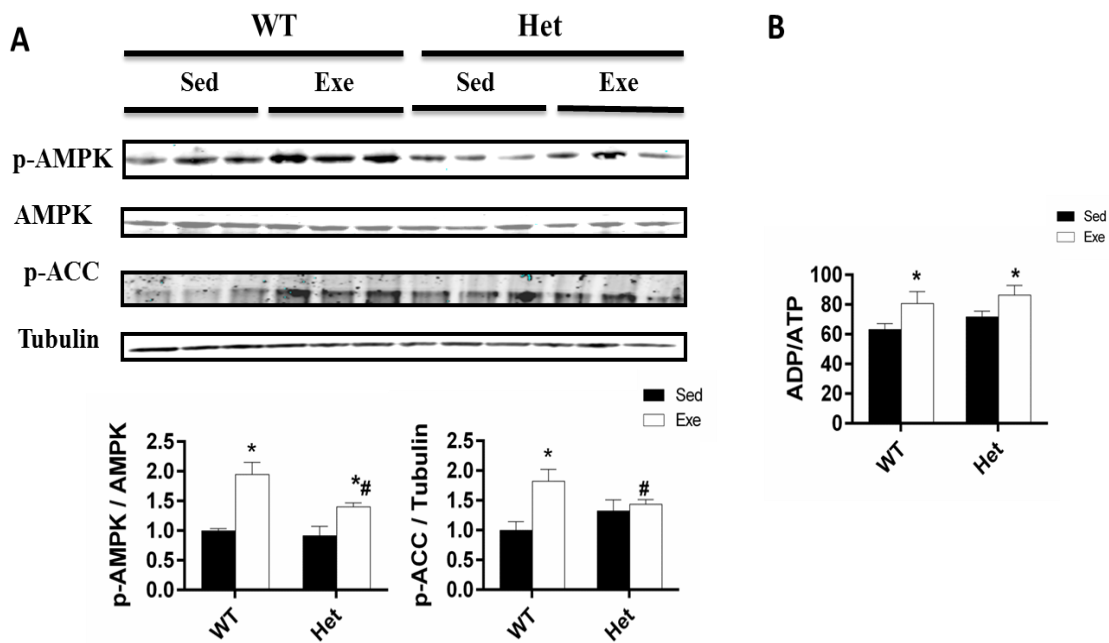


Figure 3.6 Exercise induced AMPK activation was impaired in beclin 1 heterozygous mouse hearts, but in an ADP/ATP independent manner. (A) p-AMPK, AMPK and p-ACC levels in sedentary or chronic trained mouse hearts, n=3. (B) ADP/ATP ratio was measured in sedentary or chronically trained mouse hearts, n=3. *p<0.05 compared to sedentary mice, #p<0.05 compared to WT mice.

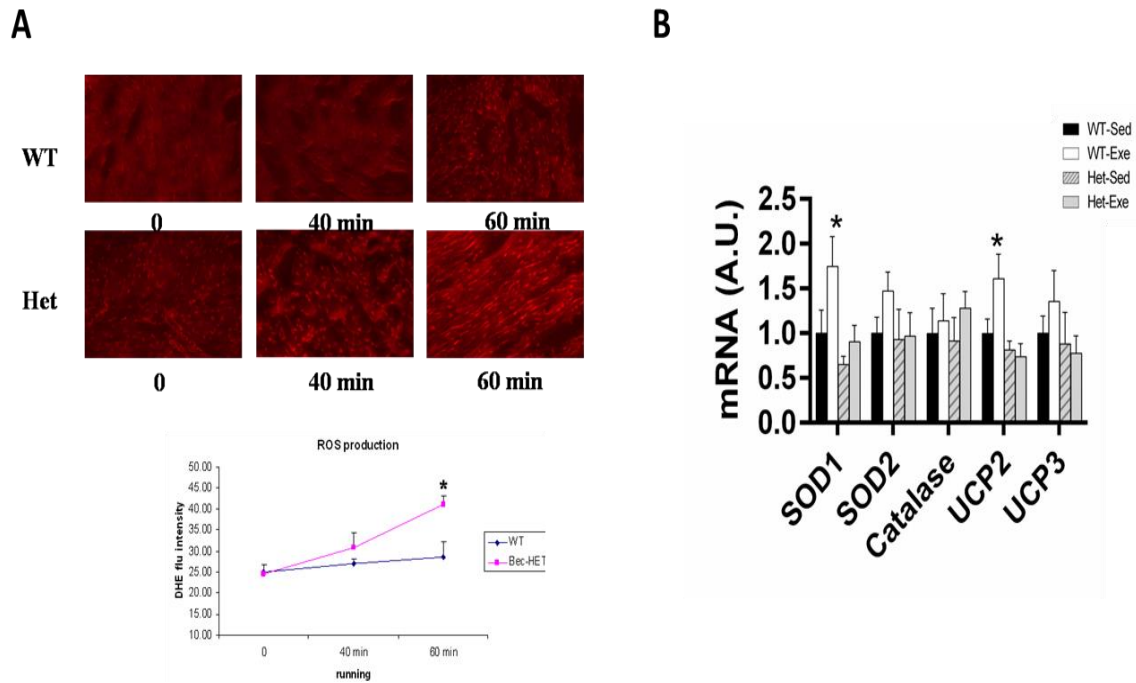


Figure 3.7 Cardiac anti-oxidation response was impaired in beclin 1 heterozygous mouse heart as response to exercise training. (A) DHE staining of WT and beclin 1 heterozygous mouse heart sections after 0, 40 min and 60 min exercise training, n=3. (B) mRNA expression of anti-oxidant genes in sedentary or chronic trained WT and beclin 1 heterozygous mouse hearts, n=6. *p<0.05 compared to sedentary mice.

Table 3.1 Primer sequences for Real time-PCR.

Gene	Forward	Reverse
RPL13a	CTCTGGCCTTTTCCTTTTTG	CCGAAGAAGGGAGACAGTTC
SOD1	CGGCGGATGAAGAGAGGCA	TCACACGATCTTCAATGGACACA
Catalase	GCAGATACCTGTGAACTGTC	GTAGAATGTCCGCACCTGAG
Cyto C	ATCTCCACGGTCTGTTCTGGG	TCCCAGGTGATGCCTTTGT
PGC-1	GTAATCTGCGGGATGATGG	AGCAGGGTCAAATCGTCTG
NRF1	CTTCAGAACTGCCAACCACA	GCTTCTGCCAGTGATGCTAC
NRF2	AGTCTTCACCACCCCTGATC	TCTGTCAGTGTGGCCTCTGG
TFAM	GCAAAGGATGATTCGGCTC	TCTGCTCTTCCCAAGACTTCA
UCP2	TTCTACAAGGGGTTTCATGCC	AGAAGGGTAAAGGGTGTGAG
SOD2	CAGACCTGCCTTACGACTATGG	CTCGGTGGCGTTGAGATTGTT

CONCLUSION

It is well-established that autophagy is involved in various cardiovascular diseases; however, the exact role of autophagy in the heart is incompletely understood. Moreover, the detailed molecular mechanism by which autophagy modulates cardiac bioenergetics and cardiac metabolism needs to be clearly elucidated.

Before our study, there were two animal models used to study the role of autophagy in the heart, beclin 1 heterozygous mice and cardiac-specific ATG5 KO (cATG5 KO) mice. But there are some limitations for these two models. Although beclin 1 heterozygous disruption resulted in reduced autophagy in liver and spleen, the constitutive autophagy in the heart of beclin 1 heterozygous mice was still preserved under basal conditions, which may explain the fact that the cardiac function in beclin 1 heterozygous mice is well preserved [1]. Then cardiac-specific ATG5 KO mice were generated, and ATG5 deletion in the heart caused aging-dependent cardiomyopathy at 8 months old [2]. However, ATG5 has diverse role beyond autophagy regulation. For example, ATG5 regulates apoptotic cell death signaling by interaction with Bcl family, and is also involved in necrosis signaling [3]. Thus the detrimental consequence of ATG5-deficiency in the heart might be the consequence of apoptosis rather than a secondary effect of autophagy inhibition.

Compared to ATG5 and beclin 1, ATG3 is a more specific autophagy-related protein, which is required for autophagosome membrane elongation [4]. Therefore, we generated a novel cardiac specific autophagy deficient mouse model by deleting ATG3 in cardiomyocytes. Compared to WT mice, cATG3 KO mice exhibited decreased ATG3

expression and blocked autophagic flux under basal and starvation conditions in a heart-specific manner. Thus our newly generated cATG3 KO mice provide a novel animal model to study the role autophagy in the heart.

Importantly, cATG3 KO mice exhibited cardiac contractile dysfunction at as early as 4 weeks old. More interestingly, metabolomics data showed that glycolytic and TCA cycle intermediates in ATG3 deficient heart were dramatically changed starting at 1 week old, when cardiac function was still preserved. After birth, the preference of cardiac substrate is switched from glucose to fatty acid, which is known as metabolic switch; however, the mechanism of this cardiac programming is poorly understood [5]. The accumulation of glycolytic intermediates and decreased fatty acid oxidation gene expression in ATG3 deficient heart indicate autophagy may be required for this metabolic transmission in fetal heart. Our finding in ATG3-deficient heart reveals the importance of autophagy in directing cardiac metabolic programming and facilitating cardiac development.

Most interestingly, we found NAD^+ metabolism was dramatically altered in ATG3-deficient hearts, characterized by increased NNMT expression and accelerated NAD^+ breakdown. In cultured cardiomyocytes, increasing NNMT expression repressed mitochondrial respiration, while inhibiting NNMT activity prevented mitochondrial dysfunction in autophagy deficient cardiomyocytes, suggesting NNMT induction may contribute to the mitochondrial dysfunction in autophagy deficient heart. In previous studies, NNMT inhibition by anti-sense oligonucleotide or its inhibitor MeNAM prevented obesity and fatty liver following high-fat diet, which reflects the importance of NNMT in metabolic disease [6]; however, the exact role of NNMT in cardiac function was never studied before. Our results for the first time showed NNMT promotes NAM degradation to MeNAM, and exerts an adverse effect on mitochondrial respiration in the heart. So NNMT is becoming a potential therapeutic target in the treatment of heart failure

mediated by autophagy inhibition.

NAD⁺ homeostasis has been long known to be crucial for cardiac function. For instance, certain agonists, such as angiotensin-II or isoproterenol, induce cardiac hypertrophy and heart failure by causing myocardial NAD⁺ depletion, and exogenous NAD⁺ blocks above cardiac hypertrophic response [7]. In our study, NMN or NR increased cardiac NAD⁺ content and rescued cardiac contractile dysfunction in cATG3 KO mice. Our results highlight the importance of NAD⁺ homeostasis in maintaining normal heart function.

We also demonstrate that autophagy may contribute to the beneficial effects of exercise training in the heart. In our study, we found that autophagy was induced in the heart as a response to acute and chronic exercise training. Interestingly, exercise training increased cardiac contractile function and enhanced cardiac mitochondrial respiration in WT mouse hearts, while inhibiting autophagy by heterozygous deletion of beclin 1 gene impaired autophagy response and blunted cardiac remodeling in response to exercise training. These data illustrate the important role of autophagy in maintenance of cardiac function in response to exercise training.

In this study, we found that cardiac mitochondrial biogenesis, which is a very important adaptive response to exercise training in the heart, also requires autophagy. Autophagy is a general response under cellular stress conditions, and mitochondrial biogenesis is also upregulated in response to stress for cellular survival [8]. But it is still unclear how autophagy and mitochondrial biogenesis are cross-talked under stress conditions. Our studies identify autophagy as an important factor to induce mitochondrial biogenesis following exercise training in the heart.

It is possible that autophagy induced by exercise training triggers certain signaling to promote mitochondrial biogenesis in the heart. Based on our finding, AMPK may be as a potential target that connects autophagy and mitochondrial biogenesis

under exercise conditions. However, the detailed mechanism by which autophagy regulates AMPK activity following exercise training is still unclear. In future studies, it will be very interesting to identify potential AMPK activator or inhibitor based on our newly generated ATG3 KO mouse model, which may help explain how autophagy mediates the beneficial effect of exercise training in the heart.

References

1. Qu, X., et al., Promotion of tumorigenesis by heterozygous disruption of the beclin 1 autophagy gene. *J Clin Invest*, 2003. 112(12): p. 1809-20.
2. Taneike, M., et al., Inhibition of autophagy in the heart induces age-related cardiomyopathy. *Autophagy*, 2010. 6(5): p. 600-6.
3. Yousefi, S., et al., Calpain-mediated cleavage of Atg5 switches autophagy to apoptosis. *Nat Cell Biol*, 2006. 8(10): p. 1124-32.
4. Yamaguchi, M., et al., Autophagy-related protein 8 (Atg8) family interacting motif in Atg3 mediates the Atg3-Atg8 interaction and is crucial for the cytoplasm-to-vacuole targeting pathway. *J Biol Chem*, 2010. 285(38): p. 29599-607.
5. Gong, G., et al., Parkin-mediated mitophagy directs perinatal cardiac metabolic maturation in mice. *Science*, 2015. 350(6265): p. aad2459.
6. Hong, S., et al., Nicotinamide N-methyltransferase regulates hepatic nutrient metabolism through Sirt1 protein stabilization. *Nat Med*, 2015. 21(8): p. 887-94.
7. Pillai, V.B., et al., Exogenous NAD blocks cardiac hypertrophic response via activation of the SIRT3-LKB1-AMP-activated kinase pathway. *J Biol Chem*, 2010. 285(5): p. 3133-44.
8. Cherry, A.D. and C.A. Piantadosi, Regulation of mitochondrial biogenesis and its intersection with inflammatory responses. *Antioxid Redox Signal*, 2015. 22(12): p. 965-76.